

---

# **Regulation of expression and functional characterization of human HIF-3 $\alpha$**

**Florian Rieß**

---



München 2015



---

# **Regulation of expression and functional characterization of human HIF-3 $\alpha$**

**Florian Rieß**

---

Dissertation  
der Fakultät für Biologie  
der Ludwig-Maximilians-Universität  
München

vorgelegt von  
Florian Rieß  
aus München

Erstgutachter:  
Zweitgutachter:  
Tag der mündlichen Prüfung:

Prof. Dr. Heinrich Leonhardt  
Prof. Dr. Bettina Kempkes  
13.10.2015

Erklärung

Hiermit erkläre ich, Florian Rieß, dass die Dissertation nicht ganz oder in wesentlichen Teilen einer anderen Prüfungskommission vorgelegt worden ist. Weiterhin erkläre ich, dass ich mich anderweitig einer Doktorprüfung ohne Erfolg nicht unterzogen habe.

München, den \_\_\_\_\_

---

Florian Rieß

Eidesstattliche Erklärung

Ich versichere hiermit an Eides statt, dass die vorgelegte Dissertation von mir selbstständig und ohne unerlaubte Hilfe angefertigt ist.

München, den \_\_\_\_\_

---

Florian Rieß

Dissertation eingereicht am: 18.12.2014

1. Gutachter Prof. Dr. Heinrich Leonhardt

2. Gutachter Prof. Dr. Bettina Kempkes

Mündliche Prüfung am: 13.10.2015

*Meiner Familie*

## Table of contents

Index of figures.....	I
Index of tables.....	II
Abbreviations .....	III
Gene symbols .....	VI
1    Introduction .....	2
1.1    Responses to hypoxia.....	3
1.1.1    Systemic effects .....	4
1.1.2    Cellular effects.....	6
1.1.3    Regulation of gene expression .....	9
1.2    Hypoxia inducible factors .....	9
1.2.1    ARNT.....	12
1.2.2    HIF-1 $\alpha$ .....	12
1.2.3    HIF-2 $\alpha$ .....	14
1.2.4    HIF target genes.....	16
1.2.5    HIF-3 $\alpha$ .....	17
1.3    Angiogenesis .....	20
1.3.1    Endothelial cells.....	21
1.3.2    Angiogenesis in physiology and pathophysiology .....	22
1.3.3    Cancer and its hallmarks .....	23
1.3.4    Epigenetics .....	24
2    Aims of this study.....	26
3    Materials and Methods.....	27
3.1    Materials .....	27
3.1.1    Cell-lines.....	27

3.1.2 Instruments.....	28
3.1.3 Consumables.....	30
3.1.4 Chemicals.....	30
3.1.5 Buffers, solutions and media .....	33
3.1.6 Plasmid preparation (mini).....	37
3.1.7 Primers and probes .....	38
3.1.8 Plasmids.....	39
3.1.9 siRNA .....	40
3.1.10 Bacterial strains.....	40
3.1.11 Kits .....	41
3.1.12 Antibodies .....	42
3.1.13 Software .....	42
3.1.14 Online databases and algorithms.....	43
3.2 Methods .....	43
3.2.1 Cell Culture.....	43
3.2.2 Reporter Gene Assays .....	44
3.2.3 Quantitative Reverse-Transcriptase Polymerase Chain Reaction.....	45
3.2.4 Chromatin accessibility assay .....	45
3.2.5 Bisulfite sequencing.....	46
3.2.6 Plasmids and transfections.....	46
3.2.7 Immunoblot Analysis .....	47
3.2.8 Angiogenesis Assay .....	47
3.2.9 Co-Immunoprecipitation .....	48
3.2.10 <i>In vitro</i> Translation and Electrophoretic Mobility Shift Assay .....	48
3.2.11 Chromatin Immunoprecipitation .....	49
3.3 Statistical Analysis .....	49

---

4	Results .....	50
4.1	Regulation of HIF3A transcription at ambient conditions .....	50
4.1.1	<i>HIF3A</i> expression levels differs in various cell lines .....	50
4.1.2	<i>HIF3A</i> promoter is inaccessible in MCF7 .....	52
4.1.3	<i>HIF3A</i> promoter is hypermethylated in HeLa and MCF7 cells .....	54
4.1.4	<i>HIF3A</i> promoter shows open chromatin in HMEC-1 cells .....	54
4.1.5	<i>HIF3A</i> expression inversely correlates with tumor stage in lung .....	56
4.1.6	<i>HIF3A</i> is induced by hypoxia in HMEC-1 .....	57
4.2	HIF-3 $\alpha$ inhibits HIF-2 activity in endothelial cells under hypoxia .....	58
4.2.1	Time- and dose-dependent <i>HIF3A</i> induction .....	58
4.2.2	HIF-3 $\alpha$ inhibits HIF target gene expression .....	61
4.2.3	HIF-3 $\alpha$ inhibits HIF-2 mediated <i>PAI1</i> expression .....	64
4.2.4	HIF-3 $\alpha$ inhibits PAI-1-mediated angiogenesis .....	66
4.2.5	HIF-3 $\alpha$ interacts with HIF-2 $\alpha$ and ARNT .....	68
4.2.6	HIF-3 $\alpha$ /ARNT binds to <i>PAI1</i> promoter .....	70
4.2.7	Exogenous HIF-3 $\alpha$ /ARNT induces <i>PAI1</i> expression .....	72
5	Discussion .....	74
5.1	HIF3A expression in different cell lines .....	74
5.2	DNA accessibility and chromatin remodeling .....	76
5.3	DNA methylation .....	77
5.4	Histone modification .....	78
5.5	Induction of HIF3A .....	81
5.6	Limitations of the reporter gene assay .....	82
5.7	Heterogeneous effect of HIF subunit knockdown .....	83
5.8	Functional effects of HIF3A depletion .....	84
5.9	Revealing the modulatory mechanism of HIF-3 $\alpha$ by interaction studies .....	85

---

5.10	HIF-3 $\alpha$ is modulating HIF-2 $\alpha$ activity by competing for ARNT.....	86
5.11	Transactivatory properties of HIF-3 $\alpha$ .....	88
5.12	Perspectives .....	88
6	Summary.....	92
7	Zusammenfassung .....	94
8	References.....	97
	Publikationen und Auszeichnungen .....	110

# Index of figures

Figure 1: Partial pressure of oxygen in different compartments of the body. ....	2
Figure 2: Effects of hypoxia.....	4
Figure 3: Decreased pO <sub>2</sub> levels in alveoli leads to constriction of serving pulmonary arterioles.....	5
Figure 4: Role of erythropoietin in the process of erythropoiesis.....	6
Figure 5: Cellular effects of hypoxia.....	7
Figure 6: Domain structures of the HIF transcription factors and sequence comparison of alpha subunits. ....	10
Figure 7: Regulation of HIF-1 activity by degradation or stabilization of the alpha-subunit HIF-1α.....	11
Figure 8: Representation of the bHLH domain of HIF- α/β heterodimer contacting DNA containing HRE consensus motif.....	13
Figure 9: Schematic representation of exonic arrangement of suggested human HIF-3α variants. ....	19
Figure 10: Schematic representation of sprouting angiogenesis.....	22
Figure 11: Basal expression of <i>HIF3A</i> isoforms varies in different cell lines. ....	51
Figure 12: Chromatin accessibility of distal (E1a & E1b) and proximal (E1c) <i>HIF3A</i> promoter regions are increased in HMEC-1 compared to HeLa and MCF7 cells. ....	53
Figure 13: Methylation of CpG island 1 is decreased in HMEC-1 cells compared to HeLa and MCF7.55	55
Figure 14: Marker for active chromatin (H3Ac) is increased in HMEC-1 cells in <i>HIF3A</i> promoter region containing exon 1a. ....	56
Figure 15: <i>HIF3A</i> expression varies in different tissues and inversely correlates with tumor stage in lung. ....	57
Figure 16: <i>HIF3A</i> expression is induced in HMEC-1 cells but not in HeLa or MCF7 cells. ....	58
Figure 17: <i>HIF3A</i> is transcriptionally induced under hypoxia in a dose- and time-dependent manner. 60	60
Figure 18: HIF-1α and HIF-2α proteins are induced by hypoxia in HMEC-1 cells.....	61
Figure 19: HIF-3α inhibits HIF-driven luciferase activity. ....	63
Figure 20: HIF-3α inhibits HIF-2-driven <i>PAI1</i> expression. ....	65
Figure 21: HIF-3α inhibits HIF-2-driven <i>PAI-1</i> expression. ....	66
Figure 22: HIF-3α inhibits <i>PAI-1</i> -dependent angiogenesis. ....	67
Figure 23: HIF-3α binds to DNA in complex with ARNT but not with HIF-2α. ....	69
Figure 24: HIF-3α inhibits HIF-2 by outcompeting HIF-2α for the interaction with ARNT subsequently binding to DNA. ....	71
Figure 25: HIF-3α exerts transactivatory properties on <i>PAI1</i> when coexpressed with ARNT. ....	73
Figure 26: Suggested mechanism of modulatory action of HIF-3α on HIF-2α under hypoxia.....	89

## Index of tables

Table 1: Cell lines used in this study.....	27
Table 2: Instruments used in this study.....	28
Table 3: Consumables used in this study.....	30
Table 4: Chemicals used in this study.....	30
Table 5: Cell culture media and additives used in this study.....	33
Table 6: Primers and probes used in this study.....	38
Table 7: Plasmids and vectors used in this study.....	39
Table 8: siRNA used in this study.....	40
Table 9: bacterial strains used in this study.....	40
Table 10: Kits used in this study .....	41
Table 11: Antibodies used in this study.....	42
Table 12: Software used in this study.....	42
Table 13: Online databases and algorithms used in this study.....	43

# Abbreviations

<i>AhR</i>	aryl hydrogen receptor (protein)
<i>ANOVA</i>	analysis of variance
<i>APS</i>	ammonium persulfate
<i>ARNT</i>	aryl hydrocarbon receptor nuclear translocator (protein)
<i>ATP</i>	adenosine triphosphate
<i>bHLH</i>	basic helix-loop-helix
<i>bp</i>	base pairs
<i>caC</i>	5-carboxylcytosine
<i>CA-IX</i>	carbonic anhydrase IX
<i>CBP</i>	CREB binding protein
<i>cDNA</i>	coding desoxyribonucleic acid
<i>ChIP</i>	chromatin immunoprecipitation
<i>CpG</i>	—C—phosphate—G—
<i>CTAD</i>	C-terminal transactivation domain
<i>DEPC</i>	diethylpyrocarbonate
<i>DMEM</i>	Dulbecco's modified Eagle's medium
<i>DMSO</i>	dimethylsulfoxide
<i>DNA</i>	desoxyribonucleic acid
<i>DTT</i>	dithiothreitol
<i>ECM</i>	extracellular matrix
<i>EDTA</i>	ethylene diamine tetraacetic acid
<i>EGF</i>	endothelial growth factor
<i>EGTA</i>	ethylene glycol tetraacetic acid
<i>eIF4E</i>	eukaryotic translation initiation factor 4E (protein)
<i>EMSA</i>	electrophoretic mobility shift assay
<i>EPAS1</i>	endothelial PAS protein 1
<i>EPO</i>	erythropoietin (protein)
<i>EST</i>	expressed sequence tag
<i>FADH<sub>2</sub></i>	flavin adenine dinucleotide
<i>fC</i>	5-formylcytosine
<i>FCS</i>	fetal calf serum
<i>FIH-1</i>	factor inhibiting HIF-1
<i>H3Ac</i>	acetylated histone 3
<i>H3K9me3</i>	trimethylated lysine 9 of histone 3
<i>HBSS</i>	Hank's balanced salt solution
<i>HEPES</i>	4-(2-hydroxyethyl)-1-piperazineethanesulfonic acid

---

<i>HIF</i>	hypoxia inducible factor (protein)
<i>HIF-1<math>\alpha</math></i>	hypoxia-inducible factor 1-alpha (protein)
<i>HIF-2<math>\alpha</math></i>	hypoxia-inducible factor 2-alpha (protein)
<i>HIF-3<math>\alpha</math></i>	hypoxia-inducible factor 3-alpha (protein)
<i>HLF</i>	<i>HIF1<math>\alpha</math></i> -like factor
<i>hmC</i>	5-hydroxymethylcytosine
<i>HRE</i>	<i>HIF</i> -response element
<i>HRF</i>	<i>HIF</i> -related factor
<i>IgG</i>	immunoglobulin G
<i>IPAS</i>	inhibitory PAS domain protein
<i>kb</i>	kilobases
<i>K<sub>m</sub></i>	Michaelis constant
<i>kPa</i>	kilopascal
<i>MeCP2</i>	methyl CpG binding protein 2
<i>mmHg</i>	millimeters of mercury
<i>MOP</i>	member of PAS family
<i>mRNA</i>	messenger ribonucleic acid
<i>mTOR</i>	mammalian target of rapamycin
<i>NADH</i>	nicotinamide adenine dinucleotide
<i>NLS</i>	nuclear localization signal
<i>NTAD</i>	N-terminal transactivation domain
<i>ODD</i>	oxgen dependent degradation
<i>PAGE</i>	polyacrylamide gel electrophoresis
<i>PAI-1</i>	plasminogen activator inhibitor 1 (protein)
<i>PAS</i>	Per-Arnt-Sim homology
<i>PBS</i>	phosphate buffered saline
<i>PDH</i>	pyruvate dehydrogenase (protein)
<i>PDK1</i>	pyruvate dehydrogenase kinase, isozyme 1 (protein)
<i>PGK1</i>	phosphoglycerate kinase 1 (protein)
<i>PHD</i>	prolyl hydroxylase domain protein
<i>PMSF</i>	phenylmethanesulfonyl fluoride
<i>pO<sub>2</sub></i>	partial pressure of oxygen
<i>pVHL</i>	von Hippel-Lindau protein
<i>qPCR</i>	quantitative polymerase chain reaction
<i>RLU</i>	relative light units
<i>RNAi</i>	RNA interference
<i>ROS</i>	reactive oxygen species
<i>rRNA</i>	ribosomal ribonucleic acid

---

<i>RT-qPCR</i>	quantitative reverse-transcriptase polymerase chain reaction
<i>SDS</i>	sodium dodecyl sulfate
<i>siRNA</i>	small interfering RNA
<i>TCA</i>	tricarboxylic acid
<i>TEMED</i>	tetramethylethylenediamine
<i>TET</i>	ten-eleven translocation (protein)
<i>TRIS</i>	tris(hydroxymethyl)aminomethane
<i>VEGF-A</i>	vascular endothelial growth factor A (protein)

## Gene symbols

<i>ACTB</i>	actin, beta
<i>CA12</i>	carbonic anhydrase XII
<i>CA9</i>	carbonic anhydrase IX
<i>CCND1</i>	cyclin D1
<i>CD82</i>	<i>CD82</i> molecule
<i>CDH5</i>	cadherin 5, type 2
<i>EGLN3</i>	<i>egl-9</i> family hypoxia-inducible factor 3
<i>EPO</i>	erythropoietin
<i>GAPDH</i>	glycerine aldehyde 3 phosphate dehydrogenase
<i>GLUT1</i>	glucose transporter 1
<i>HBB</i>	hemoglobin, beta
<i>HIF1A</i>	hypoxia inducible factor 1, alpha subunit
<i>HIF2A</i>	hypoxia inducible factor 2, alpha subunit
<i>HIF3A</i>	hypoxia inducible factor 3, alpha subunit
<i>KDR</i>	kinase insert domain receptor
<i>PAI1</i>	plasminogen activator inhibitor 1
<i>PGK1</i>	phosphoglycerate kinase 1
<i>POU5F1</i>	<i>POU</i> class 5 homeobox 1
<i>RHO</i>	rhodopsin
<i>VEGFA</i>	vascular endothelial growth factor A

Listed symbols resemble human genes and are italicized in continuous capitals according to Guidelines for Human Gene Nomenclature (Wain et al. 2002). Murine gene symbols differ in only having the first letter capitalized.

# 1 Introduction

The availability of molecular dioxygen,  $O_2$ , plays an essential role for cellular respiration in aerobic organisms, amongst them virtually all eukaryotes, including mammals. The central metabolic role of oxygen is its utilization in the process of cellular respiration. In the generation of energy *via* oxidative phosphorylation,  $O_2$  serves as the final electron acceptor in the respiratory chain (Alberts et al. 2002). The transport of oxygen and thus an optimal oxygenation of all cells occur through the uptake *via* the lungs over the downstream transport *via* erythrocytes to the different tissues eventually reaching mitochondria. During that process the partial pressure of oxygen ( $pO_2$ ) in air, which is 21 kPa at sea level drops on the one hand by physically limited solubility in aqueous solution and on the other hand continuous consumption down to 0.5 kPa once the oxygen reaches the mitochondria (Østergaard and Gassmann 2011).

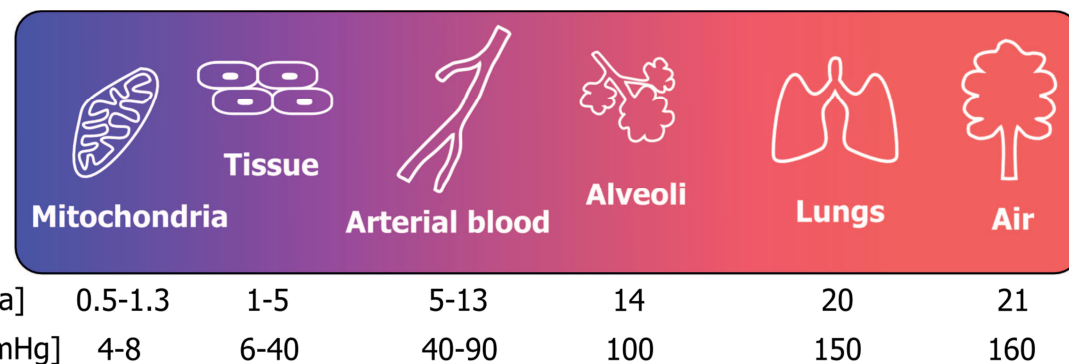


**Figure 1: Partial pressure of oxygen in different compartments of the body.**

Normoxic dry air has a  $pO_2$  of 21 kPa (160 mmHg). With entering the lungs it is reduced to 20 kPa (150 mmHg) by humidification. The subsequent constant removal of oxygen by the pulmonary capillaries, the  $pO_2$  in the alveolae is around 14 kPa (100 mmHg), whereas oxygen tension in the blood is physiologically between 5 and 13 kPa (40-90 mmHg), venous to arterial side, respectively. In tissues and single cells, the  $pO_2$  goes down to 1-5 kPa (6-40 mmHg), in mitochondria down to 0.5-1.3 kPa (4-8 mmHg). At an ambient pressure of 100 kPa,  $pO_2$  levels given in kPa correspond to the relative fraction given in percent. (Figure adapted from Østergaard and Gassmann 2011)

However, when the supply with oxygen does not longer meet the demand in tissues or cells, the resulting condition is called hypoxia.

The expression “hypoxia” derives from the Greek terms *hypo* (= under, sub-) and oxygen [Anc Greek: *oxys* (= sharp) + *genos* (= generation, produced by) meaning acid-

former because oxygen was thought to be essential in the formation of acid]. Hypoxia describes the situation in which the body or tissues or cells encounter insufficient oxygen supply, which can occur by dysfunction of either delivery or utilization on cellular level (Legrand et al. 2008). It is important to note that hypoxia is not only involved in pathophysiological conditions like cancer or fetal heart defects but is also crucial in development like in the establishment of the embryonic cardiovascular system (Ruan et al. 2009; Dunwoodie 2009).

Thus, in order to maintain the supply with energy by efficient oxidative phosphorylation oxygen homeostasis is absolutely crucial. This process comprises several responses amongst them the precise establishment and regulation of blood vessels, the physiological infrastructure for  $O_2$  delivery supply.

## ***1.1 Responses to hypoxia***

The adaptation to hypoxia occurs on different levels, depending on the severity and duration of hypoxia. An immediate body wide response occurs by vasoconstriction of underventilated areas in the lung to ensure an efficient oxygenation of areas that are ventilated (systemic effects) (Evans et al. 2011). A prolonged adaption involves a switch from aerobic to anaerobic metabolism. This includes a change in post-glycolytic processes when pyruvate is not longer decarboxylated to form acetyl-CoA but to form lactate by fermentation (cellular effects) (Goda and Kanai 2012). An additional effect is the hypoxia triggered secretion of EPO which confers further capacity in the transport of oxygen. Ultimately, it includes the activation of genes in order to counteract the negative effects of sustained hypoxia (regulation on gene expression level) (Semenza 2010).

### 1.1.1 Systemic effects

Upon low oxygen, peripheral vessels dilate, whereas vessels of pulmonary vasculature constrict thus rapidly modulating pulmonary ventilation and perfusion to optimize the supply of metabolising tissues with  $O_2$  by shunting blood from poorly ventilated areas. The immediate systemic response to altered  $O_2$  supply is regulated by specialized chemoreceptors, the carotid and neuroepithelial bodies (Figure 2) (Ward 2008). While the carotid body is located close to the bifurcation of the carotid artery, the neuroepithelial bodies are found in the intrapulmonary epithelium mainly at the bifurcation of the bronchi. These clusters of chemoreceptors are sensing changes in  $pO_2$  levels in a yet to be identified way and secrete neurotransmitters which activate afferent neurons. Subsequently, the cardiovascular center of the brain gets stimulated and causes besides other effects a change of breathing rate, heart rate and tone of pulmonary and peripheral vessels.

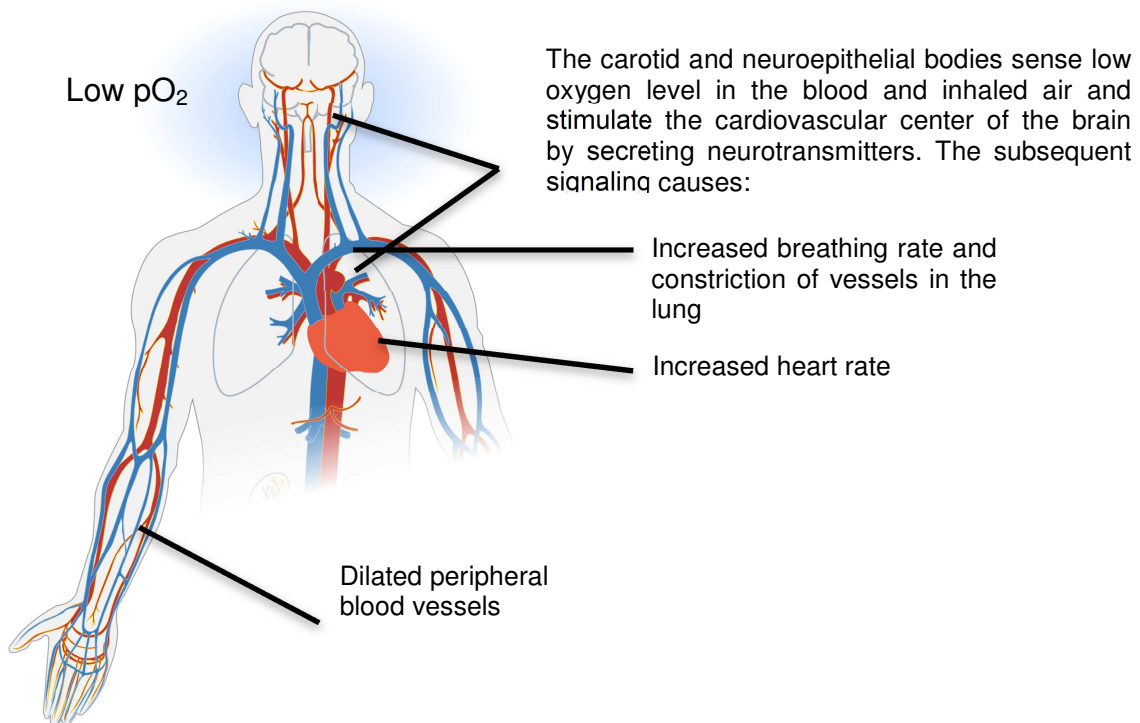


**Figure 2: Effects of hypoxia.**

Upon low levels of  $pO_2$ , the carotid body and the neuroepithelial bodies detect the changed oxygen content in blood and inhaled air, respectively. The triggered secretion of neurotransmitters in the brain leads to an increase of heart and breathing rate and a constriction of vessels in the lung, while peripheral blood vessels dilate (figure adapted from LadyofHats).

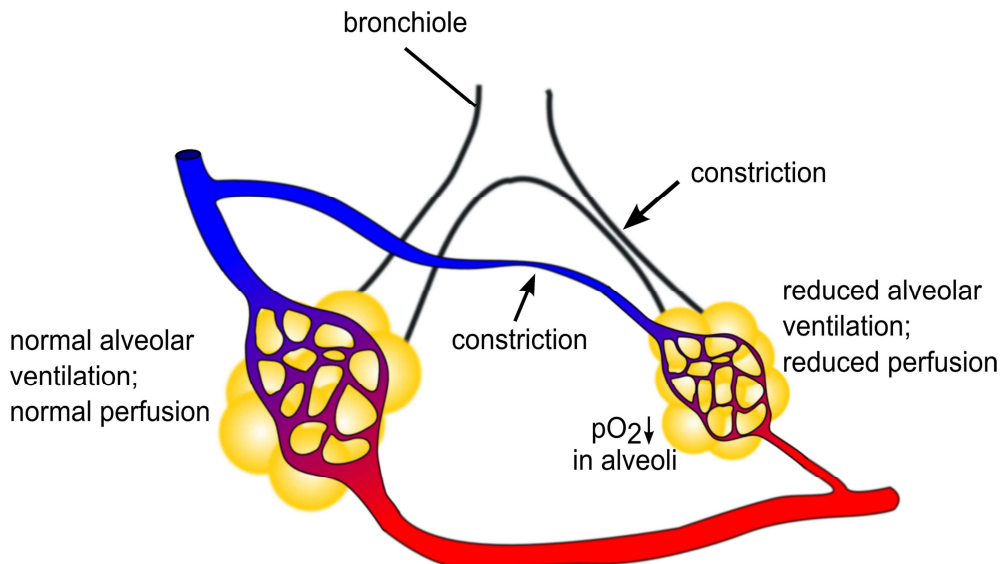


**Figure 3: Decreased  $pO_2$  levels in alveoli leads to constriction of serving pulmonary arterioles.**

In case of reduced alveolar ventilation, the excessive perfusion of capillaries is downregulated by a constriction of the respective serving pulmonary arterioles upon decreased  $pO_2$  levels in alveoli (figure modified after de Leval and Deanfield 2010).

However, the aforementioned effects are beneficial only in acute phase hypoxia; with sustained hypoxic conditions, the systemic effects may lead to pathologic side effects. Due to the hypoxia mediated vasoconstriction of pulmonary arteries an increased resistance and thus an increased blood pressure occurs, which leads to pathological vascular remodeling including endothelial dysfunction and smooth muscle cell hypertrophy (Aggarwal et al. 2013). The subsequent right heart hypertrophy due to the increased workload is known as pulmonary hypertension (Voelkel et al. 2011). In contrast to the short-term adaptation, vascular remodeling is majorly irreversible even after being back to normoxia, at least the form which occurs due to increased proliferation of endothelial cells (Hirota and Martin 2013).

In addition, the reduced  $pO_2$  triggers enhanced  $O_2$  delivery by erythropoiesis. Unlike increased ventilation and cardiac output (probably resulting from heightened sympathetic drive), the production and release of erythropoietin (EPO) from renal peritubular fibroblasts is less costly in terms of energy and can easily be sustained for extended periods (Boron and Boulpaep 2008). Released EPO acts selectively on burst forming unit erythroid cells and colony forming unit erythroid cells to stimulate cell proliferation and differentiation to proerythroblasts, usually occurring in the bone

marrow (Rifkind et al. 1976). The further maturation of cells downstream of erythroblasts does not require EPO (Figure 4). The increased number of mature erythrocytes ultimately compensates for the lack of oxygen by improved capacity of oxygen transport. However, this organism wide response is not only beneficial in the adaptation to hypoxia but is also used as a trigger the endurance performance of sportsmen by altitude training.

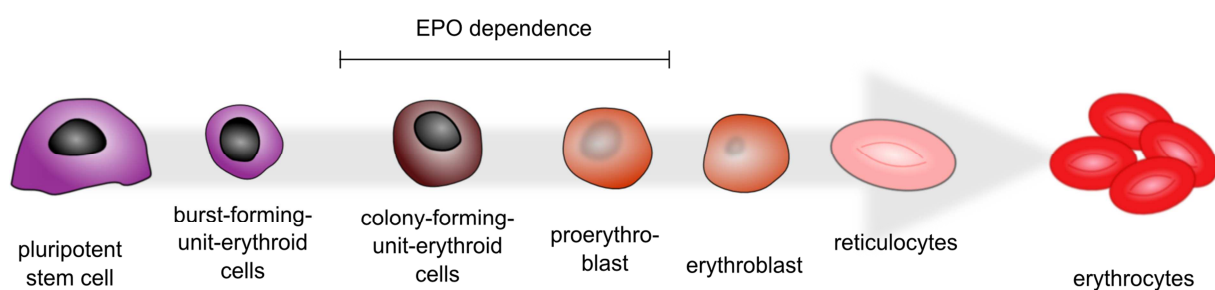


**Figure 4: Role of erythropoietin in the process of erythropoiesis.**

Erythropoiesis starts from pluripotent stem cells, which differentiate into burst-forming-unit-erythroid cells before EPO triggers the formation of colony-forming-unit-erythroid cells. The subsequent differentiation into proerythroblasts is again EPO-dependent. During the maturation of erythroblasts and reticulocytes the nucleus is extruded. Eventually, fully differentiated erythrocytes are formed (figure adapted from Elliott et al. 2014).

### 1.1.2 Cellular effects

Besides the systemic responses, an appropriate adaptation to hypoxia on cellular level is fundamental. An efficient supply with energy is vital for each cell, with hydrolysis of ATP being the predominant source of energy. Homeostasis of intracellular environment through ion pumps are mainly dependent on ATP and can consume up to 80% of energy produced (Boutilier 2001). Mitochondria are regarded as the central compartment for the generation of energy rich phosphate bonds by cellular respiration. In this process also known as oxidative phosphorylation electrons are transferred from a donor by an electron transport chain to the acceptor. In eukaryotic cells, the electrons are gained by the oxidation of NADH or  $\text{FADH}_2$  and transported by five main protein complexes that are located in the inner membrane of the mitochondria (Cooper 2000). In each of these steps of the electron transport chain, free energy gets released as  $\text{H}^+$  ions, which are pumped from the matrix into the intermembrane

space to create a proton gradient across the inner mitochondrial membrane. This potential drives the synthesis of ATP by complex V, the ATP synthase (Figure 5). Under hypoxic conditions, respiratory chain reaction is inhibited while proton leakage is increased (Wheaton and Chandel 2011). The resulting loss of ATP causes a failure of ion-motive ATPase, thus an uncontrolled influx of  $\text{Ca}^{2+}$  through voltage dependent ion channels, induced by membrane depolarization. Subsequently, Calcium dependent phospholipases and proteases are activated, resulting in cell swelling concomitant to damaging of cellular components and ultimately necrosis of the cell (Michiels 2004).

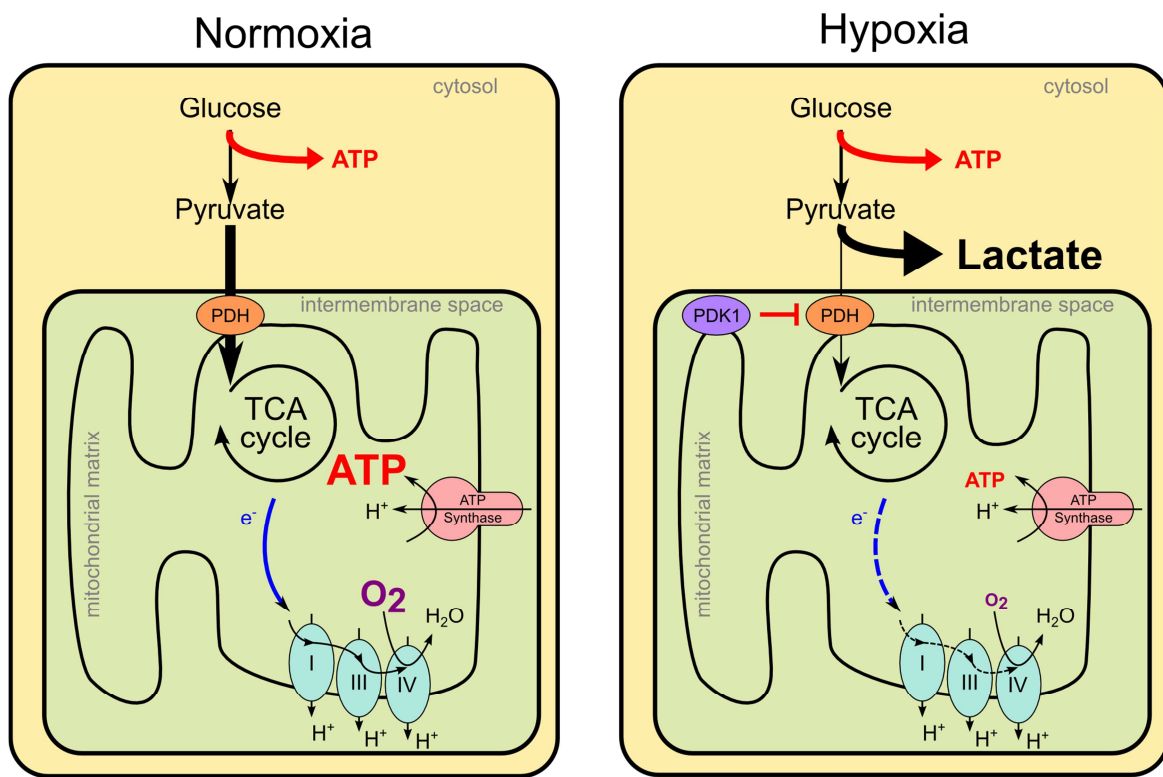


**Figure 5: Cellular effects of hypoxia**

Under normoxic conditions, ATP production occurs majorly by proton driven ATP synthase after glycolysis with subsequent TCA cycle and oxidative phosphorylation. Under hypoxic conditions, cells switch their catabolic pathway to respiratory chain independent mechanism by changing to an anaerobic ATP production. The post-glycolysis processes switches from acetyl-CoA formation by decarboxylating pyruvate to a fermentation of pyruvate to lactate (ATP: adenosine triphosphate; TCA cycle: tricarboxylic acid cycle; blue ovals resemble complex I, III and IV of the respiratory chain, respectively; PDH: pyruvate dehydrogenase; PDK1: pyruvate dehydrogenase kinase isozyme 1). Figure modified after Aragonés et al. 2008).

It is worth to mention, that although decreased  $O_2$  availability leads to a diminished final electron acceptor, activity of complex IV is not the main limiting factor as inhibition of mitochondrial respiration occurs at  $pO_2$  levels way above the  $K_m$  of complex IV, meaning at higher  $pO_2$ -levels (Gnaiger et al. 1995).

In order to counteract the pathological effects of hypoxia, cells decrease energy consuming processes concomitantly with an upregulation of energetic efficiency of ATP-producing pathways, concretely increased anaerobic processing of pyruvate after glycolysis (Hochachka et al. 1993)

The main metabolic processes of energy consumption in cells are ion shuttling by ATPases pumps and protein synthesis (Boutilier 2001). Thus inhibition of protein synthesis as well as  $Na^+/K^+$  and  $Ca^{2+}$  pumping is contributing in the first instance to reduce the need for ATP, of which the supply is limited under hypoxia. The orchestration of decreased energy consumption on translational level is amongst others controlled by the eukaryotic translation initiation factor 4E (eIF4E). The initial step of protein synthesis, the binding of eIF4E to the 5'-located 7-methylguanosine triphosphate cap of messenger RNAs, is repressed with low oxygen tension by sequestering eIF4E through mammalian target of rapamycin (mTOR)-dependent mechanisms (Uniacke et al. 2012).

Simultaneously, cells change their catabolic pathways producing ATP from the oxygen dependent oxidative phosphorylation to the oxygen independent fermentation (known as “Pasteur effect” (Racker 1974)). However, the net production of ATP is remarkably lower in glycolysis compared to mitochondrial respiration (2:36) (Lodish et al. 2000). To overcome this limitation, activity of several glycolytic enzymes is induced, either by kinases or by transcriptional induction (Seagroves et al. 2001) (Figure 5). Interestingly,  $O_2$  is not limiting in ATP production by oxidative phosphorylation. In hypoxic cells increased glycolytic flux to pyruvate and its reduction to lactate by lactate-dehydrogenase is stimulated. This change in the metabolism is additionally triggered by hypoxia-induced PDK1 inhibiting the multi-enzyme complex PDH activity that contributes to the transformation of pyruvate into acetyl-CoA, which is subsequently used in the tricarboxylic acid (TCA) cycle (Kim et al. 2006) (Figure 5). The resulting attenuation of oxidative phosphorylation is essential to prevent the genera-

tion of reactive oxygen species (ROS) resulting from ineffective electron transport under hypoxic conditions (Kim et al. 2006).

### 1.1.3 Regulation of gene expression

The above-described systemic and cellular responses to hypoxia occur within minutes to a few hours and are mainly based on preexisting components of the cell. To maintain or even improve the response to prolonged hypoxic conditions, newly synthesized enzymes, transporters, growth factors and even peptide hormones are necessary. To this end, a special family of transcription factors evolved which mediate the synthesis of key factors involved in the adaptation to low oxygen tension. These transcription factors belong to the family of hypoxia inducible factors (HIFs) and are described in detailed below.

## **1.2 Hypoxia inducible factors**

For an appropriate cellular adaptation to reduced availability of oxygen (hypoxia) transcription factors of the HIF (hypoxia-inducible factor) family are essential, ensuring metabolism (Semenza 2012) and proliferation (Kaelin and Ratcliffe 2008). HIFs were postulated as master regulators under hypoxia (Wang and Semenza 1993), shown to mediate proliferative responses of vascular endothelial cells, such as division (Iyer et al. 1998), sprouting and angiogenesis (Maxwell et al. 1997; Carmeliet et al. 1998).

HIFs are heterodimers belonging to the bHLH-PAS (basic helix-loop-helix/Per-Arnt-Sim homology) protein superfamily containing domains for heterodimerization and DNA binding (bHLH and PAS-A/PAS-B domain, respectively) (Semenza 2009). The HIF-family comprises the constitutively expressed  $\beta$ -subunit HIF-1 $\beta$ , also known as the aryl hydrocarbon receptor nuclear translocator (ARNT) and regulated  $\alpha$ -subunits (HIF-1 $\alpha$ , HIF-2 $\alpha$ ) resulting in an inducible transcription factor under hypoxia (Jiang et al. 1996). The alpha subunits contain an additional domain determining its protein stability (Huang et al. 1998) – oxygen dependent degradation domain (ODD) - as well

as a N- and C-terminal activation domain (NTAD and CTAD, respectively) (Ruas et al. 2002) providing the means to act as transcription factors (Figure 6).

The third member of the HIF alpha subunits, HIF-3 $\alpha$ , initially described by Gu et al. (1998) in mice also belongs to the bHLH-PAS protein family, but lacks the CTAD, suggesting a distinct role in comparison to HIF-1 $\alpha$  and HIF-2 $\alpha$ . Since only little is known about human HIF-3 $\alpha$ , its regulation and function was investigated in this thesis.

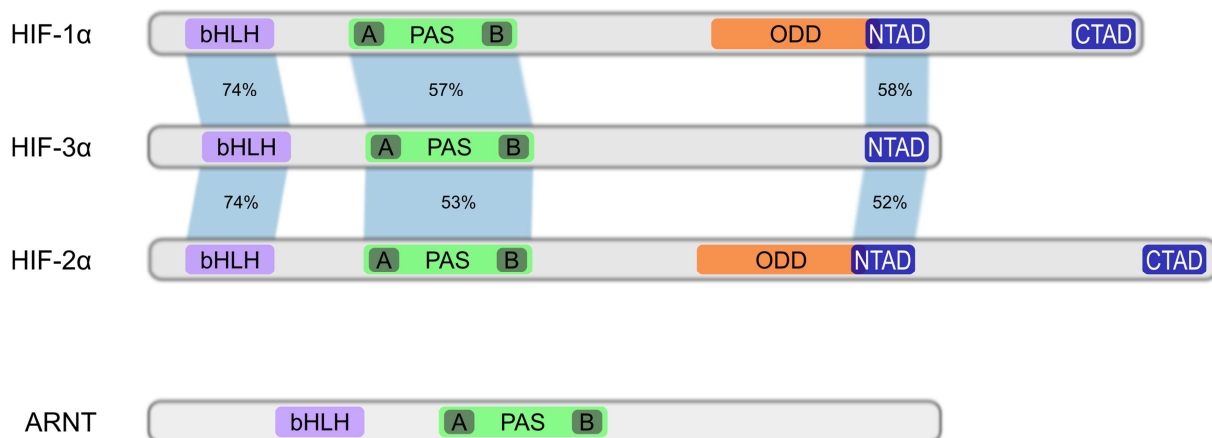


**Figure 6: Domain structures of the HIF transcription factors and sequence comparison of alpha subunits.**

The three HIF- $\alpha$  paralogues, HIF-1 $\alpha$ , HIF-2 $\alpha$  and HIF-3 $\alpha$  and the  $\beta$ -subunit ARNT all contain bHLH and PAS domains. Whereas HIF-1 $\alpha$  and HIF-2 $\alpha$  contain ODDs, NTADs and CTADs, HIF-3 $\alpha$  only contains a NTAD. Percentages of identity between HIF-3 $\alpha$  and HIF-1 $\alpha$  or HIF-2 $\alpha$  are indicated. bHLH: basic helix-loop-helix domain, PAS: Per-Arnt-Sim homology domain, ODD: oxygen dependent degradation domain, NTAD/CTAD: N- and C-terminal transactivation domain (adapted from Lisy and Peet 2008).

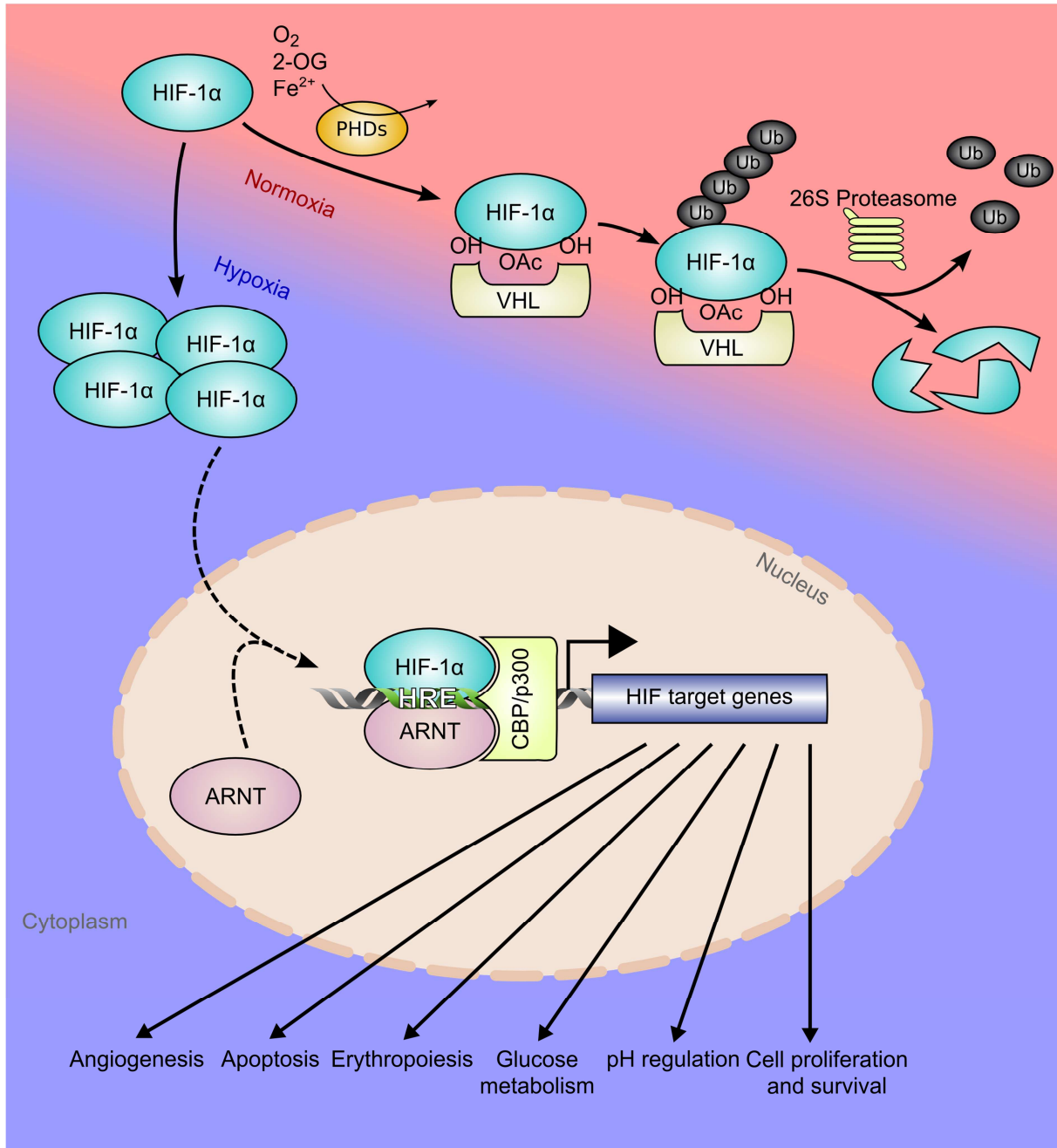


**Figure 7: Regulation of HIF-1 activity by degradation or stabilization of the alpha-subunit HIF-1 $\alpha$ .**

Under normoxic conditions, the HIF-1 $\alpha$  gets hydroxylated by prolyl hydroxylases (PHDs) using O<sub>2</sub>, 2-Oxoglutarate and Fe<sup>2+</sup> as cofactors. Tagged HIF-1 $\alpha$  is recognized and complexed by von Hippel-Lindau protein (VHL), a subunit of E3 ubiquitin ligase, and subsequently marked for proteasomal degradation. Thus HIF-1 $\alpha$  is inactive under normoxic conditions. However, under hypoxia, activity of PHDs is abrogated causing an accumulation of HIF-1 $\alpha$  subunits in the cytoplasm. After translocation to the nucleus, HIF-1 $\alpha$  interacts with the ubiquitous ARNT and binds as a heterodimer to HIF response elements (HRE) present in the regulatory regions of HIF targets. By recruiting the cofactor CBP/p300, transcriptional induction of target genes involved in different processes is triggered.

### 1.2.1 ARNT

The ubiquitously expressed  $\beta$ -subunit ARNT was initially described as the activating ligand-bound aryl hydrogen receptor (AhR) (Reyes et al. 1992). The AhR/ARNT complex is activating genes upon the stimulation by aromatic hydrocarbons, which explains the name. In addition, ARNT is also known to be the major interaction partner of HIF-1 $\alpha$  and is therefore also known as HIF-1 $\beta$ . Although ARNT has been suggested to function as a homodimer (Sogawa et al. 1995), the biological relevance of this complex remains unclear.

ARNT contains two major domains, namely bHLH and PAS domains for both heterodimerization and binding to the target DNA. Hence ARNT is crucial for the formation of a functional heterodimeric transcription factor. Several studies suggest that apart from ARNT its orthologues ARNT2 and ARNT3 can act as  $\beta$ -class HIF subunits (Wang et al. 1995; Hirose et al. 1996; Hogenesch et al. 1997). However, as ARNT is described as the predominant  $\beta$ -subunit in HIF-1 and HIF-2 due to its ubiquitous expression over the restricted expression of ARNT2 and ARNT3 in the central nervous system (Crews 2003), this work focuses on ARNT and its role in the response to hypoxia.

### 1.2.2 HIF-1 $\alpha$

The hypoxia inducible  $\alpha$ -subunit HIF-1 $\alpha$  (Hypoxia-inducible factor 1-alpha) was initially described by Wang and Semenza, identified by affinity purification using oligonucleotides from the 3'-UTR of the human erythropoietin gene *EPO* (Wang and Semenza 1993). With physiological levels of oxygen present (normoxia), the constantly translated HIF-1 $\alpha$  proteins are degraded *via* the 26S proteasome with half-life of less than 5 minutes (Huang et al. 1996; Yu et al. 1998). The underlying mechanism is based on hydroxylation of Pro<sup>402</sup> or Pro<sup>564</sup>, or both, by the prolyl hydroxylase domain proteins (PHD1-3) for which they use molecular oxygen as a substrate and  $\alpha$ -ketoglutarate as a cosubstrate (Marxsen et al. 2004). The hydroxylation of proline residues located in the ODD (oxygen dependent degradation domain) of HIF-1 $\alpha$  enables the interaction with the von Hippel-Lindau (pVHL) protein, which is a component of an E3 multiprotein ubiquitin-ligase complex (Jaakkola et al. 2001). The subsequent

polyubiquitination of HIF-1 $\alpha$  triggers its degradation. Using the same set of substrates, a third residue (N<sup>803</sup>) gets hydroxylated by factor inhibiting HIF-1 (FIH-1). In contrast to the hydroxylation of proline residues, the hydroxylation of the asparagine residue inhibits the binding of coactivators such as p300 and its parologue CREB-binding protein (CBP), histone acetyltransferases, which act as a cofactor in the transactivation of target genes (Ruas et al. 2002). Both, degradation as well as preventing the interaction with cofactors tightly controls HIF-1 $\alpha$  and therefore the activity of HIF-1 under normoxia (Figure 7). However, when oxygen availability drops, hydroxylation of all three mentioned residues is attenuated, contributing to an accumulation of HIF-1 $\alpha$  subunits which translocate to the nucleus due to its potential nuclear localization signal (NLS) located at positions 718-721. Subsequently, HIF-1 $\alpha$  and the obligate nuclear located ARNT dimerize via the N-terminal bHLH and PAS domains of each subunit. This heterodimeric complex binds to DNA sequences with the canonical motif 5'-RCGTG-3', so called HIF response elements (HREs), located in the promoter or enhancer of the respective target genes (Figure 8) (Wang and Semenza 1993; Semenza 1999; Kaelin and Ratcliffe 2008).

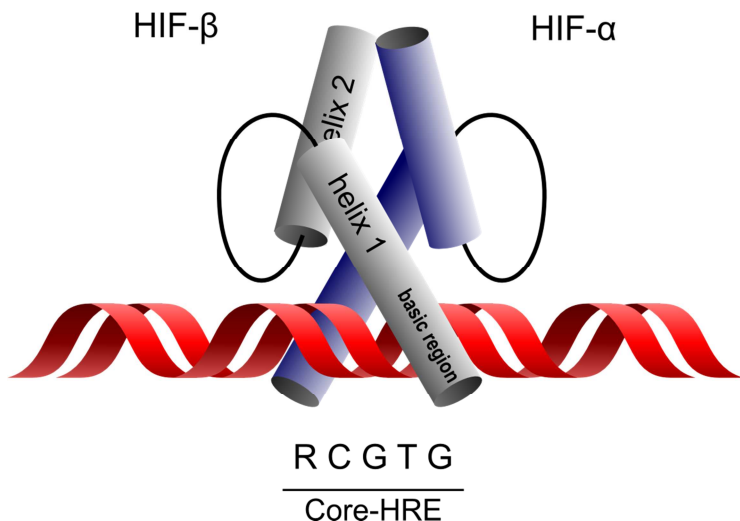


**Figure 8: Representation of the bHLH domain of HIF- α/β heterodimer contacting DNA containing HRE consensus motif.**

Cylinders represent helix domains that are connected by a loop. The basic residues near the N-terminus of each subunit contact the nucleotides of the core-HRE (adapted from Lisy and Peet 2008).

The recruitment and interaction with CBP/p300 occurs *via* the TAD domain of the HIF complex. This cofactor exerts intrinsic histone acetyl transferase activity, thus changing the chromatin structure and subsequently recruiting basal transcription machinery. Eventually, the initiation of transcription of genes whose products are involved in triggering - amongst other processes - erythropoiesis, glycolysis and angiogenesis takes place (Kaelin and Ratcliffe 2008; Semenza 2009) (Figure 7).

The expression of HIF-1 $\alpha$  is described as ubiquitous, with HIF-1 $\alpha$ /ARNT dimers being the primary factors regulating the hypoxic response (Ke and Costa 2006). However, recent studies indicate, that HIF-1 $\alpha$  exerts its uniqueness in hypoxic response rather by target gene specificity than by tissue or cell selective expression (Hu et al. 2003; Warnecke et al. 2004). HIF-1 $\alpha$  regulates a variety of genes, amongst them *PGK1*, *CA9* and *EGLN3*. The *PGK1* encoded protein phosphoglycerate kinase 1 catalyzes the production of 3-phosphoglycerate from 1,3-bisphosphoglycerate during glycolysis (Hu et al. 2003), while CA-IX, encoded by the gene *CA9* (Grabmaier et al. 2004) is a major factor in controlling pH homeostasis. *EGLN3* encodes for PHD3 thereby enabling an negative feedback loop in the HIF-1 activation (Marxsen et al. 2004). HIF-1 $\alpha$  was shown to be important not only in cellular homeostasis but also in development. Homozygous *Hif1a* knockout mice die at day E10.5 with vascular defects and cardiac malfunction (Kotch et al. 1999), underlining the significance of HIF-1 $\alpha$  as a component in hypoxic conditions like vascular diseases and cancer. The protein abundance of HIF-1 $\alpha$  protein under hypoxic condition is also contributing to its function. Several studies suggest an immediate accumulation within a few minutes after the onset of hypoxia, with decay after several hours (Jewell et al. 2001; Holmquist-Mengelbier et al. 2006). This data provides evidence for HIF-1 $\alpha$  being involved in the fast response to hypoxia (meaning several minutes to few hours) and dealing with the acute effects of it (Holmquist-Mengelbier et al. 2006).

### 1.2.3 HIF-2 $\alpha$

HIF-2 $\alpha$  was identified in 1997 by several independent groups (initially called endothelial PAS protein 1 (EPAS1) (Tian et al. 1997), HIF-related factor (HRF) (Flamme et al. 1997), HIF1 $\alpha$ -like factor (HLF) (Ema et al. 1997), and member of PAS family 2

(MOP2) (Hogenesch et al. 1997). The description of HIF-2 $\alpha$  extended the complexity of the HIF response. Hypoxia inducible factor 2 (HIF-2) consists, similarly to HIF-1, of the  $\beta$ -subunit ARNT and HIF-2 $\alpha$ , a parologue of HIF-1 $\alpha$ . The regulation of its activity was shown to be comparable to that of HIF-1 $\alpha$ , namely by destabilization of the  $\alpha$ -subunit HIF-2 $\alpha$  by 26S proteasome. The residues which get hydroxylated are P<sup>405</sup>, P<sup>531</sup> and N<sup>847</sup>. Although it was shown, that HIF-1 $\alpha$  protein levels are detectable in a huge variety of cells (hepatocytes, macrophages muscle cells (Wiesener et al. 2003)), the overall expression on tissue level is nevertheless maximal in blood vessels and therefore in highly vascularized organs like lung or placenta.

While HIF-1 $\alpha$  is ubiquitously expressed, HIF-2 $\alpha$  is detected most prominently in hypoxic vascular endothelial cells during embryonic development (Tian et al. 1997; Hu et al. 2003). In addition to being present in endothelial cells, murine *Hif2a* mRNA has also been detected postnatally in different rat tissues, amongst them kidney fibroblasts, liver hepatocytes and heart myocytes (Wiesener et al. 2003; Hu et al. 2003). In contrast to *in vivo* restricted expression patterns, quite a few transformed human cell lines exhibit HIF-2 $\alpha$  expression, amongst them HEK293, HeLa, HepG2, and Hep3B (Wiesener et al. 1998; Hu et al. 2003). Moreover, HIF-2 $\alpha$  has been shown to be expressed in perinecrotic areas as well as vascular cell lines like HUVEC and HMEC-1 (Onita et al. 2002; Hu et al. 2003). These data indicate that HIF-2 might play an important role in a broad range of cells in addition to endothelial cells as well as in tumorigenesis.

HIF-2 is known to regulate the expression of kinase insert domain receptor (*KDR*) (Elvert et al. 2003), and cadherin 5, type 2 (*CDH5*) (Le Bras et al. 2007), which suggests an important role for HIF-2 in angiogenesis. Besides, other described target genes of HIF-2 $\alpha$  are *CCND1* (Cyclin D1) and *POU5F1* (POU class 5 homeobox 1) (Raval et al. 2005; Covello et al. 2006) as well as *CD82* (CD82 molecule) and *PAI1* (plasminogen activator inhibitor 1) (Hu et al. 2007; Nagao and Oka 2011).

In contrast to HIF-1 $\alpha$ , HIF-2 $\alpha$  protein is reported to be induced more slowly, meaning in the range of several hours to a few days (Holmquist et al. 2005). Concomitantly, its presence under hypoxia is prolonged with protein levels detectable even after several days (Holmquist-Mengelbier et al. 2006). Thus, HIF-2 $\alpha$  is rather involved on the long-

term regulation of cellular homeostasis under hypoxic condition (Koh and Powis 2012).

HIF-1 and HIF-2 are closely related, especially when it comes to their preferential binding partner ARNT, the regulation of their activity, and their mechanism in activating HRE dependent gene expression (Loboda et al. 2010). However, HIF-1 and HIF-2 seem to be non-redundant as shown by studies with knockout mice and differ both in their expression pattern on tissue level and their prevalent target genes. In addition, several functional studies suggest distinct roles for HIF-1 $\alpha$  and HIF-2 $\alpha$  during development and tumor progression. Whereas Covello et al. observed an increase in size and proliferation of teratomas in *Hif2a* knock-in mice, another group described a reciprocal interaction between HIF-1 $\alpha$  and HIF-2 $\alpha$  levels in RCC4 cell line suggesting retarding and promoting functions, respectively (Covello et al. 2005; Raval et al. 2005). Yet, there are a vast number of hypoxia inducible genes which are described to be regulated by both HIF-1 $\alpha$  and HIF-2 $\alpha$ , amongst them *VEGFA* (vascular endothelial growth factor A) and *GLUT1* (glucose transporter 1) (Hu et al. 2006). The underlying mechanism of target genes specificity is still not fully understood, with different properties regarding DNA binding or transactivation being discussed. By replacing the NTAD of HIF-2 $\alpha$  with that of HIF-1 $\alpha$ , Hu et al. (2007) could show that the N-terminal transactivation domain confers target gene specificity of HIF-1 $\alpha$  and HIF-2 $\alpha$ . It is worth to mention, that apart from hypoxia, several stimuli are described to induce HIF-1 $\alpha$  and HIF-2 $\alpha$  activity, amongst them iron chelators and divalent cations like Co<sup>2+</sup> (Woo et al. 2006).

#### 1.2.4 HIF target genes

The distinct assignment of hypoxia regulated genes to either HIF-1 or HIF-2 is a complex issue, as factors like cell type or tissue as well as duration and intensity of hypoxia contribute to which gene gets activated at a defined time point. Currently, many of the known HIF target genes are regarded as general target genes, like *GLUT1*, *CA12* and *VEGFA* (Keith et al. 2012). Whereas the group of genes which are published to be selectively activated by HIF-1 is comparably huge, only a small subset of them are described to be specifically induced by HIF-2. Interestingly, Stiehl

et al. suggested that the HIF- $\alpha$  isoforms determine target gene kinetics rather than specificity (2011). Nevertheless, so far reported unique HIF-1 target genes comprise *GAPDH* (Denko 2008) and *PGK1* (Hu et al. 2003) whose protein counterparts are involved in glycolysis as well as *EGLN3* (encodes for the prolyl hydroxylase PHD3) (Stiehl et al. 2011), whereas the identification of unique HIF-2 target genes brought up only few candidates, amongst them *POU5F1* (encodes for Oct4, which is involved in the self-renewal of undifferentiated embryonic stem cells) (Covello et al. 2006), *CD82* (its protein is a membrane glycoprotein) (Nagao and Oka 2011) and *PAI1* (Hu et al. 2007). Whereas the alleged HIF-1 $\alpha$  target genes are often involved in the immediate metabolic response (e.g. upregulation of glycolytic enzymes), some of the supposed HIF-2 $\alpha$  unique genes are reported to be critical in the long term adaptation, like in the case of *PAI1* in the regulation of angiogenesis. In general, the ability of HIF-1 and HIF-2 to activate specific target genes appears to be context dependent and therefore each target gene must be carefully defined in terms of HIF-1 and HIF-2 responsiveness when examined within a specific context (Koh and Powis 2012).

### 1.2.5 HIF-3 $\alpha$

The third member of the HIF-alpha family HIF-3 $\alpha$  was initially described by the report of the murine *Hif3a* locus based on sequence similarity of EST (expressed sequence tags) with known HIF alpha subunits (Gu et al. 1998). Concomitantly, Gu et al. mapped the human *HIF3A* gene locus on chromosome 19 and verified its alpha subunit properties together with ARNT in a successful gel shift assay on HRE containing probes. Cloning and sequencing of rat *Hif3a* mRNA from cultured rat hepatocytes by Kietzmann et al. (2001) led to a more profound knowledge about domain architecture (35% identity with murine HIF-1 $\alpha$ ), transactivation (activation of episomal reporter constructs in rat hepatocytes) and localization (*Hif3a* predominantly occurs in the perivenous zone of the hepatic acinus and in endothelial cells of the central vein). Later on, Makino et al. described a splice variant of *Hif3a* in mice called inhibitory PAS domain protein (*Ipas*), giving rise to the N-terminal part of full length HIF-3 $\alpha$  containing only the bHLH-PAS domains. The protein IPAS was reported to exert an inhibitory effect on HIF-1, thereby abolishing hypoxia-induced *Vegfa* expression in

murine cornea (Makino et al. 2001). This report was the starting point for a still ongoing controversial discussion about the corresponding human HIF-3 $\alpha$ , its regulation, and function including underlying mechanism. Subsequently, it was reported that also human HIF-3 $\alpha$  suppresses HIF-mediated gene expression, however only *in vitro* (Hara et al. 2001). Characterization of the human *HIF3A* locus showed, similar to the mouse locus, several splice variants (Maynard et al. 2003; Pasanen et al. 2010) (Figure 9). However, neither of its encoded proteins showed structural similarity to IPAS, although HIF-3 $\alpha$ 1 (RefSeq accession number: NM\_152794) and HIF-3 $\alpha$ BC (RefSeq accession number: BC\_026308) were shown to have inhibitory effects on HIF driven gene assays (Hara et al. 2001; Maynard et al. 2005; Maynard et al. 2007; Heikkilä et al. 2011). With ARNT in excess, HIF-3 $\alpha$  was proposed to be a weak transcription factor (Hara et al. 2001; Heikkilä et al. 2011). Nevertheless, a role of HIF-3 $\alpha$  as a suppressor of HIF-mediated gene expression was favored by numerous studies (Hara et al. 2001; Maynard et al. 2005; Maynard et al. 2007; Augstein et al. 2011; Heikkilä et al. 2011). The suggested underlying mechanism for HIF-3 $\alpha$  inhibiting the classical HIF system is based on the observation of an interaction with the respective HIF-alpha subunit. However, the interaction was only observed with both interaction partners, HIF-3 $\alpha$  and HIF-1 $\alpha$  or HIF-2 $\alpha$  overexpressed in different cell lines (Maynard et al. 2003; Maynard et al. 2005; Jang et al. 2005; Heikkilä et al. 2011). Similarly, the interaction of HIF-3 $\alpha$  with ARNT was described by different groups (Maynard et al. 2005; Heikkilä et al. 2011). Yet, the favored approach for the inhibitory role of HIF-3 $\alpha$  is a competition with the respective alpha subunit.

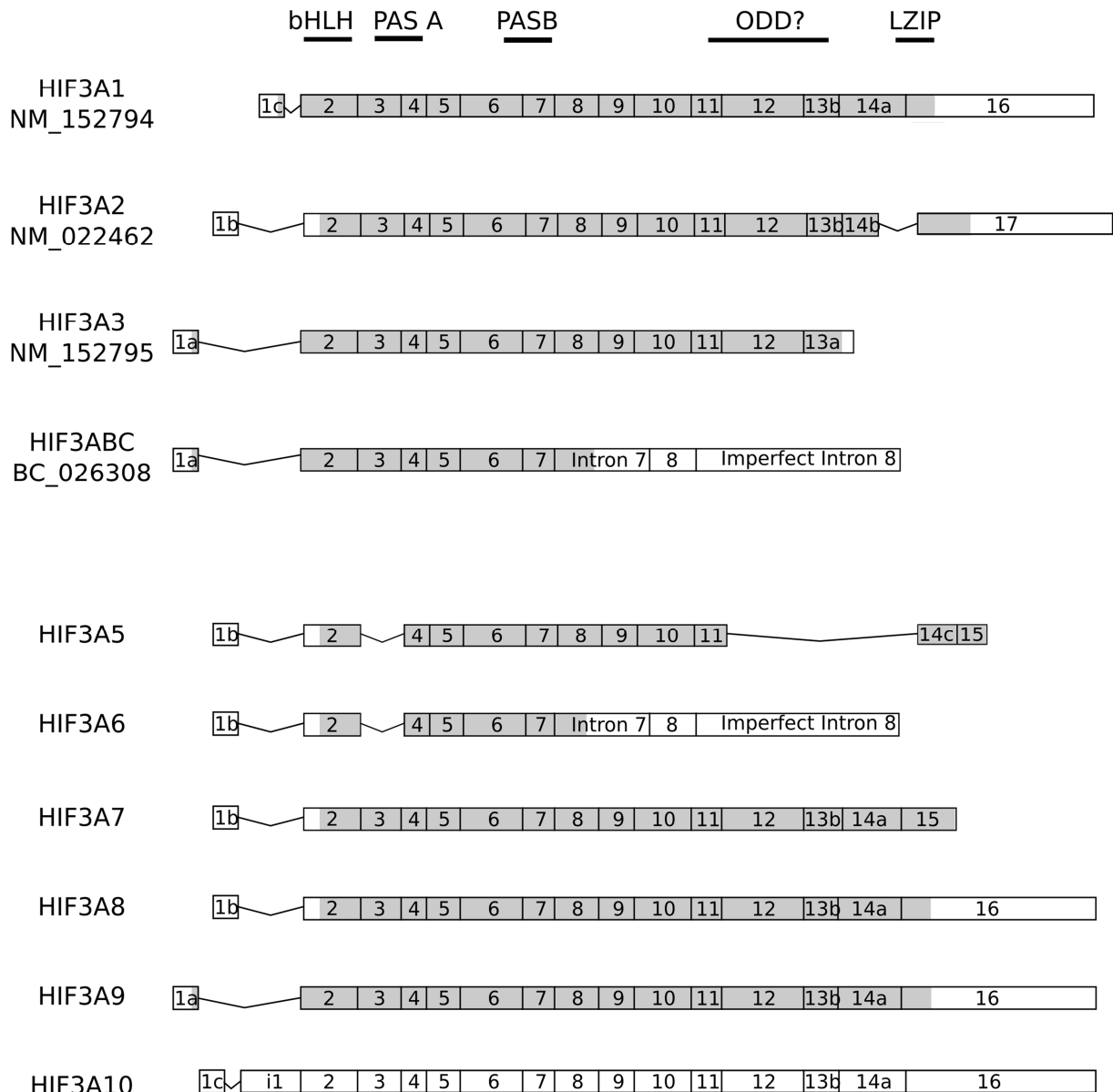


**Figure 9: Schematic representation of exonic arrangement of suggested human HIF-3 $\alpha$  variants.**

This scheme represents the arrangement of exons of the so far published *HIF3A* isoforms. Areas coding for distinct domains are indicated in the upmost position. Coding regions are indicated in grey (adapted from Pasanen et al. 2010).

The role of the human HIF-3 $\alpha$  is also determined by the specific expression of HIF-3 $\alpha$  in different tissues and cell types. Whereas the usage of different antibodies against the murine HIF-3 $\alpha$  was reported (Makino et al. 2001), the unambiguous detection of any of the published variants of human HIF-3 $\alpha$  on endogenous level has not yet been shown. Of note, Maynard et al. report that HIF-3 $\alpha$  protein gets degraded by hypoxia

*in vitro* by binding to pVHL through proline residue at position 490, analogue to HIF-1 $\alpha$  and HIF-2 $\alpha$  (2003). However, the presence of an ODD and thus the regulation of endogenous HIF-3 $\alpha$  protein by oxygen is still controversially discussed, as endogenous HIF-3 $\alpha$  protein was so far not identified free of doubt. Thus, the detection of human *HIF3A* mRNA evolved as an index for the presence of its protein counterpart HIF-3 $\alpha$ . On this basis, Maynard et al. proposed *HIF3A* to be majorly expressed in heart, placenta and lung, as shown by multiple tissue northern blot (2003). These findings were extended by Pasanen et al. showing an expression also in fetal organs like liver and kidney (2010). The suggested expression patterns of *HIF3A* are linked with *HIF3A* being detected majorly in endothelial cells and vascular smooth muscle cells, as shown by Augstein et al., who also confirmed the absence of *HIF3A* in blood (2011).

Another criterion that indicates the functional properties is the kinetics of HIF-3 $\alpha$  upon hypoxic stimulation. Again, due to missing reliable antibodies, current knowledge about endogenous HIF-3 $\alpha$  is mainly restricted to its regulation on transcriptional level. In contrast to *HIF1A* and *HIF2A*, *HIF3A* was suggested to be upregulated under sustained hypoxia (Pasanen et al. 2010; Augstein et al. 2011), which qualifies it as a component in the adaptation to hypoxia. However, suggested HIF target genes that are modulated by *HIF3A* are so far rather elusive, especially as only few of them are characterized on endogenous level.

In general, the HIF-system (maybe including HIF-3 $\alpha$ ) is not only known to trigger the already mentioned erythropoiesis under hypoxia but is also involved in the process of angiogenesis.

### **1.3 Angiogenesis**

The distribution of gases, liquids and nutrients in vertebrates is achieved by the network of blood vessels, contributing to homeostasis in the organism. The proper formation of this network is vital in growth and development and is achieved by sprouting and branching of capillaries. Thereby new blood vessels are formed from preexisting blood vessels. This procedure named sprouting angiogenesis is closely

connected with hypoxia and comprises different biological processes like cell proliferation, migration and differentiation, including remodeling.

### 1.3.1 Endothelial cells

Endothelial cells are key components of the angiogenic system, lining the interior surface of the vasculature. The starting point in the formation of new vessels are growth factors that activate its respective receptors in preexisting endothelial cells. The predominant angiogenic signal is VEGF-A, which can be secreted by many types of cells, but usually not endothelial cells themselves (McIlhenny et al. 2002). The paracrine stimulation leads to proliferation of selected endothelial cells, called tip cells. Concomitantly, the sprouting cells acquire invasive properties and secrete highly efficient plasminogen activators in order to locally degrade the basement membrane (Figure 10). To tightly control this process, their physiological inhibitor PAI-1, a serine protease inhibitor, is secreted in parallel. PAI-1 is involved in remodelling of the extracellular matrix, fibrinolysis, proliferation and angiogenesis (Bajou et al. 1998; Diebold et al. 2008).

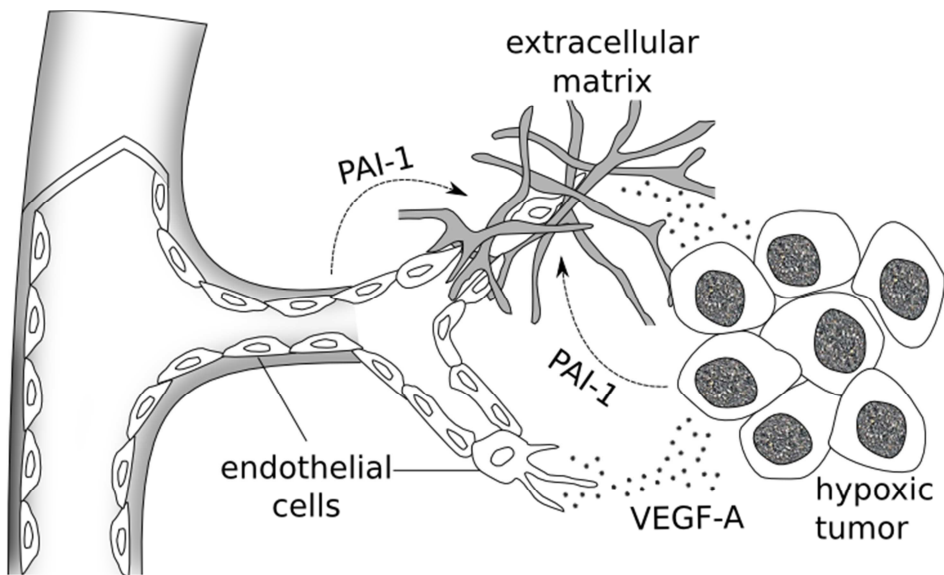


**Figure 10: Schematic representation of sprouting angiogenesis.**

The emergence of new blood vessels in response to a hypoxic area is schematically shown. Hypoxic cells do secrete VEGF-A in order to stimulate sprouting of migrating endothelial cells. The latter one as well as hypoxic cells secrete PAI-1 leading to a remodeling of the extracellular matrix thus further supporting the angiogenic process. Figure modified and adapted from Dorsam and Gutkind 2007; ten Dijke and Arthur 2007).

Apart from inhibiting the ECM degradation, PAI-1 is suggested to also exert proangiogenic properties by modulating cell migration. However, the exact mechanisms how PAI-1 can modulate vascular function are not fully understood (Diebold et al. 2008). Subsequent to ECM degradation, activated endothelial cells proliferate into the extracellular matrix and form sprouts that extend in the direction of the stimulus.

### 1.3.2 Angiogenesis in physiology and pathophysiology

The above-described angiogenesis is a process that occurs both in physiological and pathophysiological conditions. The truly initial phase of life, the development of the embryo, is also the beginning of vascular network formation, which starts by vasculogenesis followed by angiogenesis to expand the preexisting blood vessels (Marcelo et al. 2013). Notably, the vasculature continues to remodel dynamically even as the organs function. But also in adults, physiological angiogenesis occurs during wound healing, skeletal growth, the menstrual cycle, and pregnancy (Hoeben et al. 2004).

The physiological control of angiogenesis is achieved by a tight balance between factors that induce the formation of blood vessels and those that inhibit the process. When this balance is disturbed, it can result in pathological angiogenesis which causes increased blood-vessel formation in diseases that depend on angiogenesis, amongst them arthritis, psoriasis and most notably tumorigenesis (Hoeben et al. 2004). The transition of benign tumors to malignant ones is characterized by uncontrolled angiogenesis (Hanahan and Weinberg 2000).

It is worth to mention, that a major difference between physiological and pathophysiological angiogenesis is the state of vessel maturity, i.e. vascular perfusion will not be achieved in case of disease (Krock et al. 2011; Fakhrejahani and Toi 2012).

### 1.3.3 Cancer and its hallmarks

Induction of uncontrolled angiogenesis is one of the hallmarks of solid malignant tumors. Together with sustaining proliferative signaling, evading growth suppressors, resisting cell death, enabling replicative immortality, and activating invasion and metastasis, its one of the inevitable acquired properties of cancer (Hanahan and Weinberg 2000). The ability of triggering angiogenesis is closely linked to the hypoxic microenvironment, which occurs in the core solid tumors that are beyond the size of 2-3 mm in diameter (Ribatti 2008). This is the critical distance when diffusion of oxygen is limited and active transport of nutrients and gases is essential for cell survival (Hoeben et al. 2004). Thus, hypoxic areas in solid tumors do promote tumor progression *via* triggering angiogenesis, mainly by secretion of VEGF-A.

Cancers are caused by both internal factors (such as inherited mutations, hormones, and immune conditions) and environmental/acquired factors (such as tobacco, diet, radiation, and infectious organisms) (Anand et al. 2008). The onset of cancer however is characterized by a transformation of a normal cell into a tumor cell, which is the effect of genetic alterations (Sarkar et al. 2013). Affected genes can be separated in oncogenes, which promote proliferation of cells, and tumor suppressor genes, which inhibit cell division (Sarkar et al. 2013). The transformation of a normal into a tumor cell usually requires several changes allowing the cell to escape the controls that limit normal tissue growth (Fearon and Vogelstein 1990).

### 1.3.4 Epigenetics

In addition, also epigenetical alterations are reported to drive cancer (Jones and Baylin 2002; Sarkar et al. 2013). These changes are not directly linked to the plain nucleotide sequence level but rather above (epi- (ancient Greek): over, outside of, around). Thus, loss or gain of function is not necessarily linked to aberrant DNA sequence but is determined by epigenetical mechanisms (Baylin and Ohm 2006).

Concretely, epigenetic mechanisms comprise in the first instance DNA and histone modifications (e.g. methylation or acetylation). Methylated cytosines in CpG sites are considered as the fifth base and are associated with repressed transcriptional activity by recruitment of chromatin remodeling factors (Leonhardt and Cardoso 2000). Interestingly, recent studies reported several on-top-modifications, namely 5-hydroxymethylcytosine (hmC), 5-formylcytosine (fC) and 5-carboxylcytosine (caC). These modifications are catalyzed by the TET protein family through oxidation of methylcytosine. Interestingly, these TET proteins are Fe(II)- and 2-oxoglutarate dependent (Dickson et al. 2013) thus showing a remarkable overlap with PHDs regulating the stability of HIF-1 $\alpha$  and HIF-2 $\alpha$ . It is suggested that TET proteins prompt the demethylation of CpG sites (Spruijt et al. 2013; Müller et al. 2014). Modifications of histones are completing the classical understanding of epigenetic mechanisms. Histones were considered for a long time as inert packing material for eukaryotic nuclear DNA, when Turner described their regulating properties. Later on, their detailed function were specified (Turner 1998; Rea et al. 2000; Chi et al. 2010). Although it is accepted, that modifications of histone tails alter the interaction of DNA and histones and thereby the chromatin structure, the exact mechanism is still vague. Yet, there are some distinct changes, which are well described. One of the best-described modifications is the methylation of lysine 9 of histone 3. While mono-methylation of this residue is found in actively transcribed promoters, its triple methylation is connected with repression of transcription (Strahl and Allis 2000; Rea et al. 2000). The second modification that is extensively studied is acetylation, particularly that of lysine 9 and 14 of histone 3. These modified residues are explicitly associated with an active transcription of the respective gene (Turner 1998; Strahl and Allis 2000).

It is becoming increasingly apparent that epigenetics also plays a crucial role in the cellular response to hypoxia (Watson et al 2010). Amongst other effects, hypoxia provokes a decrease of general transcription that seems to rely in part on epigenetic changes (Perez-Perri et al 2011). In this process, epigenetic regulation may work hand in hand with the HIF family or may contribute to the maintenance of a hypoxia-adapted cellular phenotype after HIF has initiated the immediate response pathways (Watson et al 2010). In this study, we sought to investigate the role of the youngest member of the human HIF protein family HIF-3 $\alpha$  in the response to hypoxia by characterization of its expression as well as its functional properties.

## 2 Aims of this study

Hypoxia is an important trigger of development but is also known to contribute to the malignancy of tumors besides others by activation of uncontrolled angiogenesis. This is mainly based on the transactivation properties of HIF-1 and HIF-2.

Whereas in mice the description of the *Hif3a* isoform Ipas apparently is linked with an inhibitory characteristic (Makino et al. 2001; Yamashita et al. 2008), an unambiguous role of *HIF3A* in human has yet to be identified.

Hence, this study sought to deal with the following issues:

1. Analyse the expression pattern of human *HIF3A* transcript variants in different human cell types.

Differential expression of *HIF3A* has been reported not only on tissue levels, but also in several cell lines. Whereas transcripts of *HIF3A* were detected in the endothelial cell line HUVEC and human neuroblastoma cell line Kelly, they were absent in other cells like the cervical cancer cell line HeLa or the breast cancer cell line MCF7. We hypothesized, that the basal expression levels of *HIF3A* are differing due to epigenetic regulation in different cell lines.

2. Analyse the mechanisms of *HIF3A* function under hypoxia.

HIF-2 $\alpha$  was initially described in endothelial cells and, in contrast to HIF-1 $\alpha$ , shown to be sustained even after long term hypoxia. In line, we hypothesized, that HIF-3 $\alpha$  may exert an inhibitory function on HIF-2 $\alpha$  and its target genes in sustained hypoxia.

### 3 Materials and Methods

#### 3.1 Materials

##### 3.1.1 Cell-lines

Cell lines HEK293T, HeLa and MCF7 were obtained from Leibniz Institute DSMZ-German Collection of Microorganisms and Cell Cultures, Braunschweig, Germany. Cell line HMEC-1 was purchased from the Center for Disease Control CDC, Atlanta, USA. Cell line PASMC was purchased from Lonza, Basel, Switzerland. Cell lines LNCaP and DU145 were a kind gift of Dr. Thomas Schwend. Preadipocyte cell line was a kind gift of Dr. Isabelle Mack.

**Table 1: Cell lines used in this study.**

Name	Reference number	Derived from	morphology	Ref
<b>HEK293T</b>	ATCC CRL-11268	Human embryonic kidney	Monolayer, epithelial-like	(Graham et al. 1977)
<b>HMEC-1</b>	CDC E036-91/0	Human microvascular endothelium	Cobblestone-like	(Ades et al. 1992)
<b>HeLa</b>	ATCC CCL-2	Human cervix adenocarcinoma	Monolayer, epithelial	(Gey and Bang 1951)
<b>MCF7</b>	ATCC HTB-22	metastatic site of human mammary gland	Monolayer, epithelial	(Russo et al. 1976)
<b>PASMC</b>	CC-2581 (Lonza)	Human pulmonary artery	Monolayer	
<b>SGBS (preadipocytes)</b>	Not given	patients with Simpson-Golabi-Behmel syndrome	monolayer	(Wabitsch et al. 2001)
<b>LNCaP</b>	ATCC CRL-1740	Prostate; derived from metastatic site of lymph node	adherent, single cells and loosely attached clusters	(Horoszewicz et al. 1980)
<b>DU145</b>	ATCC® HTB-81	prostate; derived from metastatic site in brain	Monolayer, adherent	(Stone et al. 1978)

### 3.1.2 Instruments

**Table 2: Instruments used in this study.**

Device	Product name	Manufacturer, City, Country
<b>Analytical balance</b>	BP 211D	Sartorius, Goettingen, Germany
<b>Autoclave</b>	KSG-116-2-ED	KSG, Erlangen, Germany
<b>Balance</b>	LP5200P	Sartorius, Goettingen, Germany
<b>Bunsen burner</b>	Vulcan	Heraeus, Hanau, Germany
<b>Centrifuges</b>	Biofuge fresco	Heraeus, Hanau, Germany
	Biofuge pico	Heraeus, Hanau, Germany
	Biofuge stratos	Heraeus, Hanau, Germany
	MegaFuge 1.0R	Heraeus, Hanau, Germany
	Varifuge 3.0R	Heraeus, Hanau, Germany
<b>Deep-freezer (-70°)</b>	Hera freeze	Heraeus, Hanau, Germany
<b>Fluorescence microscope</b>	IX50	Olympus, Tokio, Japan
	Hg-Lamp U-RFL-T	Olympus, Tokio, Japan
	Camera Controller	Hamamatsu Photonics, Hamamatsu, Japan
	Filtermodule improvisation Orbit	PerkinElmer, Waltham, USA
	Hg-Lamp U-RFL-T	Olympus, Tokio, Japan
<b>Liquid-N<sub>2</sub>-Dewar</b>	Locator 6 Plus	Thermolyne, Dubuque, USA
<b>Freezer</b>	comfort	Liebherr, Bulle, Switzerland
<b>Fridge</b>	profi line	Liebherr, Bulle, Switzerland
<b>Fridge</b>	Premium	Liebherr, Bulle, Switzerland
<b>Fridge-freezer</b>		Liebherr, Bulle, Switzerland
<b>Gel documentation system</b>	Gel Doc 2000	Bio-Rad, Munich, Germany
<b>Heating block</b>	Thermomixer comfort	Eppendorf, Hamburg, Germany
<b>Heating plate</b>	CM1850	Leica, Solms, Germany
<b>Hypoxia workstation</b>	InVIVO400	Ruskinn Technology, Bridgend, South Wales
<b>Incubator</b>	Hera Cell	Heraeus, Hanau, Germany
<b>Incubator</b>	CB 210	Binder, Tuttlingen, Germany
<b>Isopropanol freezing box</b>		
<b>Laboratory dishwasher</b>	G7783CD Mielabor	Miele, Guetersloh, Germany
<b>Laminar airflow cabinet</b>	Hera Safe	Heraeus, Hanau, Germany
<b>Luminometer</b>	AutoLumat plus	Berthold Technologies, Bad Wildbad, Germany

Device	Product name	Manufacturer, City, Country
<b>Magnetic stirrer + heater</b>	MR3001	Heidolph, Schwabach, Germany
<b>Magnetic stirrer without heater</b>	MR3000	Heidolph, Schwabach, Germany
<b>Microscope</b>	Axiovert 25	Zeiss, Oberkochen, Germany
<b>Microwave</b>		Whirlpool, Stuttgart, Germany
<b>Millipore water supply</b>	Milli-Q synthesis	Millipore, Darmstadt, Germany
<b>Mini-table-top-centrifuge</b>	Capsulefuge PMC-060	Tomtech, Carson, USA
<b>pH Meter</b>	pH 540 GLP	WTW, Weilheim, Germany
<b>Photometer</b>	NanoDrop 2000c	Thermo Fisher Scientific, Waltham, USA
<b>Platereader</b>	Safire	Tecan, Maennedorf, Switzerland
<b>Power supplies</b>	Power Pac 200	Bio-Rad, Munich, Germany
	Power PAC 300	Bio-Rad, Munich, Germany
	Power Pac 3000	Bio-Rad, Munich, Germany
<b>Pump</b>	CVC 2000	Vacuubrand, Wertheim, Germany
<b>Roller mixer</b>	RM5 Assistent	Karl Hecht, Sondheim / Rhoen, Germany
<b>Rotator</b>		Froebel Labortechnik, Lindau, Germany
<b>Electrophoresis system</b>	Mini-Protean 3	Bio-Rad, Munich, Germany
<b>Shaker</b>	Duomax 1030	Heidolph, Schwabach, Germany
	IKA-Schüttler MTS2 electronic	IKA-Werke, Staufen, Germany
	Polymax 1040	Heidolph, Schwabach, Germany
<b>Shaker-incubator</b>	C24 Incubator Shaker	Eppendorf, Enfield, USA
<b>Standdewar</b>		KGW Isotherm, Karlsruhe, Germany
<b>Thermocycler</b>	PCR System 9700	PE Applied Biosystems, Foster City, USA
<b>Thermocycler</b>	Rotor-Gene 6000	Corbett Life Sciences, Sydney, Australia
<b>UV-Stratalinker</b>	Stratalinker 1800	Stratagene, La Jolla , USA
<b>Vortexer</b>	Reax top	Heidolph, Schwabach, Germany
<b>Water bath</b>	SUB Aqua Plus	Grant Instruments, Cambridge, UK
<b>Imaging system</b>	Typhoon Trio	GE Healthcare, Buckinghamshire, UK
<b>Water bath</b>	unknown	Memmert, Schwabach, Germany

### 3.1.3 Consumables

**Table 3: Consumables used in this study.**

Item	Supplier, City, Country
<b>T25, T75 and T150 flasks</b>	Greiner Bio-One, Kremsmuenster, Austria
<b>10 and 6 cm dishes</b>	Sarstedt, Nuembrecht, Germany
<b>6-, 24- and 96-well plates</b>	Greiner Bio-One, Kremsmuenster, Austria
<b>2, 5, 10 and 25 ml pipettes</b>	Sarstedt, Nuembrecht, Germany
<b>1.5 and 2 ml Eppendorf tubes</b>	Sarstedt, Nuembrecht, Germany
<b>15 ml and 50 ml tubes</b>	Sarstedt, Nuembrecht, Germany
<b>Cryovials</b>	Greiner Bio-One, Kremsmuenster, Austria
<b>15-well µ-Slide</b>	Ibidi, Planegg / Martinsried, Germany
<b>Nitrocellulose Protran Membrane (0.45 µM)</b>	GE Healthcare, Buckinghamshire, UK

### 3.1.4 Chemicals

**Table 4: Chemicals used in this study.**

Name	Supplier, City, Country
<b>Acetic acid</b>	Carl Roth, Karlsruhe, Germany
<b>Acrylamide/Bis-acrylamide, ratio 37:1</b>	Sigma-Aldrich, St. Louis, USA
<b>Actinomycin D</b>	Sigma-Aldrich, St. Louis, USA
<b>Adenosinetriphosphate (ATP)</b>	Sigma-Aldrich, St. Louis, USA
<b>Agar</b>	Carl Roth, Karlsruhe, Germany
<b>Agarose NEEO Ultra quality</b>	Carl Roth, Karlsruhe, Germany
<b>Alamar Blue</b>	BioSource International, Camarillo, USA
<b>Amidoblack</b>	Carl Roth, Karlsruhe, Germany
<b>Ammonium persulfate (APS)</b>	Carl Roth, Karlsruhe, Germany
<b>Ampicillin</b>	Calbiochem, San Diego, USA
<b>Biotin</b>	Sigma-Aldrich, St. Louis, USA
<b>Bovine serum albumin</b>	Sigma-Aldrich, St. Louis, USA
<b>Brilliant Blue G250</b>	Carl Roth, Karlsruhe, Germany
<b>Calcein AM (1mg/mL solution in anhydrous DMSO)</b>	BD Biosciences, Germany
<b>Calciumchlorid-Dihydrate</b>	Merck, Darmstadt, Germany
<b>Calcium pantothenate</b>	Sigma-Aldrich, St. Louis, USA
<b>Chloroform</b>	Merck, Darmstadt, Germany

Name	Supplier, City, Country
<b>Coumaric acid</b>	Sigma-Aldrich, St. Louis, USA
<b>D-(+)-Glucose</b>	Sigma-Aldrich, St. Louis, USA
<b>DEPC</b>	Carl Roth, Karlsruhe, Germany
<b>Dimethylsulfoxide (DMSO)</b>	Carl Roth, Karlsruhe, Germany
<b>Dithiothreitol (DTT)</b>	Carl Roth, Karlsruhe, Germany
<b>Endothelial growth factor (EGF) (human, recombinant)</b>	Invitrogen, Carlsbad, USA
<b>Ethanol</b>	Merck, Darmstadt, Germany
<b>Ethidium bromide</b>	Carl Roth, Karlsruhe, Germany
<b>Ethylene diamine tetraacetic acid (EDTA)</b>	Carl Roth, Karlsruhe, Germany
<b>Ethylene glycol tetraacetic acid (EGTA)</b>	Carl Roth, Karlsruhe, Germany
<b>Formaldehyde 37%</b>	Merck, Darmstadt, Germany
<b>FuGENE HD reagent</b>	Roche, Basel, Switzerland
<b>Glycerol</b>	Carl Roth, Karlsruhe, Germany
<b>Glycine</b>	Carl Roth, Karlsruhe, Germany
<b>Hank's balanced salt solution (HBSS)</b>	Life Technologies, Carlsbad, USA
<b>Hydrochloric acid</b>	VWR, Radno, USA
<b>Hydrocortisone</b>	Life Technologies, Carlsbad, USA
<b>Hydrogen peroxide</b>	Merck, Darmstadt, Germany
<b>Igepal CA-630</b>	Sigma-Aldrich, St. Louis, USA
<b>Ionomycine</b>	Sigma-Aldrich, St. Louis, USA
<b>Isoamylalcohol</b>	Merck, Darmstadt, Germany
<b>Isopropanol</b>	VWR, Radno, USA
<b>Kanamycin Sulfate</b>	Calbiochem, San Diego, USA
<b>Lipofectamin RNAiMAX</b>	Life Technologies, Carlsbad, USA
<b>Lithium Chloride</b>	AppliChem, Darmstadt, Germany
<b>Lithium Iodide-hydrate</b>	Merck, Darmstadt, Germany
<b>Lucigenin</b>	Sigma-Aldrich, St. Louis, USA
<b>Luminol</b>	Sigma-Aldrich, St. Louis, USA
<b>Magnesium Carbonate Hydroxide</b>	Sigma-Aldrich, St. Louis, USA
<b>Magnesium Chloride-Hexahydrate</b>	Carl Roth, Karlsruhe, Germany
<b>Magnesiumsulfat-heptahydrat</b>	AppliChem, Darmstadt, Germany
<b>Maleic Acid</b>	Sigma-Aldrich, St. Louis, USA
<b>Manganese-(II)-Chloride</b>	Merck, Darmstadt, Germany
<b>Matrigel, growth factor reduced</b>	BD Biosciences, San Jose, USA

Name	Supplier, City, Country
<b>N-Acetyl-Cysteine</b>	Sigma-Aldrich, St. Louis, USA
<b>N-Lauryl-Sarcosine</b>	Sigma-Aldrich, St. Louis, USA
<b>N-Nitro-L-Arginine</b>	Calbiochem, San Diego, USA
<b>Non-fat dry milk powder</b>	Merck, Darmstadt, Germany
<b>ortho-Nitrophenyl-β-galactoside (ONPG)</b>	Carl Roth, Karslruhe, Germany
<b>PBS-Tablettes</b>	Life Technologies, Carlsbad, USA
<b>Phenylmethanesulfonyl fluoride (PMSF)</b>	Sigma-Aldrich, St. Louis, USA
<b>Phorbol 12-Myristate 13 Acetate</b>	Sigma-Aldrich, St. Louis, USA
<b>Poly-dIdC</b>	Roche, Basel, Switzerland
<b>Ponceau S</b>	Carl Roth, Karslruhe, Germany
<b>Potassium Acetate</b>	Merck, Darmstadt, Germany
<b>Potassium Carbonate</b>	Merck, Darmstadt, Germany
<b>Potassium Chloride</b>	Merck, Darmstadt, Germany
<b>Potassium Dihydrogen Phosphate</b>	Merck, Darmstadt, Germany
<b>Potassium Hydrogencarbonate</b>	Merck, Darmstadt, Germany
<b>Potassium Hydroxide</b>	Carl Roth, Karslruhe, Germany
<b>Protease inhibitors “complete”</b>	Roche, Basel, Switzerland
<b>Protein A agarose beads</b>	Roche, Basel, Switzerland
<b>Roti-Aqua-Phenol</b>	Carl Roth, Karslruhe, Germany
<b>Rotiphorese Gel 30%</b>	Carl Roth, Karslruhe, Germany
<b>SDS ultra-pure</b>	Carl Roth, Karslruhe, Germany
<b>Sodium acetate</b>	Merck, Darmstadt, Germany
<b>Sodium chloride</b>	Carl Roth, Karslruhe, Germany
<b>Sodium citrate</b>	Carl Roth, Karslruhe, Germany
<b>Sodium deoxycholate</b>	Sigma-Aldrich, St. Louis, USA
<b>Sodium dihydrogen phosphate</b>	Sigma-Aldrich, St. Louis, USA
<b>Sodium fluoride</b>	Merck, Darmstadt, Germany
<b>Sodium orthovanadate</b>	Merck, Darmstadt, Germany
<b>Sucrose</b>	Sigma-Aldrich, St. Louis, USA
<b>Sulfuric acid</b>	Carl Roth, Karslruhe, Germany
<b>SYBR Green FastMix PerfeCTa</b>	Quanta BioSciences
<b>TEMED</b>	Carl Roth, Karslruhe, Germany
<b>Trifluoroacetic acid</b>	Sigma-Aldrich, St. Louis, USA
<b>TRIS ultra</b>	Carl Roth, Karslruhe, Germany
<b>Triton X-100</b>	Sigma-Aldrich, St. Louis, USA

Name	Supplier, City, Country
Trypan blue (C.I. 23850)	Merck, Darmstadt, Germany
Tryptone	Carl Roth, Karlsruhe, Germany
TWEEN20	Sigma-Aldrich, St. Louis, USA
Xylenecyanol	Carl Roth, Karlsruhe, Germany
Yeast extract	Carl Roth, Karlsruhe, Germany
β-Mercaptoethanol	Carl Roth, Karlsruhe, Germany

### 3.1.5 Buffers, solutions and media

All solutions were prepared with double distilled water if not otherwise stated.

#### 3.1.5.1 Cell culture

**Table 5: Cell culture media and additives used in this study.**

Cell culture media and additives	Supplier, City, Country
Dulbecco's Modified Eagle's Medium (DMEM) High glucose (4.5 mg/ml) Low glucose (1.5 mg/ml)	PAA, Pasching, Austria
Dulbecco's Modified Eagle Medium: Nutrient Mixture F-12 (DMEM/F12)	Life Technologies, Carlsbad, USA
MCDB 131	PAA, Pasching, Austria
RPMI 1640	PAA, Pasching, Austria
SmGM-2 BulletKit	Lonza, Basel, Switzerland
Fetal calf serum (FCS)	PAN Biotech, Aidenbach, Germany
Endothelial basal Medium	PAA, Pasching, Austria
Penicillin /Streptomycin	PAA, Pasching, Austria
Trypsin-EDTA	PAA, Pasching, Austria
PBS	PAA, Pasching, Austria
HBSS with Mg/Ca	PAA, Pasching, Austria

#### Cell lysis buffer

Tris pH 7.5	50 mM
NaCl	150 mM
SDS	0.1%
Igepal	1%
Sodium-Deoxycholate	0.5%
Protease Inhibitors	1 tablet per 50 ml

### 3.1.5.2 Luciferase assay solutions

#### *Luciferase lysis buffer*

Tris pH 7.8	5 mM
trans-CDTA	0.4 mM
Glycerol	50%
DTT	2 mM
Triton X-100	5%

DTT and Triton X-100 are added freshly after autoclaving

#### *Luciferase substrate*

Tris pH 7.8	20 mM
(MgCO <sub>3</sub> ) <sub>4</sub> Mg(OH) <sub>2</sub> 5H <sub>2</sub> O	1.07 mM
MgSO <sub>4</sub>	2.67 mM
EDTA	0.1 mM
DTT	33.3 mM
D-Luciferin	460 mM
ATP	580 mM

#### *β-Galactosidase substrate*

MgCl <sub>2</sub>	1.1 mM
ONPG	1 mg/ml
Na <sub>2</sub> HPO <sub>4</sub>	82 mM
NaH <sub>2</sub> PO <sub>4</sub>	18 mM
β-Mercaptoethanol	50 mM

### 3.1.5.3 Western Blot

#### *Separation gel*

	8%	10%	12%
H <sub>2</sub> O	3.4 ml	2.8 ml	2.1 ml
30% Acrylamid / 0.8% Bisacrylamid	2.7 ml	3.3 ml	4.0 ml
1 M Tris HCl pH 8.8	3.7 ml	3.7 ml	3.7 ml
10% SDS	100 µl	100 µl	100 µl
10% Ammoniumpersulfate	80 µl	80 µl	80 µl
TEMED	10 µl	10 µl	10 µl

#### *Stacking gel (5%)*

H <sub>2</sub> O	2.14 ml
30% Acrylamide	488 µl
1 M Tris/HCl pH 6.8	375 µl
10% SDS	30 µl
10% APS	15 µl
TEMED	3 µl

*Laemmlie buffer (3x)*

Tris/HCl pH 6.8	187 mM
SDS	6%
Glycerol	30%
Bromphenol blue	0.06%
DTT	15 mM
EDTA	60 mM

*Running buffer*

Tris	25 mM
Glycin	200 mM
SDS	0.5%

*Transfer buffer*

Tris	25 mM
Glycin	200 mM
Methanol	20%

*Stripping buffer*

SDS	2%
Tris pH 6.8	62.5 mM
$\beta$ -Mercaptoethanol	0.07%

*TBS-T*

Tris	50 mM
NaCl	150 mM
HCl	0.3%
Tween	0.3%
pH was set to 7.5	

*ECL-Chemoluminescence reagent 1*

Tris pH 8.8	100 mM
Luminol	2,5 mM
Cumaric acid	0,4 mM

*ECL-Chemoluminescence reagent 2*

Tris pH 8.8	100 mM
$H_2O_2$	0.15%

### 3.1.5.4 Cultivation of *E. coli*

#### *TB medium*

HEPES	10 mM
CaCl <sub>2</sub>	15 mM
KCl <sub>2</sub>	250 mM

The solution was adjusted to pH 6.7 with KOH and MnCl<sub>2</sub> was added to a final concentration of 55 mM. The solution was then sterile filtered and stored at 4°C.

#### *SOC medium*

Yeast Extract	0.5%
Trypton	2%
NaCl	0.05%
KCl	2.5 mM

The solution was adjusted to pH 7.0 and then autoclaved with a subsequent addition of 20 ml of glucose (1 M, final concentration 5 mM) and 5 ml MgCl<sub>2</sub> (2 M, final concentration 0.5 mM).

#### *LB Medium*

Yeast Extract	0.5%
Trypton	1%
NaCl	1%

The solution was adjusted to pH 7.0 and then autoclaved

#### *LB Agar plates*

Agar	1.5%
LB Medium	98.5%

The solution was autoclaved and cooled down; required antibiotic was added at approximately 60°C (ampicillin 100 µg/ml, kanamycin 100 µg/ml). The solution was mixed and filled to appropriate dishes.

### 3.1.6 Plasmid preparation (mini)

*P1*

Tris	50 mM
EDTA	10 mM

The solution was adjusted to pH 8.0

*P2*

NaOH	200 mM
SDS	1.0%

*P3*

Na-Acetate pH 5.5	3.1 M
-------------------	-------

#### 3.1.6.1 Agarose gel electrophoresis

*TAE buffer*

Tris	0.5 M
Sodiumacetate	0.2 M
EDTA	0.02 M

The solution was adjusted to pH 7.0 using acetic acid

*Orange G loading buffer*

Glycerol	7.5%
Orange G dye	0.2%

#### 3.1.6.2 Co-IP buffers

*Non-denaturating lysis buffer*

Tris-HCl pH 7.4	50 mM
NaCl	300 mM
EDTA	5 mM
TritonX-100	1%
complete protease inhibitors	

*Washing buffer*

Tris-HCl, pH 7.4	50 mM
NaCl	300 mM
EDTA	5 mM
TritonX-100	0.1%

### 3.1.6.3 EMSA reaction buffer

Tris/HCl pH 7.5	10 mM
KCl	50 mM
NaCl	50 mM
MgCl <sub>2</sub>	1 mM
EDTA	1 mM
Glycerol	5%

### 3.1.7 Primers and probes

Primers were designed either with the primer3 online algorithm or adapted from Universal Probe Library. Uniqueness in the human genome was rechecked by BLAT analysis against NCBI build 36.1. Oligonucleotides were purchased from metabion, Planegg, Germany.

**Table 6: Primers and probes used in this study.**

Name	ID	Sequence (5'-3')
PApro fw2	oFR003	CAGAGGGCAGAAAGGTCAAG
PApro rev2	oFR004	CTCTCTGGGACTTGCTGAGG
NMfw2	oFR005	GATGGCCCTTCAGCCAAC
hPAI1-RT fw	oFR079	CACAAATCAGACGGCAGCACT
hPAI1-RT rev	oFR080	CATCGGGCGTGGTGAACTC
hHIF1A-RT fwd	oFR083	GAAGACATCGCGGGGAC
hHIF1A-RT rev	oFR084	TGGCTGCATCTCGAGACTTT
hHIF3A-RT rev1	oFR090	AGCACCTCGGTCTCCTGGCTGC
hHIF3A1-RT fw2	oFR091	CCCACTCCTGAACCTGAATG
hHIF3A1-RT rev2	oFR092	GGCAGATGGGGAGAGGGAG
hHIF3A3-RT fw	oFR095	CTCAGCCTGGTGTGTTGGG
hHIF3A3-RT rev	oFR096	CCTGCCCTCTCTGGTTTC
hHIF3A-RT fw1	oFR097	ACTGTGACGACAGGATTGCAG
hHIF3ABC-RT rev	oFR098	CATGTGGCAGCTGGCTTCGCAC
hHIF3A-RT fw3	oFR100	GCCTGGACATGAAGTTCAAC
hHIF3A-RT rev3	oFR101	GTACTCGTAGGCAGAACAGC
h18S-RT fw	oFR118	GTAACCCGTTGAACCCATT
h18S-RT rev	oFR119	CCATCCAATCGGTAGTAGCG
hPGK1-RT fw	oFR168	CTGTGGCTTCTGGCATAACCT
hPGK1-RT rev	oFR169	CGAGTGACAGCCTCAGCATA
hEPAS1-RT fw	oFR170	GACATGAAGTTCACCTACTGTGATG
hEPAS1-RT rev	oFR171	GCGCATGGTAGAATTCAAGG
hACTB-RT fw3	oFR174	GTTGTCGACGACGAGCG

Name	ID	Sequence (5'-3')
hACTB-RT rev3	oFR175	GCACAGAGCCTCGCCTT
hEGLN3-RT fw	oFR180	ATCGACAGGCTGGCTCTCA
hEGLN3-RT rev	oFR181	GATAGCAAGCCACCATTGC
hCD82-RT for	oFR214	TGCACTGGTTCTGTGAAAG
hCD82-RT rev	oFR215	TGGTGACTTGTACAGGCTGA
hHIF3A 1c EpiQ fw	oFR216	TGAGGGAAAAGGGCAGAGGGAGGTGA
hHIF3A 1c EpiQ rev	oFR217	GTCTTGCCAGTCCATGGTGCCTCTG
hHIF3Apro1aChIP fw	oFR222	AGTACTGGCGTTGGCACTTC
hHIF3Apro1aChIP rev	oFR223	ACTTCCTCGGCAGTGTATCC
hHIF3Apro1cChIP fw	oFR224	CGAGTCACCACCAGTGAATG
hHIF3Apro1cChIP rev	oFR225	TGGTACAGCACCTCGGTCTC
hHIF3A 1a EpiQ fw	oFR226	GCGTTGGCACTTCAGAGGCTGGACT
hHIF3A 1a EpiQ rev	oFR227	GAGCCCTCGGAGGGCCCTAGCC
hUntr4 fw	oFR228	CTCCCTCCTGTGCTTCTCAG
hUntr4 rev	oFR229	AATGAACGTGTCTCCAGAA
PAI1-HREwt, sense		Cy5-TCTTACACACGTACACACA
PAI1-HREmut, sense		Cy3-TCTTACACACGTACACACA
RHO EpiQ fw		AGGTCACTTATAAGGGCTGGGGG
RHO EpiQ rev		AGTTGATGGGAAGGCCAGCACGAT
GAPDH EpiQ fw		ACCTCCCATGGGCCAATCTCAGTC
GAPDH EpiQ rev		GGCTGACTGTCGAACAGGAGGAGCA
hHIF3Apro1aBS fw		AGAGGTTGGATTAGAGAAGG
hHIF3Apro1aBS rev		CAATTCCAAAACCTCCTACC
hHIF3Apro1cBS-1 fw		AGAGGTTGGATTAGAGAAGG
hHIF3Apro1cBS-1 rev		AAACCCTCCTAACCCCTAATTTT
hHIF3Apro1cBS-2 fw		TAATATATTATTGGGAGGTTG
hHIF3Apro1cBS-2 rev		CAAAACCTCCCAAAAATAAC

### 3.1.8 Plasmids

Table 7: Plasmids and vectors used in this study.

Cloning vectors	Function	Reference
pGL3-Basic	Luciferase assay	Promega, Mannheim, Germany
pGL3-Promoter	Luciferase assay	Promega, Mannheim, Germany
pSV- $\beta$ -Galactosidase Control Vector plasmid	Luciferase assay	Promega, Mannheim, Germany
pGL3-hPAI-796	Luciferase assay	(Kietzmann et al. 2003)
pGL3-EPO-HRE	Luciferase assay	(Görlach et al. 2001)
pcDNA3.1-	Cloning	Life Technologies, Carlsbad, USA
pcDNA3.1D/ V5-His-hHIF-1 $\alpha$	Overexpression	(Klein et al. 2008)

Cloning vectors	Function	Reference
pcDNA3.1-HIF-2 $\alpha$	Overexpression	Kind gift of Prof. T. Kietzmann
pcDNA3.1-HIF-3 $\alpha$ 1	Overexpression	PhD thesis Steve Bonello
pcDNA3.1-HIF-3 $\alpha$ 1-V5	Overexpression	PhD thesis Steve Bonello
pcDNA3.1-ARNT	Overexpression	Kind gift of Prof. T. Kietzmann

### 3.1.9 siRNA

Table 8: siRNA used in this study.

Target	Company	target-sequence
<b>None (control)</b>	Eurogentec	gacuacuggucguugaagudTdT
<b>HIF1A</b>	Eurogentec	ucaaguugcuggucaucagdTdT targeting 1543 to 1561 bp of the human <i>HIF1A</i> mRNA (NCBI accession number NM_001530)
<b>HIF2A</b>	Qiagen	cggauagacuuauugccadTdT targeting 4742 to 4760 bp of the human <i>HIF2A</i> mRNA (NCBI accession number NM_001430)
<b>HIF3A</b>	Invitrogen	ccugugaccaagaggagcuucagga targeting 447 to 471 bp of the human <i>HIF3A</i> mRNA (NCBI accession number NM_152794)

### 3.1.10 Bacterial strains

Table 9: bacterial strains used in this study

E.coli strain	Supplier, City, Country
<b>DH5<math>\alpha</math></b>	Invitrogen, Carlsbad, USA
<b>XL-1 Blue</b>	Agilent Technologies, Santa Clara, USA
<b>JM109</b>	Sigma-Aldrich, St. Louis, USA

See manufacturer's manuals for genotypes.

### 3.1.11 Kits

**Table 10: Kits used in this study**

Name	Company , City, Country
<b>ABI PRISM BigDye Terminator v1.1 Cycle Sequencing Kit</b>	Applied Biosystems, Carlsbad, USA
<b>BrdU proliferation assay</b>	Roche, Basel, Switzerland
<b>Nucleo Seq sequencing clean-up kit</b>	Macherey-Nagel, Dueren, Germany
<b>RNeasy Mini Kit</b>	Qiagen, Hilden, Germany
<b>Qiagen Plasmid Maxi Kit</b>	Qiagen, Hilden, Germany
<b>SuperScriptIII Reverse Transcriptase</b>	Invitrogen, Carlsbad, USA
<b>Phusion High-Fidelity DNA Polymerase</b>	New England Biolabs, Frankfurt am Main, Germany
<b>High Capacity cDNA Reverse Transcription Kit</b>	Applied Biosystems, Carlsbad, USA
<b>TnT T7 Quick Coupled Transcription/Translation System</b>	Promega, Mannheim, Germany
<b>StrataClone PCR Cloning Kit</b>	Agilent Technologies, Santa Clara, USA
<b>EpiQ chromatin analysis kit</b>	Bio-Rad, Munich, Germany
<b>NucleoSpin Tissue kit</b>	Macherey-Nagel, Germany, Dueren
<b>EZ DNA Methylation-Gold kit</b>	Zymo Research, Germany, Freiburg
<b>HotStarTaq Master Mix Kit</b>	Qiagen, Hilden, Germany
<b>Cancer Survey cDNA Array 96 - I</b>	OriGene, Rockville, USA

### 3.1.12 Antibodies

**Table 11: Antibodies used in this study.**

Antigen	Host, isotyp, modification	Supplier, city, country	Dilution
<b>β-Actin</b>	goat, IgG	Santa Cruz Biotechnology, Heidelberg, Germany	1:1000
<b>HIF-1α</b>	mouse, IgG	BD Transduction Laboratories, Heidelberg, Germany	1:1000
<b>HIF-2α</b>	mouse, IgG	Merck Chemicals, Schwalbach, Germany	1:1000
<b>HIF-3α</b>	Rabbit IgG	Abcam, Cambridge, UK	1:1000
<b>ARNT</b>	Rabbit IgG	Abcam, Cambridge, UK	1:2000
<b>V5</b>	mouse, IgG	Invitrogen, Carlsbad, USA	1:5000
<b>PAI-1</b>	Maus, IgG	American Diagnostica, Pfungstadt, Germany	1:200
<b>goat, IgG</b>	rabbit, IgG, Peroxidase	Calbiochem, San Diego, USA	1:10000
<b>Mouse IgG</b>	Rabbit IgG, peroxidase	Calbiochem, San Diego, USA	1:10000
<b>rabbit, IgG</b>	goat, IgG, Peroxidase	Calbiochem, San Diego, USA	1:10000
<b>PAI-1 (inhibitory)</b>	Mouse IgG	MyBioSource, San Diego, USA	1 µg/ml
<b>unspecific</b>	mouse IgG1, monoclonal	Abcam, Cambridge, UK	1 µg/ml
<b>H3Ac</b>	Rabbit, polyclonal	Merck, Darmstadt, Germany	Millipore
<b>H3K9me3</b>	Mouse IgG2b, monoclonal	Active motif, La Hulpe, Belgium	

### 3.1.13 Software

**Table 12: Software used in this study.**

Software	Version	Manufacturer	Used for
<b>Image J software</b>	1.43b	Wright Cell Imaging Facility, Toronto, Canada	Analysis of tube formation
<b>Rotor-Gene 6000 Application Software</b>	1.7	Corbett Life Sciences, Sydney, Australia	Analysis of qPCR data
<b>Openlab Modular Software</b>	4.0.4	PerkinElmer, Waltham, USA	Capturing images from microscope
<b>BiQ Analyzer</b>		Max-Planck-Institute for Informatics, Saarbruecken, Germany	visualization and quality control for DNA methylation data from bisulfite sequencing
<b>Adobe Photoshop</b>	CS2	Adobe Systems, Munich, Germany	Editing of captured images from microscopy and western blot
<b>ApE (A plasmid Editor)</b>	2.0.36	M. Wayne Davis	DNA sequence analysis software
<b>Microsoft Office</b>	2007	Microsoft, Unterschleissheim, Germany	Documentation
<b>Nanodrop Software</b>	3.2.1	PEQLAB Biotechnologie, Erlangen, Germany	Determination of DNA and RNA concentration

Software	Version	Manufacturer	Used for
<b>Image lab software</b>		Bio-Rad, Munich, Germany	Capturing images from agarose gels on UV transluminator
<b>ImageQuantTL</b>		GE Healthcare, Buckinghamshire, UK	Analysis of images captured by Typhoon Trio instrument
<b>Inkscape</b>	0.47	Open Source Software	Creating vector images
<b>REST 2009</b>	1	M. Pfaffl (Technical University Munich) and QIAGEN	gene expression analysis
<b>GraphPad Prism</b>	4	GraphPad Software, Inc.	2D graphing and statistics

### 3.1.14 Online databases and algorithms

**Table 13: Online databases and algorithms used in this study.**

Name	URL	Reference
<b>Blast: the Basic Local Alignment Search Tool</b>	<a href="http://blast.ncbi.nlm.nih.gov/Blast.cgi">http://blast.ncbi.nlm.nih.gov/Blast.cgi</a>	(Altschul et al. 1990)
<b>BLAT (BLAST-like alignment tool)</b>	<a href="https://genome.ucsc.edu/cgi-bin/hgBlat?command=start">https://genome.ucsc.edu/cgi-bin/hgBlat?command=start</a>	(Kent 2002)
<b>ClustalW2</b>	<a href="http://www.ebi.ac.uk/Tools/msa/clustalw2/">http://www.ebi.ac.uk/Tools/msa/clustalw2/</a>	(Thompson et al. 2002)
<b>RefSeq: NCBI Reference Sequence Database</b>	<a href="http://www.ncbi.nlm.nih.gov/refseq/">http://www.ncbi.nlm.nih.gov/refseq/</a>	(Pruitt et al. 2007)
<b>Primer3web (version 4.0.0)</b>	<a href="http://primer3.ut.ee/">http://primer3.ut.ee/</a>	(Rozen and Skaletsky 2000)
<b>UCSC Genome Browser</b>	<a href="http://genome.ucsc.edu/">http://genome.ucsc.edu/</a>	(Kuhn et al. 2009)

## 3.2 Methods

### 3.2.1 Cell Culture

HMEC-1 (Human microvascular endothelial cells) cell line was obtained from the Center for Disease Control at passage 12, and used before passage 25. Cells were grown in Endothelial Basal Medium - MCDB 131 supplemented with 10% fetal calf serum, 100 U/ml penicillin, 100 µg/ml streptomycin, 1 µg/ml hydrocortisone and 10 ng/ml human recombinant endothelial growth factor. Cells were cultivated according to manufacturer's instructions and placed with endothelial basal medium supplemented with 2% fetal calf serum 16 hours prior to stimulation.

HeLa cells were cultured according to manufacturer's instructions in Dulbecco's Modified Eagle's Medium (DMEM) supplemented with 4.5 g/l glucose, 10% fetal calf serum, 100 U/ml penicillin, and 100 mg/ml streptomycin.

MCF7 cells were cultured according to manufacturer's instructions in RPMI 1640 medium supplemented with 10% fetal calf serum, 100 U/ml penicillin, and 100 mg/ml streptomycin.

SGBS preadipocytes were cultured in DMEM/F-12 containing 10% fetal calf serum, 33  $\mu$ M biotin, 17  $\mu$ M pantothenate, 100 U/ml penicillin and 100  $\mu$ g/ml streptomycin.

PASMC cells were cultured according to manufacturer's instructions in SmGM-2 BulletKit (SMBM plus SmGM-2 SingleQuots).

DU145 and LNCaP cells were cultured in high glucose DMEM and RPMI 1640 medium, respectively, which were supplemented with 10% fetal calf serum, 100 U/ml penicillin, and 100 mg/ml streptomycin.

For luciferase and coimmunoprecipitation assays human embryonic kidney cells (HEK293T) were used. HEK293T cells were cultured in Dulbecco's Modified Eagle's Medium - DMEM supplemented with 4.5 g/l glucose, 10% fetal calf serum, 100 U/ml penicillin, and 100 mg/ml streptomycin. All cells were grown at 37°C under an atmosphere of 5% carbon dioxide. If stated that hypoxic induction was carried out, cells were exposed to hypoxia (0.1-10% O<sub>2</sub> and 5% CO<sub>2</sub>) in a Hypoxia work station.

### 3.2.2 Reporter Gene Assays

HEK293T cells grown to 50-70% confluence in 24-well plates were transiently cotransfected with 400 ng of overexpression constructs, 50 ng of the reporter constructs and 50 ng of pSV- $\beta$ -galactosidase control vector plasmid. Transfection with the host vector (pGL3basic or pGL3promoter) served as a control. The transfected cells were incubated for 16 hours either at 0.1 or 21% oxygen prior to lysis in Luciferase Lysis Buffer. Luciferase activities were measured in a luminometer and  $\beta$ -galactosidase activities were determined spectrophotometrically as described in the manufacturer's protocol. Data are presented as relative light units (RLU) normalized to  $\beta$ -galactosidase activities for the control of transfection efficiencies.

The pGL3-hPAI-796 plasmid, containing the human *PAI1* gene promoter 5'-flanking region from -796 to +13 as well as the pGL3-EPO-HRE plasmid have been described previously (Görlach et al. 2001; Kietzmann et al. 2003).

### 3.2.3 Quantitative Reverse-Transcriptase Polymerase Chain Reaction

Total RNA was isolated by the use of RNeasy Mini Kit according to the manufacturer's protocol. First-strand cDNA synthesis was performed with 1 µg of total RNA using High Capacity cDNA Reverse Transcription Kit according to manufacturer's instructions. Two percent of the volumes of the reaction products were used for quantitative real time PCR amplification with PerfeCTa SYBR Green FastMix. qPCR was performed in a Rotor-Gene 6000 Real-Time PCR System using gene-specific primers for the quantitative Reverse-Transcriptase Polymerase Chain Reaction (RT-qPCR) listed as follows (detailed sequence information can be found in chapter 3.1.7): *HIF3A* consensus (*HIF3Atv1-4*); *HIF3Atv1* (NM\_152794); *HIF3Atv2* (NM\_022462); *HIF3Atv3* (NM\_152795); *HIF3AtvBC* (BC\_026308); *HIF1A* (NM\_001530); *HIF2A* (NM\_001430); *PGK1* (NM\_000291); *EGLN3* (NM\_022073); *CD82* (NM\_002231); *PAI1* (NM\_000602); *ACTB* (NM\_001101); 18S rRNA (X03205). The samples were loaded in triplicate for each primer pair, and the result of each sample was normalized to *ACTB* mRNA. Fold-change was calculated as a ratio of treatment over control (Ctr) with "comparative quantification" module of REST software. Agarose DNA gels were run and/or melting curve analysis was performed to verify the absence of non-specific products. A negative control without addition of reverse transcriptase was run in each assay to assess the overall specificity. All data was analyzed by the Corbett Rotor-Gene 6000 application software with subsequent calculation of relative change by REST software.

### 3.2.4 Chromatin accessibility assay

Chromatin accessibility assay was done using the EpiQ chromatin analysis kit according to manufacturer's instruction. In brief, chromatin was digested with DNaseI or not, before genomic DNA was prepared. Samples were analyzed using qPCR performed in a Rotor-Gene 6000 Real-Time PCR System. Following primers were used (detailed sequence information can be found in chapter 3.1.7): Reference gene *RHO*; control gene *GAPDH*; *HIF3A* E1a; *HIF3A* E1c. By comparing the amount of digested versus undigested DNA material of two regions of the *HIF3A* promoter, the accessibility of these areas was calculated.

### 3.2.5 Bisulfite sequencing

DNA was extracted from HeLa, MCF7 and HMEC-1 cells using NucleoSpin Tissue kit. 1.5 µg of DNA was treated with bisulfite solution derived from EZ DNA Methylation-Gold kit under the following conditions: 98°C for 10 min, 64°C for 180 minutes, thereby converting cytosine residues to uracil, but leaving 5-methylcytosine residues unaffected. Converted DNA was purified according to the manufacturer's instructions and 1/20th was used per amplification of the regions covering exon 1a or exon 1c. PCRs were performed in PCR buffer with the addition of 200 µM betaine, 400 µM tetramethyl ammonium chloride 0.25 mM dNTPs, 0.1 unit/µl HotStarTaq DNA Polymerase, 0.6 µM each primer. Following primers were used: *hHIF3Apro1cBS-1* fw and *hHIF3Apro1aBS* rev; *hHIF3Apro1cBS-1* fw and *hHIF3Apro1cBS-1* rev as well as *hHIF3Apro1cBS-2* fw and *hHIF3Apro1cBS-2* rev. Cycling parameters were 5 min at 96°C, 55x (30 s at 96°C, 35 s at 54°C, 30 s at 72°C), 3 min at 72°C. PCR products were subcloned with StrataClone PCR Cloning Kit and the inserts were sequenced. Resulting sequences were analyzed with BiQ Analyzer (Bock et al. 2005).

### 3.2.6 Plasmids and transfections

The plasmid encoding V5-tagged HIF-1α (pcDNA3.1D/V5-His-hHIF-1α) and ARNT (pcDNA3.1-ARNT) were kindly provided by Prof. T. Kietzmann (Klein et al. 2008). pcDNA3.1-HIF-2α was also a kind gift of Prof. T. Kietzmann. pcDNA3.1-HIF-3α1 and pcDNA3.1-HIF-3α1-V5 expression vectors were previously described (PhD thesis Steve Bonello). The expression vector pcDNA3.1-ARNT was a kind donation from Prof. T. Kietzmann, Oulu, Finland.

For transfection, cells were plated to a density of 50-70%, cultured for 24 hours and transfected by FuGENE HD reagent according to the manufacturer's protocol. In brief, cells were freshly plated one day before transfection. Plasmid DNA and FuGENE HD was mixed in serum free medium in a ratio of 2:6 and incubated for 15 minutes at room temperature before added to the cells, which were incubated 16-72 hours before starting the experiment.

For gene silencing, following siRNAs were purchased from Eurogentec (Belgium): *siHIF1A*, *siHIF2A* and *siHIF3A*. As a negative control, we used siRNA with unspecific

sequence (labeled with siCtr). Cells were transfected with the siRNAs (10 nM final concentration) using Lipofectamin RNAiMAX according to the supplier's protocol. In brief, cells were seeded to 50-70% 24 hours before transfection. Then, Lipofectamin and siRNA are diluted separately in serum free medium and mixed before incubated for 5 minutes at room temperature. With a final concentration of 20 nM siRNA, per pmol of siRNA 0.3  $\mu$ l Lipofectamine was used. Efficiency was tested by qPCR and ranged from 65-95%.

### 3.2.7 Immunoblot Analysis

Proteins were isolated from total cellular lysates as previously described (Bonello et al. 2007). In brief, cells were washed with cold TBS, put on ice and 3x Laemmli buffer was added, before cells were collected and transferred to a reaction tube. Subsequently, tubes were put on heating block (95°C for 5 minutes) before protein concentration of lysates were assessed by dot blot counterstained with amido black solution. Western blot analyses were performed as previously described (Görlach et al. 2001). In brief, 40  $\mu$ g of isolated proteins was separated by SDS-PAGE and transferred to nitrocellulose membranes by tank blot. Next, membranes were blocked with 5% milk/TBS-T for 30 minutes on room temperature. For the subsequent immunodetection, following primary antibodies were used in the dilution 1:1000 in 5% milk/TBS-T: anti-HIF-1 $\alpha$ , anti-HIF-2 $\alpha$ , anti-HIF-3 $\alpha$  antibody, anti-PAI-1 antibody, anti-ARNT, and anti- $\beta$ -actin. Incubation with antibody was done for 16 hours at 4°C; afterwards, membranes were washed with TBS-T three times for 10 minutes. Incubation with a horseradish peroxidase-conjugated secondary antibody laster 30 minutes on room temperature before washed again three times for 10 minutes with TBS-T. Finally, membrane was rinsed with TBS and proteins were visualized applying luminol-enhanced chemiluminescence technique monitored by X-ray film. Films were developed, scanned and analyzed by using Image J software.

### 3.2.8 Angiogenesis Assay

HMEC-1 were transfected with siRNA or scrambled RNA as specified, incubated under normoxic or hypoxic conditions (21% and 0.1% oxygen, respectively) for 48

hours and supernatants were collected. Collected supernatants were used for stimulation of HMEC-1, which were previously seeded (5000 cells/well) on growth factor reduced Matrigel in 15-well  $\mu$ -Slide. As specified by experimental design, medium of one group of cells was incubated with 1  $\mu$ g/ml of an inhibitory monoclonal mouse anti-PAI-1 antibody or mouse IgG1 monoclonal antibody or not. Cells were then incubated for 16 hours at 37°C and counterstained using Calcein AM (final concentration 6.25  $\mu$ g/ml) (BD Biosciences, Germany). The formation of capillary-like structures was assessed by fluorescence microscopy using the Openlab Modular Software for Scientific Imaging and was quantified using Image J software (Schneider et al. 2012).

### 3.2.9 Co-Immunoprecipitation

HEK293T or HMEC-1 cells were cotransfected with expression vectors encoding for V5-tagged HIF-3 $\alpha$ 1 and either HIF-2 $\alpha$  or ARNT and exposed to hypoxia (0.1% oxygen). After lysis with nondenaturing lysis buffer, cells were precleared with protein A agarose beads, and subsequently incubated with protein A agarose beads bound to anti-V5 antibody, anti-ARNT antibody, or nonspecific purified mouse immunoglobulin G (IgG) for overnight at 4°C. Antibody-protein complexes were washed four times with washing buffer and once with phosphate-buffered saline and eluted with SDS-PAGE sample buffer. Precipitated proteins were detected by Western blot analysis using specific antibodies.

### 3.2.10 *In vitro* Translation and Electrophoretic Mobility Shift Assay

*In vitro* transcription/translation was carried out with TnT T7 Quick Coupled Transcription/Translation System according to manufacturer's protocol. Electrophoretic mobility shift assays (EMSA) were carried out with *in vitro* translated proteins, preincubated with poly-dIdC and DTT for 10 minutes at room temperature in a 1x reaction buffer. Fluorescently labeled oligonucleotides were annealed by mixing sense and antisense primers, heating the mixture (5 minutes at 98°C) and slow cooling down to roomtemperature (simply by switching of the heat block, leaving the tubes in there). The annealed probe was added to the protein mixture and incubated at room temperature for 20 minutes. The samples were run for 4 hours on a non-denaturing 0.4%

agarose gel at room temperature. Gels were subsequently scanned for fluorescence on a Typhoo Trio instrument. The following probes with the HIF response elements in the *PAI1* promoter were used: *PAI1*-HREwt and *PAI1*-HREmut.

### 3.2.11 Chromatin Immunoprecipitation

HeLa, MCF7 and HMEC-1 cells were grown in 10 or 15 cm dishes to 70% confluence and either incubated at ambient conditions for 48 hours or exposed to hypoxia (0.1% oxygen) for 48 hours. Cells were fixed with formaldehyde, lysed, and sonicated to obtain DNA fragments majorly ranging from 500 to 1000 bp. Chromatin was then precipitated with an antibodies against acetylated histone 3 (H3Ac), trimethylated lysine 9 of histone 3 (H3K9me3), HIF-2 $\alpha$ , or ARNT for overnight at 4°C. Real-time PCR was performed using a Rotor-Gene 6000 Real-Time PCR System with following primers. *HIF3A* exon 1a: h*HIF3A*pro1aChIP fw and h*HIF3A*pro1aChIP rev; *HIF3A* exon 1c: h*HIF3A*pro1cChIP fw and h*HIF3A*pro1cChIP rev; *PAI1* promoter (flanking the potential HRE -188/-193 bp): PAIpro fw2 and PAIpro rev2. A gene-deficient region on chromosome 4 (Untr4) served as a negative control (hUntr4 fw and hUntr4 rev). As background control, chromatin immunoprecipitation (ChIP) with isotype control antibody (IgG) was performed. Quantification was performed using a standard curve of the input. H3Ac, H3K9me3, HIF-2 $\alpha$  or ARNT binding to chromatin was revealed after background subtraction as relative amount of the input used.

## 3.3 Statistical Analysis

If not otherwise stated, values are presented as means  $\pm$  SD. Results from all experiments except gene expression analysis *via* qPCR were compared by two-way ANOVA for repeated measurements followed by Student *t* test.  $p < 0.05$  was considered statistically significant. The calculation was done with the GraphPad Prism software. For relative gene expression, investigated transcripts are tested for significance by a Pair Wise Fixed Reallocation Randomisation Test and plotted using standard error (SE) estimation. This calculation was done with the REST (relative expression software tool) software. Again,  $p < 0.05$  was considered statistically significant.

## 4 Results

### 4.1 Regulation of *HIF3A* transcription at ambient conditions

#### 4.1.1 *HIF3A* expression levels differs in various cell lines

In order to investigate the regulation of expression of the *HIF3A* gene, coding for HIF-3 $\alpha$  protein, we analyzed basal transcription levels of expression of a consensus sequence in the following cell lines: HeLa (human epithelial cervix carcinoma cells), MCF7 (human epithelial adenocarcinoma cells), HMEC-1 (human immortalized microvascular endothelial cells), PASMC (human primary pulmonary artery smooth muscle cells), SGBS preadipocytes, LNCaP (human prostate adenocarcinoma cells), DU145 (human prostate cancer cells), and HEK293T (human embryonic kidney cells). In addition, we investigated the levels of different transcript variants (tv) of *HIF3A* as follows in HMEC-1, HeLa and MCF7 cells: *HIF3Atv1* (RefSeq accession number: NM\_152794); *HIF3Atv2* (NM\_022462); *HIF3Atv3* (NM\_152795) and *HIF3AtvBC* (GenBank accession number: BC\_026308) (compare Figure 11A). Cells were analyzed for levels of *HIF3A* isoforms by RT-qPCR in unstimulated conditions 48 hours after plating.

The evaluation of *HIF3A* consensus levels revealed two groups of cell lines: one group with low basal expression (HeLa, MCF7, LNCaP, DU145, and HEK293T) and one group with high basal expression of *HIF3A* transcripts (HMEC-1, PASMC and SGBS) (Figure 11B). The relative difference in *HIF3A* transcripts between these groups was quantified with more than 1000-fold.

Detailed analyses of specific transcript variants were carried out only in cell lines HeLa, MCF7 and HMEC-1, which were also used for all subsequent experiments. All four distinct transcripts (*HIF3Atv1*, *HIF3Atv2*, *HIF3Atv3*, and *HIF3AtvBC*) were highly expressed in HMEC-1 cells while overall *HIF3A* transcript levels were lower in the two tumor cell lines as already shown by RT-qPCR amplifying the *HIF3A* consensus sequence (Figure 11 B-F). Consistently, HeLa cells expressed lower levels of isoforms 1, 2 and BC when compared to endothelial cells while we were not able to

detect isoform 3 (Figure 11 B-F). Similarly, in MCF7 cells *HIF3Atv1* and *HIF3Atv2* expression was lower compared to HMEC-1 cells while *HIF3Atv3* and *HIF3AtvBC* levels were not detectable (Figure 11 B-F). Overall, our results indicate a different regulation of basal *HIF3A* transcription in different cell lines.

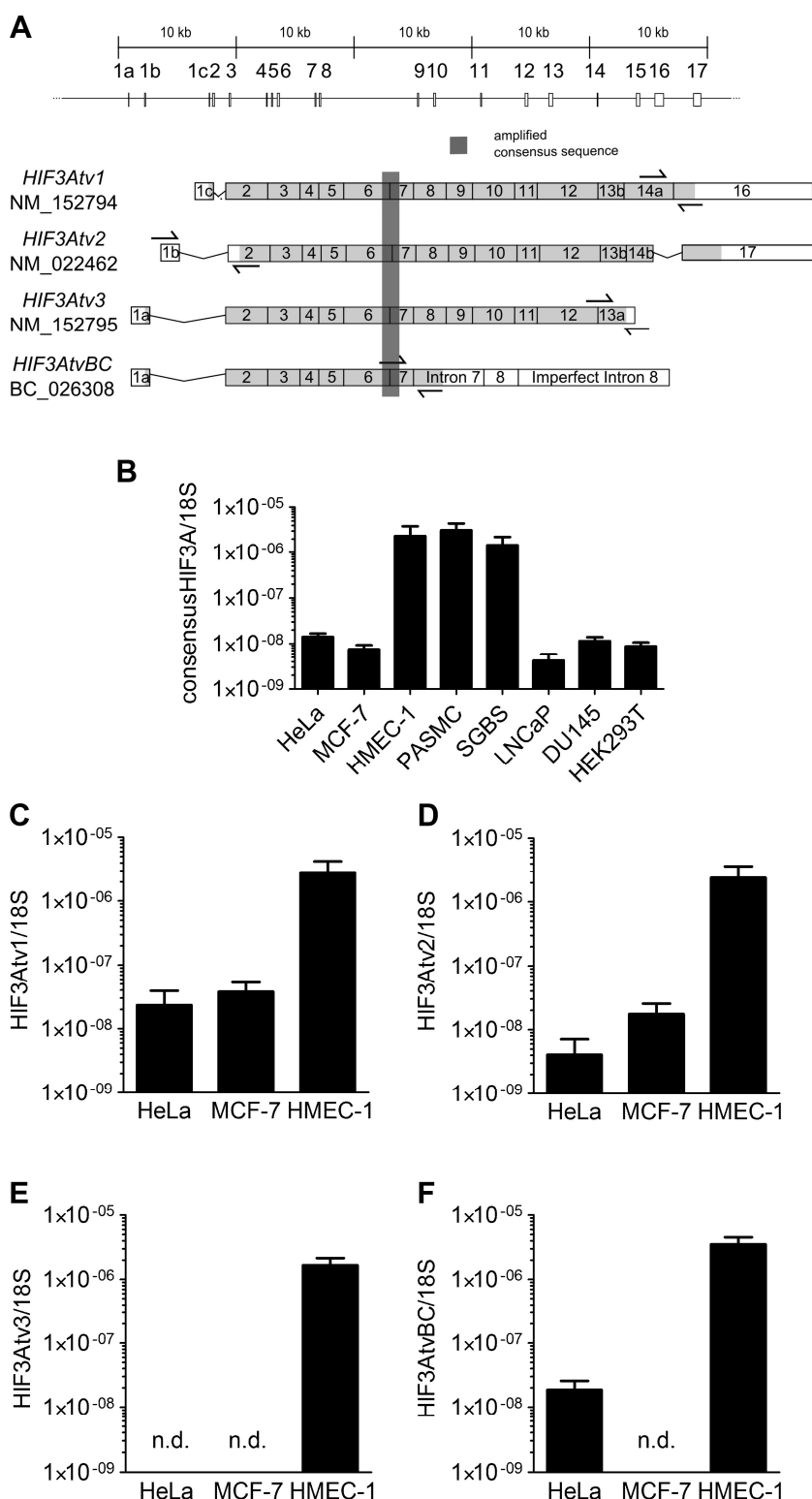


**Figure 11: Basal expression of *HIF3A* isoforms varies in different cell lines.**

(A) Schematic overview of *HIF3A* locus and transcripts. Coding regions are indicated in light grey. Opposing arrows in schemes represent position of sense and anti-sense primers, respectively. (B-F) HeLa, MCF7, HMEC-1, PASMC, SGBS preadipocytes, LNCaP, DU145 and HEK293T cells were kept under ambient conditions for 48 hours, before RNA was isolated and analyzed by RT-qPCR. In addition to levels of *HIF3A* consensus sequence (B), also individual expression levels of *HIF3Atv1* (C), *HIF3Atv2* (D), *HIF3Atv3* (E) and *HIF3AtvBC* (F) in HeLa, MCF7 and HMEC-1 were assessed. Values are displayed as ratio to 18S rRNA. (n.d.: not detected, n = 4)

#### 4.1.2 *HIF3A* promoter is inaccessible in MCF7

Variations of transcript levels are often associated with differences in chromatin accessibility. Therefore, we determined the DNasel sensitivity (and thus the accessibility) of the *HIF3A* promoter regions in the different cell lines giving rise to the different splice variants. Due to the proximity of exons 1a and 1b (distance 1300 bp), we only could distinguish between a distal region upstream of both, exon 1a and 1b, and a proximal region upstream of exon 1c, which is located more than 5 kb downstream of exon 1b. The accessibility of both *HIF3A* promoter regions was significantly higher in HMEC-1 cells compared to the tumor cell lines HeLa and MCF7. However, while HeLa cells still showed intermediate accessibility to both promoter regions (25% and 39%), *HIF3A* promoter accessibility was lowest in MCF7 cells (14% and 7%) (Figure 12). As control we assessed promoter accessibility of both the highly accessible housekeeping gene glycerol aldehyde phosphate dehydrogenase (*GAPDH*) and the commonly silenced gene encoding beta globin (*HBB*) in all three cell lines; we could observe full accessibility (> 95%) of *GAPDH* promoter and no accessibility of *HBB* promoter (Figure 12 B and C, respectively). Taken together, our results suggest a mechanism of chromatin remodeling for the distal promoter of *HIF3A* in MCF7 and HeLa cells.

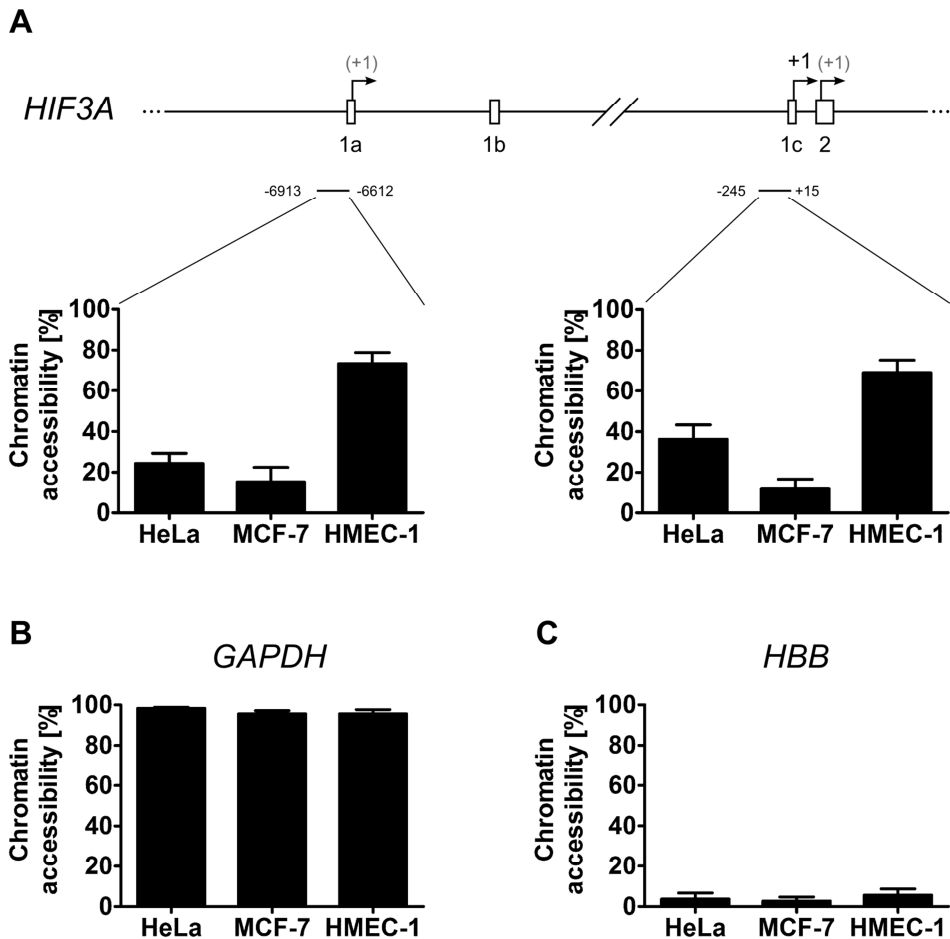


**Figure 12: Chromatin accessibility of distal (E1a & E1b) and proximal (E1c) *HIF3A* promoter regions are increased in HMEC-1 compared to HeLa and MCF7 cells.**

HeLa, MCF7 and HMEC-1 cells were treated with DNase1 or not, before genomic DNAs were isolated. (A) *HIF3A* promoter region upstream of exons 1a and 1b as well as region containing exon 1c were analyzed by qPCR. *GAPDH* (B) was used as a positive control and *HBB* (C) was used as a negative control (n = 3). Arrows on top of the exons in the genomic scheme indicate the beginning of the coding sequence (ATG) of different splice forms.

#### 4.1.3 *HIF3A* promoter is hypermethylated in HeLa and MCF7 cells

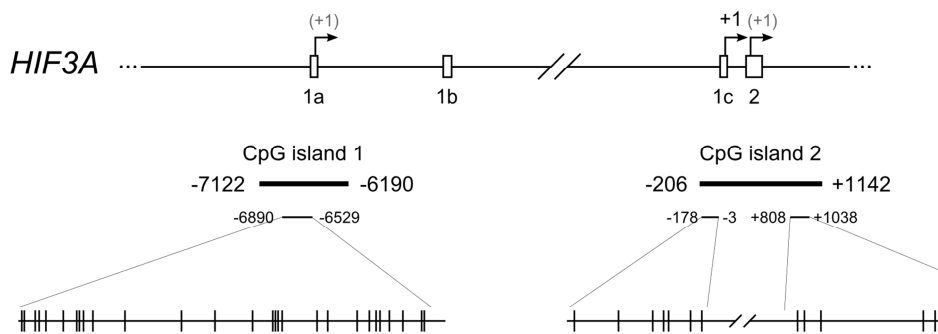
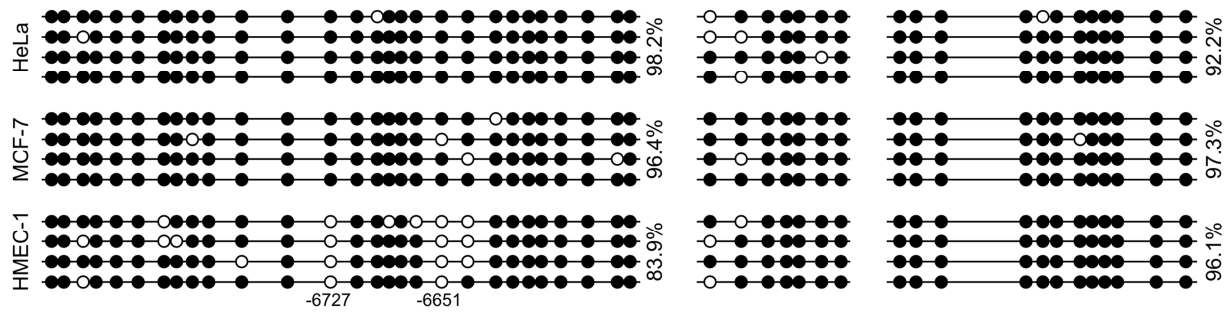
The degree of accessibility of DNA has been previously shown to be related to the level of methylation in CpG rich promoter areas (CpG islands) (Nguyen et al. 2001), of which we found two in the promoter of *HIF3A*, located around 7000 bp upstream of exon 1c (CpG island 1) and covering exons 1c and 2 (CpG island 2) (Figure 13). To assess the methylation status of the two *HIF3A* promoter regions, we performed bisulfite sequencing with genomic DNA isolated from HMEC-1, HeLa and MCF7 cells. We could show that the CpG island 1 is extensively hypermethylated in HeLa and MCF7 cells (98,2% and 96,4%, respectively), while in HMEC-1 cells less CpG sites were found to be methylated (83,9%) (Figure 13). In contrast, CpG island 2 was hypermethylated in all tested cell lines, indicating a dependency of *HIF3A* expression by the epigenetical status of the distal region upstream of exons 1a and 1b.

#### 4.1.4 *HIF3A* promoter shows open chromatin in HMEC-1 cells

Further epigenetic factors which can influence the accessibility of the DNA are histone modifications such as acetylated histone 3, in particular lysine residues 9 and 14 (H3Ac [H3K9/K14Ac]), which is considered as a marker for active open chromatin, and trimethylated lysine 9 of histone 3 (H3K9me3), which is a marker for inactive closed chromatin (Koch et al. 2007; Wang et al. 2008).

We assessed the presence of these histone modifications in the distal *HIF3A* promoter region in HeLa, HMEC-1 and MCF7 cells by chromatin immunoprecipitation using antibodies against H3Ac and H3K9me3. Co-precipitated DNA was analyzed by qPCR using primers specific for the region of the *HIF3A* promoter containing exon 1a.

Interestingly, in both tumor cell lines the amount of the repressive marker H3K9me3 was approximately double the amount of the respective permissive marker H3Ac, while in HMEC-1 cells H3K9me3 levels were even lower than the levels of H3Ac, (Figure 14), suggesting a more active chromatin structure in HMEC-1 cells compared to the tumor cell lines.

**A****B**

**Figure 13: Methylation of CpG island 1 is decreased in HMEC-1 cells compared to HeLa and MCF7.**

(A) Diagram of the region of *HIF3A* exons 1a/1b and exons 1c/2 showing the location of methylated CpGs (represented by vertical bars). Underneath, amplicons including the positions of the primers used for nested PCR are depicted. (B) Representation of the methylation pattern detected in four clones derived from the HeLa, MCF7 and HMEC-1. Cells were cultured under ambient conditions before genomic DNA was prepared. Genomic DNA was treated with bisulfite before amplification of the *HIF3A* promoter region covering exon 1a or exon 1c by PCR, fragments were subcloned and sequencing was performed. Open circles = unmethylated CpGs; filled circles = methylated CpGs. Frequency of methylated CpGs is shown next to diagram of four clones as percentage. Values indicate the average of methylated CpG sites within the analysed region. Arrows on top of the exons in the genomic scheme indicate the beginning of the coding sequence (ATG) of different splice forms.

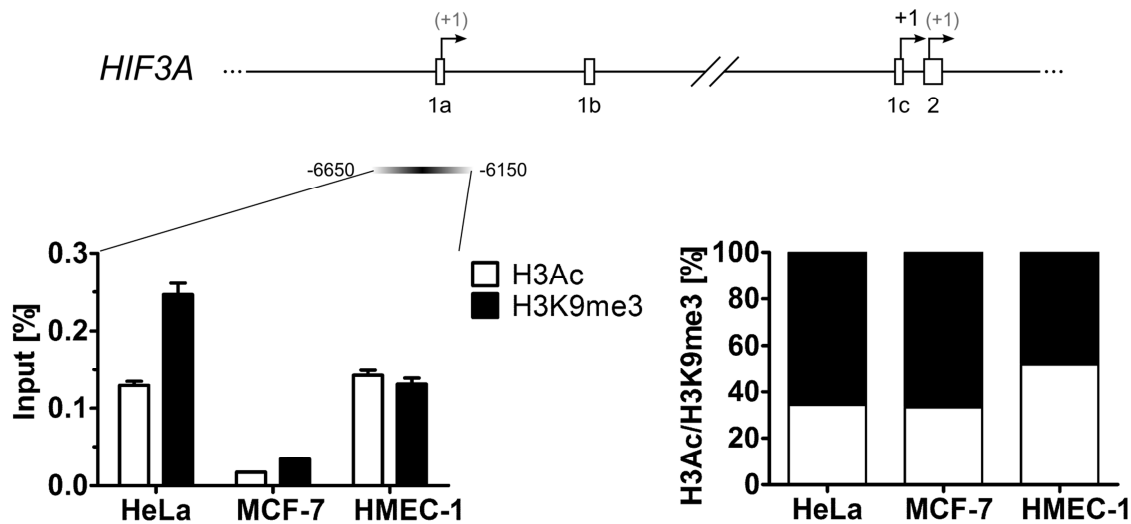


**Figure 14: Marker for active chromatin (H3Ac) is increased in HMEC-1 cells in *HIF3A* promoter region containing exon 1a.**

HeLa, MCF7 and HMEC-1 cells were cultured under ambient conditions and subsequently fixed with formaldehyde for chromatin immunoprecipitation (ChIP) assay. After cell lysis, precipitation of H3Ac and H3K9me3 was performed. Co-precipitated DNA was analyzed by qPCR using primers specific for the *HIF3A* promoter region representing the distal promoter region, containing exon 1a and 1b. Values are presented as % of the input (left panel) or as the ratio of H3Ac/H3K9me3 (%) (n = 3). Arrows on top of the exons in the genomic scheme indicate the beginning of the coding sequence (ATG) of different splice forms.

#### 4.1.5 *HIF3A* expression inversely correlates with tumor stage in lung

In order to test the association of *HIF3A* expression with tumor status, a comparison of normal and cancer tissues was done using a TissueScan Cancer and Normal Tissue cDNA Array by OriGene Inc. The used array contained 96 samples covering 8 different cancers from breast, colon, kidney, liver, lung, ovarian, prostate, and thyroid gland. For each tissue, 2-3 samples were present resembling normal tissue, taken from adjacent tumor biopsy. In addition, 1-3 samples from tumor stages I, II, III, and IV were present, respectively. The amount of provided cDNA was prenormalized by the manufacturer by  $\beta$ -actin. Thus, qPCR with primers for *HIF3A* consensus sequence was performed. Values given in Figure 15 are displayed as log2 with lowest value set to 1. We observed for all tissues heterogenous *HIF3A* expression with differences of up to 50 fold within a distinct tissue and almost 300 fold overall (Figure 15A). The overall mean relative expression of *HIF3A* in normal tissue was

1.86 fold higher compared to cancer tissue, however not statistically significant. Within the different tissues, only in lung samples an inverse correlation of tumor stage and *HIF3A* transcript levels was detected ( $r^2=0.9508$ ) (Figure 15B).

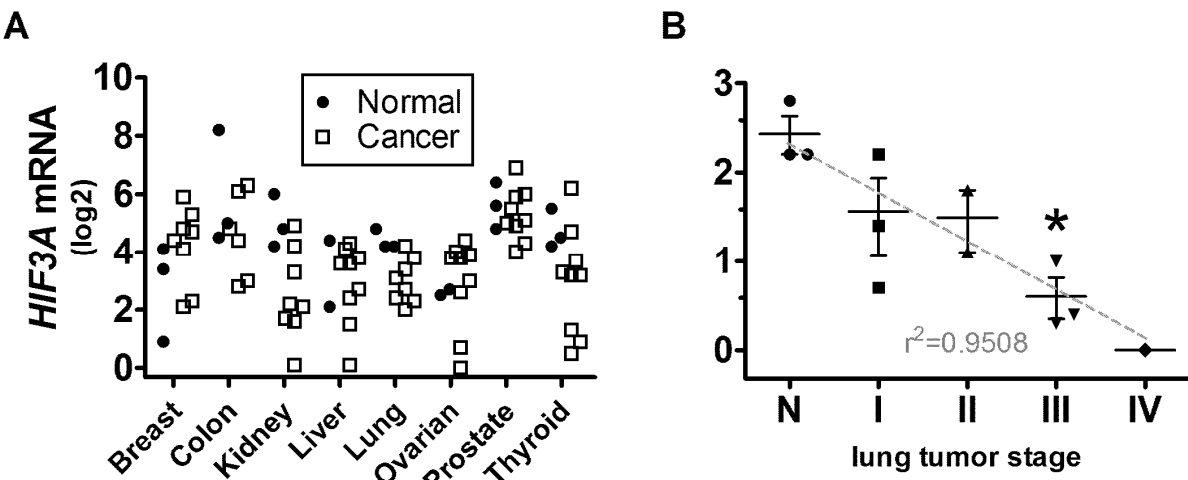


**Figure 15: *HIF3A* expression varies in different tissues and inversely correlates with tumor stage in lung.**

TissueScan Cancer and Normal Tissue cDNA Array was used for gene expression analysis of consensus *HIF3A* sequence either in all tissues (A) or specifically in lung tissues of different tumor stages (B), ranging from normal adjacent tissue (= N) over I, II and III to IV. Lowest Ct-value from qPCR was set arbitrarily to 1, either from all samples (A) or from lung tissue (B). Fold change of residual samples is given as log2-values. (B) Dashed grey line represents regression line with a correlation efficient of  $r^2=0.9508$ . mRNA data is shown as log2 values compared to the lowest value in each graph respectively ( $n = 3$ ; \* $p < 0.05$ ).

#### 4.1.6 *HIF3A* is induced by hypoxia in HMEC-1

To gain more insight into the regulation of *HIF3A* expression, HMEC-1, HeLa and MCF7 cells were exposed to 1% O<sub>2</sub> for 24 hours and mRNA levels of *HIF3A* consensus sequence were analyzed by RT-qPCR. In HeLa and MCF7 cells, *HIF3A* was detected under normoxic conditions; however no induction could be observed with hypoxic stimulus. In contrast, *HIF3A* was induced 2.4 fold by hypoxia in HMEC-1 cells indicating a role of HIF-3 $\alpha$  in the hypoxic response in these cells (Figure 16).

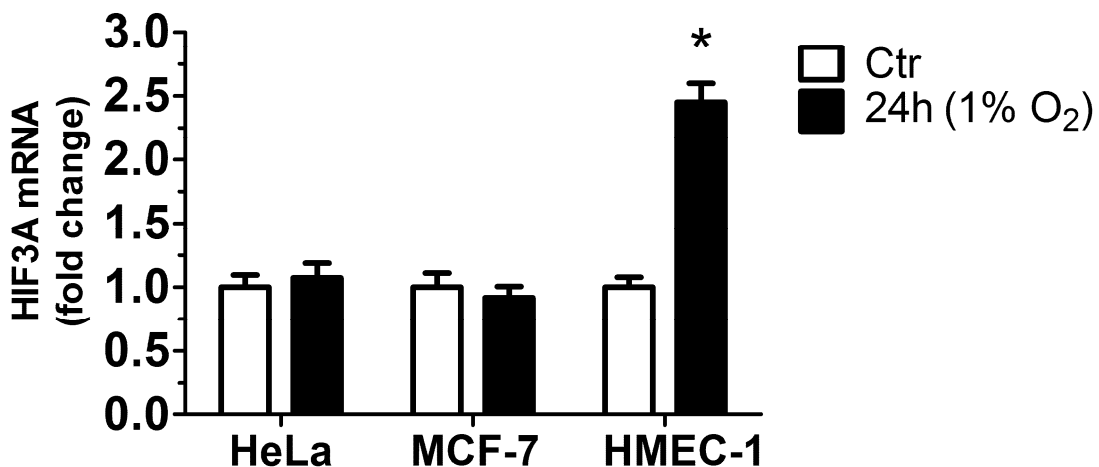


**Figure 16: *HIF3A* expression is induced in HMEC-1 cells but not in HeLa or MCF7 cells.**

HeLa, MCF7 and HMEC-1 cells were exposed to 1% O<sub>2</sub> for 24 hours before RNA was isolated and analyzed by RT-qPCR. Values were normalized to  $\beta$ -actin. Normoxic mRNA levels were set to 1. mRNA data are shown as relative increase to control (n = 4; \*p < 0.05).

## 4.2 *HIF-3 $\alpha$* inhibits *HIF-2* activity in endothelial cells under hypoxia

### 4.2.1 Time- and dose-dependent *HIF3A* induction

We detected substantial *HIF3A* basal expression as well as its induction by hypoxia in HMEC-1 cells. Thus, we chose this cell line to investigate the role of HIF-3 $\alpha$  in the context of HIF-1 $\alpha$  and HIF-2 $\alpha$  in the adaptation to hypoxia. mRNA and protein levels were analysed by RT-qPCR and Western blot, respectively. We started with exposing HMEC-1 cells to different oxygen concentrations (0.1-21% O<sub>2</sub>) and increasing time periods (2-72 hours). Of note, HMEC-1 stained with Trypan blue showed no significant change in vitality even after 48 hours of hypoxia (data not shown).

*HIF3A* mRNA levels increased dependent on the oxygen concentration with a 1.8 fold or 2.9 fold increase when exposed to 1% oxygen or 0.1% oxygen, respectively, for 24 hours (Figure 17A). A further analysis of the time dependence of *HIF3A* mRNA levels in response to severe hypoxia (0.1% O<sub>2</sub>) showed that *HIF3A* mRNA levels increased at 8 hours (1.9 fold) and peaked at 48 hours of hypoxia (3.2 fold)

(Figure 17B). To test whether the observed induction of *HIF3A* is triggered by a transcriptionally independent mechanism, we added an inhibitor of transcription, actinomycin D (5 $\mu$ g/ml), or not to the cells before exposing them to 0.1% O<sub>2</sub> for 16 hours. The previously observed hypoxic induction of *HIF3A* was completely abolished by the use of actinomycin D compared to control (Figure 17C), indicating an active transcriptional process. Differently, we found that *HIF1A* transcript levels decreased time dependently to 41% (Figure 17D). Concomitantly, *HIF2A* expression was unaffected by hypoxia (Figure 17E).

Next we determined the levels of four known HIF target genes under severe hypoxia, amongst them two HIF-1 target genes, namely phosphoglycerate kinase 1 (*PGK1*) and egl-9 family hypoxia-inducible factor 3 (*EGLN3*) and two HIF-2 target genes, namely cluster of differentiation 82 (*CD82*) and plasminogen activator inhibitor-1 (*PAI1*). mRNA levels of both, *PGK1* and *EGLN3*, were increased after 8 hours (1.9 and 1.6 fold, respectively), peaking at 24 hours (3.4 and 4.1 fold, respectively) with a decay at 48 hours (2.8 and 1.9 fold, respectively) (Figure 17F/G). Concomitantly, *PAI1* mRNA levels showed the same pattern (2 fold, 2.3 fold and 1.8 fold) (Figure 17H). However, we could not detect a significant hypoxic induction of *CD82* levels at any time point (Figure 17J). Nevertheless, our results indicate an activation of the HIF pathway in HMEC-1 cells under severe hypoxia.

In addition, we assessed protein levels of tested HIF subunits. In contrast to the corresponding mRNA, HIF-1 $\alpha$  and HIF-2 $\alpha$  protein levels peaked within the observation period at 8 hours and 24 hours of severe hypoxia, respectively (Figure 18A/B). Compared to the rapidly decreased HIF-1 $\alpha$  levels the decay of HIF-2 $\alpha$  levels was delayed within 48 hours of hypoxia (Figure 18A/B). Despite various intense approaches, we could not analyze protein levels of HIF-3 $\alpha$  due to ambiguous identification of the correct bands.

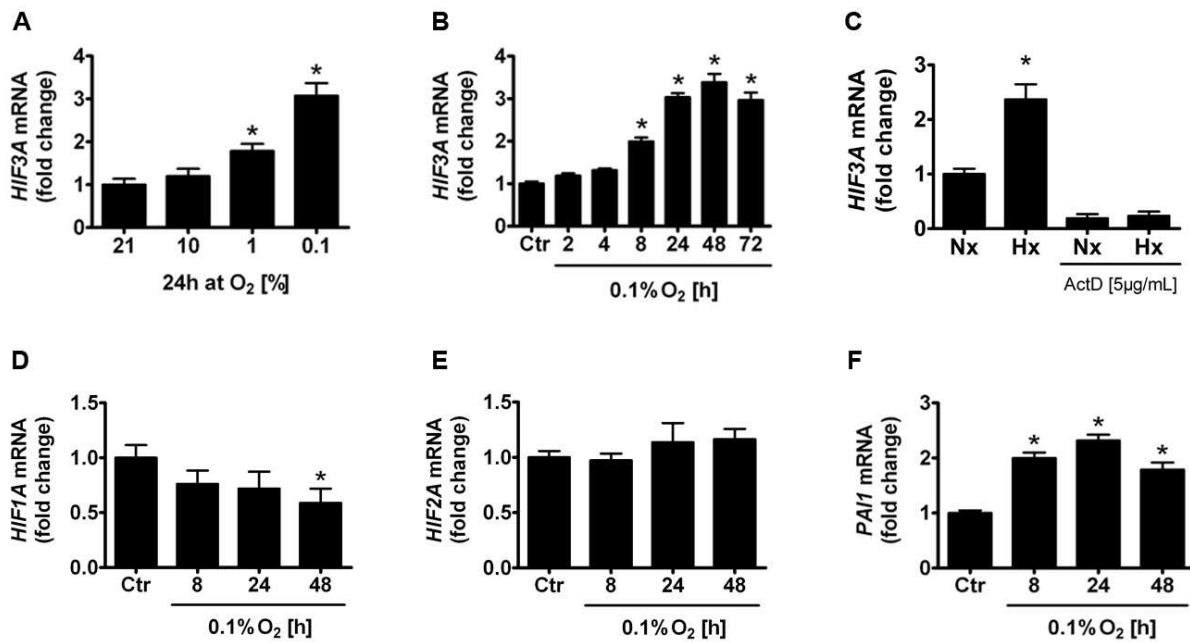


**Figure 17: *HIF3A* is transcriptionally induced under hypoxia in a dose- and time-dependent manner.**

Expression of *HIF3A* mRNA in HMEC-1 cells is dose- and time dependently increased (A, B) which is a transcriptional process as shown by means of the inhibitor of transcription Actinomycin D (C). mRNA levels of *HIF1A* are decreased (D) whereas *HIF2A* mRNA is unaffected (E). HIF-1 target genes *PGK1* and *EGLN3* peak after 24 hours of hypoxia (F, G). Also, HIF-2 target gene *PAI1* is induced (H), whereas HIF-2 target gene *CD82* is unchanged (J). RNA was analyzed by RT-qPCR. RT-qPCR values were normalized to  $\beta$ -actin. Normoxic mRNA levels were set to 1. mRNA data are shown as relative increase to control ( $n = 3$ ;  $*p < 0.05$  compared to control).

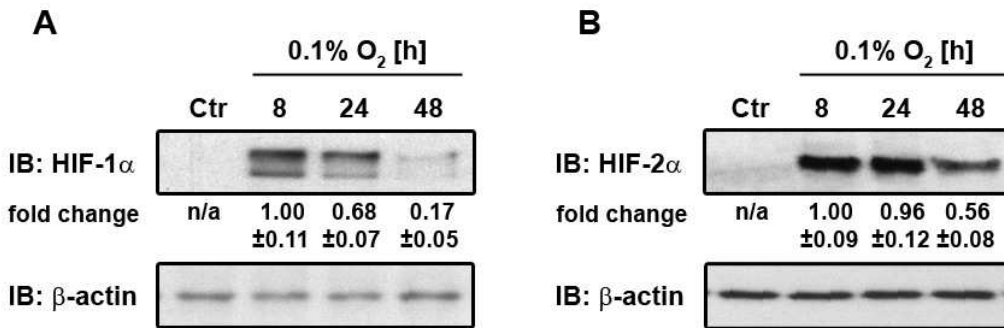


**Figure 18: HIF-1 $\alpha$  and HIF-2 $\alpha$  proteins are induced by hypoxia in HMEC-1 cells.**

Human microvascular endothelial cells (HMEC-1) were exposed for increasing time periods to 0.1% oxygen. Both, HIF-1 $\alpha$  (A) and HIF-2 $\alpha$  (B) are induced under hypoxia, peaking at 8 and 24 hours respectively. Western blot analyses were performed with antibodies against human HIF-1 $\alpha$  and HIF-2 $\alpha$ .  $\beta$ -actin served as a loading control. Western blot panels are representative for 3 independent experiments. Fold changes indicated derive from densitometry and show fold change  $\pm$  standard deviation (n/a: not available).

#### 4.2.2 HIF-3 $\alpha$ inhibits HIF target gene expression

Next, we sought to determine the involvement of HIF-3 $\alpha$  in the regulation of HIF activity. We assessed the effect of HIF-3 $\alpha$  on a luciferase constructs driven either by three hypoxia response elements (HRE) from the enhancer of the erythropoietin gene *EPO* or a construct containing the proximal 800bp fragment of the *PAI1* promoter, including a previously described HRE site (HRE-2 (Fink et al. 2002)). Control of expression was monitored by Western Blot (Figure 19, respective panel on the right hand side).

Compared to control cells, which showed significantly enhanced luciferase activity in response to hypoxia, HIF-3 $\alpha$  overexpressing cells showed decreased luciferase activity under hypoxic conditions (Figure 19A and E). Normoxic luciferase activity was not affected by overexpression of HIF-3 $\alpha$ .

In line, mimicking hypoxia by overexpression of HIF-1 $\alpha$  and, to a larger extent HIF-2 $\alpha$ , increased luciferase activity with both constructs (Figure 19B, F, C, and G). However, co-expression of HIF-3 $\alpha$  decreased HIF-1 $\alpha$ - and HIF-2 $\alpha$ -driven *PAI1* promoter activity (Figure 19B, F, C, and G). Eventually, we analysed the effect of HIF-3 $\alpha$

absence under hypoxia on luciferase constructs by introduction of siRNA directed against *HIF3A*. We confirmed the hypoxic induction of luciferase activity with both constructs under control conditions. With silenced *HIF3A* however, we observed a non-significant increase of promoter activity under normoxic and hypoxic conditions. Although the effect of *HIF3A* knockdown was less pronounced than with overexpression, we further focused on the role of HIF-3 $\alpha$  in the HIF-mediated response to hypoxia.

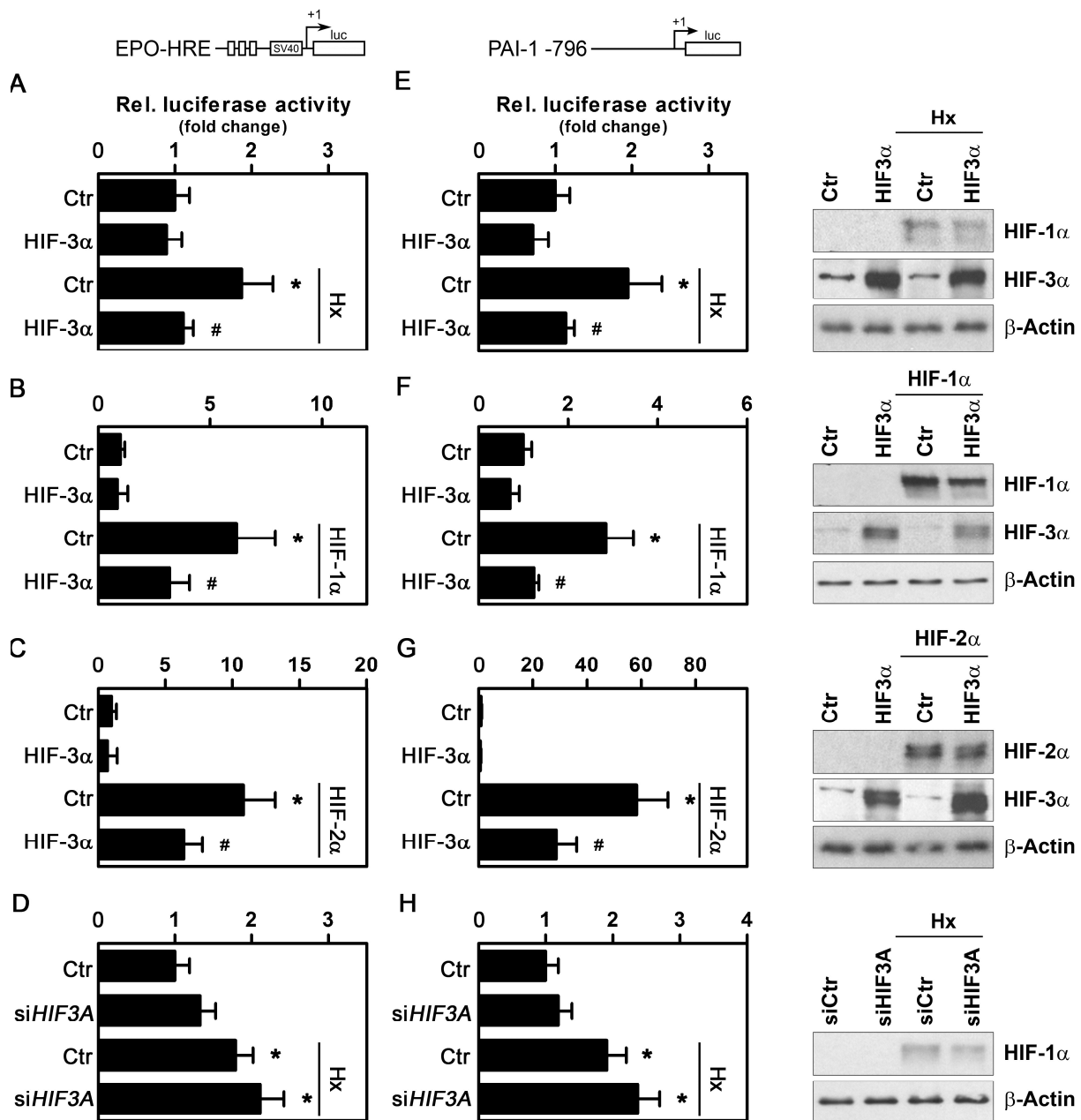


**Figure 19: HIF-3 $\alpha$  inhibits HIF-driven luciferase activity.**

HEK293T cells were cotransfected with the luciferase reporter constructs pGL-EPO-HRE (A-D) or pGL3-PAIpro-796 (E-H) and a vector encoding HIF-3 $\alpha$  (A-C, E-G) or siRNA against *HIF3A* (D and H). In addition, cells were transfected either with HIF-1 $\alpha$  (B and F) or with HIF-2 $\alpha$  (C and G) and exposed to hypoxia (A, D, E, and H) or not (B-C and F-G). Luciferase assay was performed. Values  $\pm$  SD represent the fold induction of luciferase activity ( $n = 3$ ; \* $p < 0.05$  vs. control; # $p < 0.05$  vs. Ctr under hypoxia (A and E), HIF-1 $\alpha$  (B and F) and HIF-2 $\alpha$  (C and G) respectively). Normoxic control was set to 1. On the right hand side, an expression control for respective proteins of each condition is given. Labeling on top of each panel indicates overexpressed proteins and/or stimulus. Labeling on the right hand side indicates antibodies used.

#### 4.2.3 HIF-3 $\alpha$ inhibits HIF-2 mediated *PAI1* expression

To further elucidate the mechanism underlying the inhibitory effect of HIF-3 $\alpha$  on hypoxia or HIF-1 $\alpha$ /HIF-2 $\alpha$  induced *PAI1* expression, we silenced the expression of *HIF1A* or *HIF2A* or *HIF3A* by RNAi and subsequently exposed HMEC-1 to severe hypoxia for increasing time periods. As expected, all RNAi decreased their respective target mRNAs (Figure 20A-C), as can be seen also on the protein level (Figure 21). Remarkably, silencing of *HIF1A*, but not *HIF2A*, also decreased *HIF3A* mRNA levels. The effect of silencing HIF- $\alpha$  subunits on target genes was variable. *PGK1* showed a decreased to abolished induction when *HIF1A* was silenced. However no effect was observed with the silencing of *HIF3A* (Figure 20D). When analyzing potential HIF-2 $\alpha$  target genes we observed that the hypoxic induction of *PAI1* mRNA was abolished by silencing of *HIF2A*. However, silencing of *HIF3A* increased *PAI1* expression in response to hypoxia (Figure 20E), suggesting that HIF-3 $\alpha$  modulates the HIF-2-driven induction of *PAI1* expression in vascular endothelial cells. Interestingly, depletion of *HIF1A* also increased *PAI1* mRNA levels (Figure 20E). Similar effects were obtained with another set of RNAi (data not shown).

Additionally we analyzed protein levels of HIF-1 $\alpha$ , HIF-2 $\alpha$  and of PAI-1 under severe hypoxia with distinct silencing of the HIF  $\alpha$ -subunits. For PAI-1 protein levels, we observed an enhanced hypoxic induction with silencing of *HIF3A* compared to control, similarly to the results seen with *PAI1* mRNA. With the knockdown of HIF-2 $\alpha$  hypoxic induction of PAI-1 was abolished while it was increased with HIF-1 $\alpha$  being silenced (Figure 21).

HIF-1 $\alpha$  and HIF-2 $\alpha$  showed decreased protein levels after silencing their respective gene. Interestingly, silencing of *HIF2A* increased HIF-1 $\alpha$  protein levels compared with the use of scrambled siRNA; vice versa we could not see any induction of HIF-2 $\alpha$  by the knockdown of *HIF1A* (Figure 21). Our data extends the idea, that HIF-3 $\alpha$  exerts a modulatory role on HIF-2 activity in the expression of PAI-1.

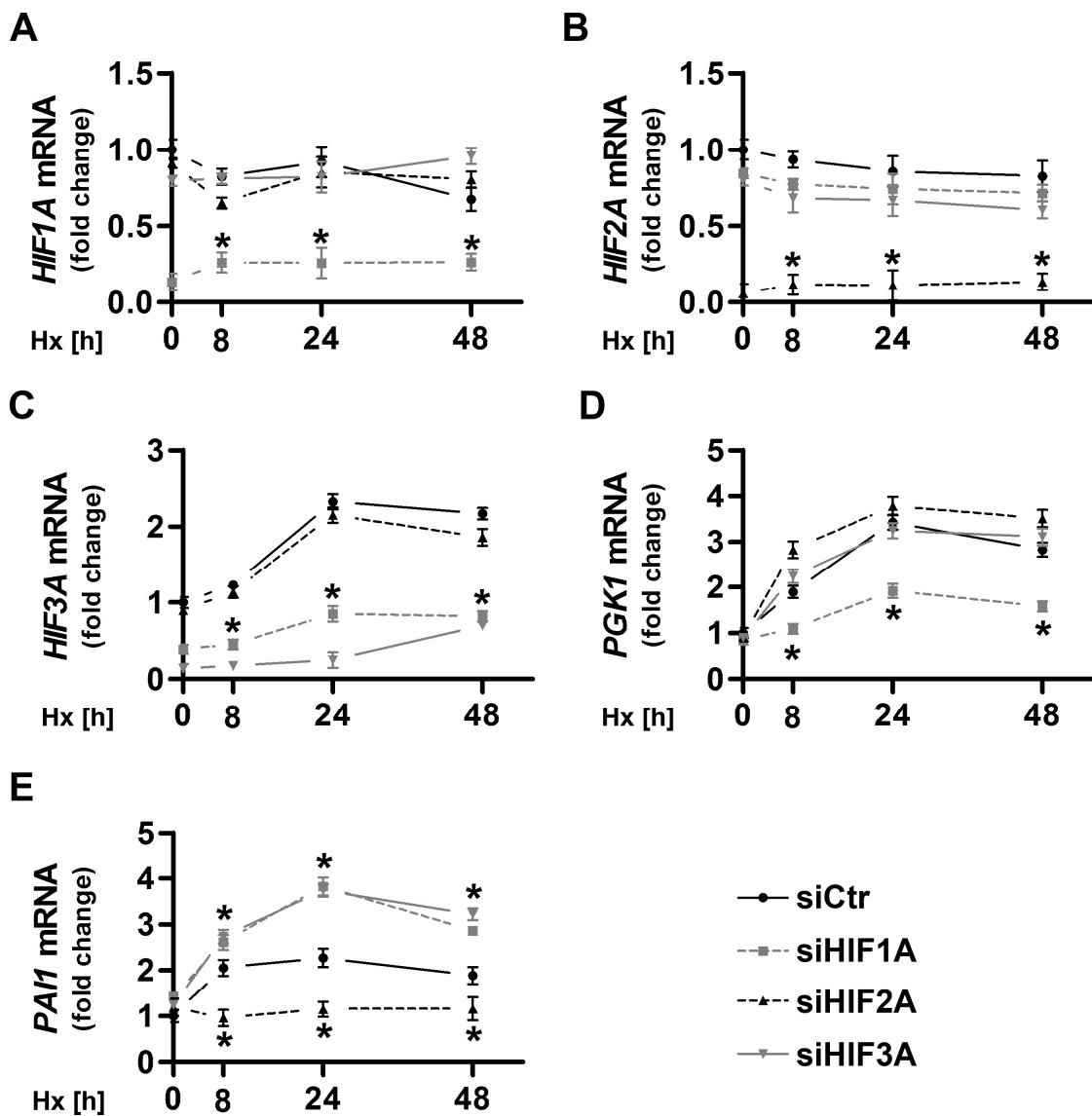


**Figure 20: HIF-3 $\alpha$  inhibits HIF-2-driven PAI1 expression.**

HMEC-1 were transfected with siRNA against either *HIF1A* or *HIF2A* or *HIF3A* or with scrambled RNA (siCtr) and exposed to hypoxia (0.1% O<sub>2</sub>) for increasing time periods. Total RNA was analyzed by RT-qPCR. (A-C) Depletion of target gene was efficient with specific siRNA as shown by quantification of levels of *HIF1A*, *HIF2A* and *HIF3A*. (C) *HIF3A* levels were induced by prolonged hypoxia. Depletion of *HIF1A* diminished this induction. (D) *PGK1* levels increased upon hypoxia and decreased with knock-down of *HIF1A* but not with that of *HIF2A* or *HIF3A*. (E) *PAI1* levels also increased after hypoxia, while depletion of *HIF2A* abolished this induction. Depletion of *HIF1A* or *HIF3A* led to an hyperinduction under hypoxic conditions. Values were normalized to  $\beta$ -actin. Normoxic mRNA levels were set to 1. Data is shown as relative increase to control (n=3; \*  $p < 0.05$  compared to respective time point in siCtr transfected cells).

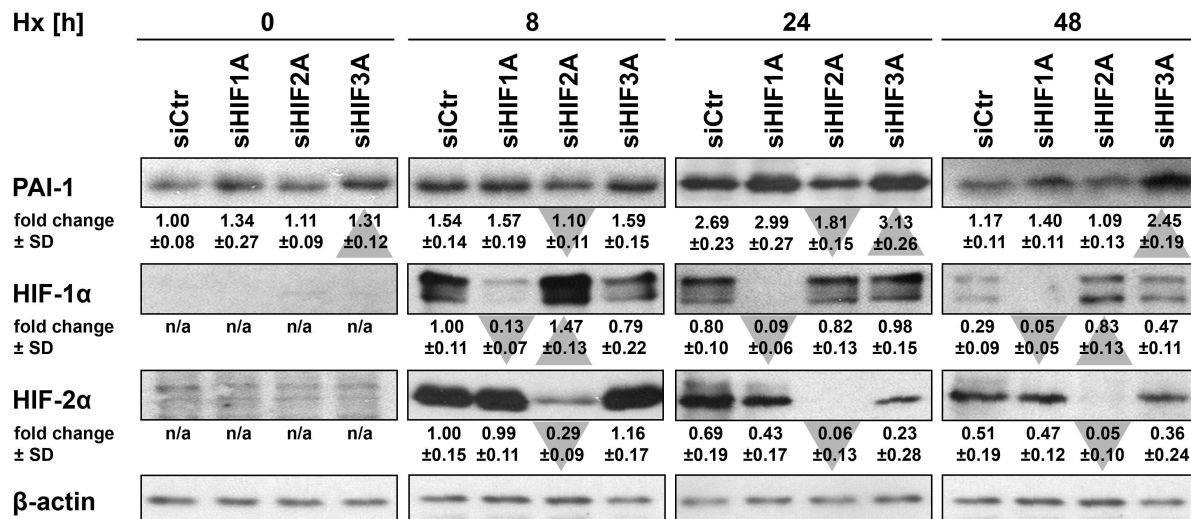


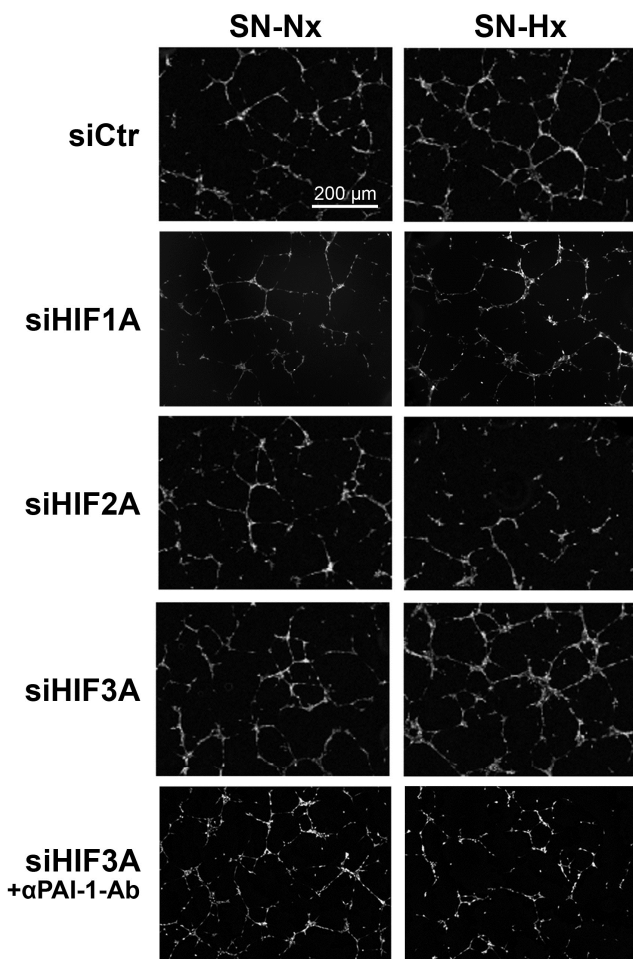
**Figure 21: HIF-3α inhibits HIF-2-driven PAI-1 expression.**

Western blot analyses were performed with antibodies against: HIF-1α, HIF-2α and PAI-1. β-actin served as loading control. Western blot panels are representative for 3 independent experiments. Below each panel the values from normalized densitometry analysis are given as fold change ± SD. (n=3; Shaded triangles resemble p < 0.05 compared to respective time point in siCtr transfected cells, indicating either statistically significant increase [up-pointing triangle] or decrease [down-pointing triangle], respectively) (n/a: not available).

#### 4.2.4 HIF-3α inhibits PAI-1-mediated angiogenesis

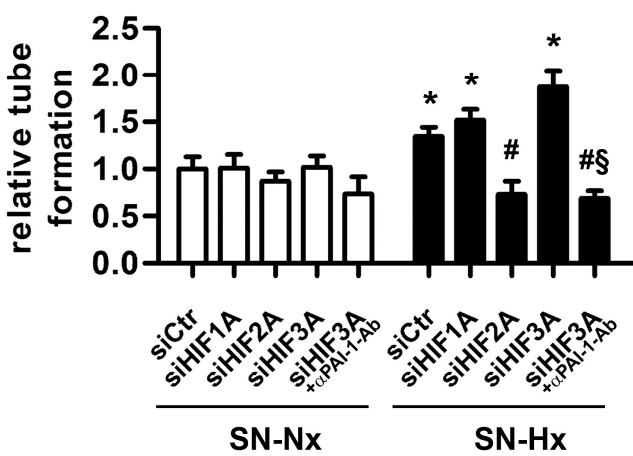
Since PAI-1 has been previously shown to promote endothelial proliferative processes, we examined the functional consequences of HIF-3α on PAI-1-mediated tube formation under hypoxic conditions. To this end, *HIF1A*, *HIF2A* or *HIF3A* were silenced by RNAi and HMEC-1 were exposed to hypoxia for 48 hours. Since PAI-1 can be secreted and exerts paracrine functions including the induction of angiogenic processes, the supernatants of the different endothelial cell cultures were collected and used to stimulate HMEC-1 plated on microslides coated with matrigel. While the supernatant from hypoxic control cells stimulated tube formation, this effect was not observed from supernatants derived from hypoxic cells deficient in *HIF2A* (Figure 22). On the contrary, supernatants from hypoxic cells deficient from *HIF3A* showed increased tube formation, supporting the finding of HIF-3α acting modulatory on HIF-2 driven *PAI1* expression. Upon addition of an inhibitory antibody against PAI-1, the proangiogenic effect of supernatants derived from HIF-3α deficient cells

was abolished, indicating that the proangiogenic effect induced in HIF-3 $\alpha$  deficient cells was mediated by PAI-1 (Figure 22). Interestingly, silencing of *HIF1A* also led to increased tube formation under hypoxic condition, supporting our previous results about HIF-1 $\alpha$  driven *HIF3A* expression.

**A**

**Figure 22: HIF-3 $\alpha$  inhibits PAI-1-dependent angiogenesis.**

HMEC-1 were transfected with siRNA against either *HIF1A* or *HIF2A* or *HIF3A* or with scrambled RNA (siCtr) and exposed to hypoxia (0.1% O<sub>2</sub>) for 48 hours or not and supernatant was collected. An aliquot of supernatant from cells silenced for *HIF3A* was mixed with an inhibitory PAI-1 antibody and incubated for 30 minutes at 37°C. Supernatants were used for stimulation of HMEC-1 plated on microslides coated with matrigel. Tube formation was monitored after 16 hours (A). Panels are representative for 3 independent experiments. Tube length was assessed by image analysis (B). Normoxic control was set to 1 (n = 3; \*p < 0.05 vs. siCtr; #p < 0.05 vs. siCtr Hx; §p < 0.05 vs. siHIF3A Hx).

**B**

#### 4.2.5 HIF-3 $\alpha$ interacts with HIF-2 $\alpha$ and ARNT

After having observed the modulatory effect of HIF-3 $\alpha$  on the function of HIF-2, we aimed to investigate the underlying mechanisms. Based on the structural similarity of HIF subunits, we determined whether HIF-3 $\alpha$  would be able to interact with the HIF-subunits involved in the activation of PAI-1 expression, HIF-2 $\alpha$  or ARNT, using co-immunoprecipitation. Human embryonic kidney cells (HEK293T) were cotransfected with V5-tagged HIF-3 $\alpha$  and either HIF-2 $\alpha$  or ARNT. Western blot analysis showed that HIF-3 $\alpha$  can bind to both, HIF-2 $\alpha$  and ARNT, *in vitro* (Figure 23A).

Next, we investigated whether both HIF-3 $\alpha$ /ARNT and HIF-3 $\alpha$ /HIF-2 $\alpha$  complexes can bind to HRE sequences on DNA. To this end, we performed an electromobility shift assay (EMSA). In brief, *in vitro* translated HIF-subunits (HIF-2 $\alpha$ , ARNT and HIF-3 $\alpha$ ) were mixed with fluorescence labeled DNA probes containing either the wildtype HRE sequence of the human *PAI1* promoter (*PAI1*-HREwt) (Fink et al. 2002) or a mutated and therefore defective HRE sequence (*PAI1*-HREmut). The mixture was separated on an agarose gel and formation of DNA-protein complexes were detected by a fluorescence scanner. While the HIF-3 $\alpha$ /ARNT complex bound to the wildtype HRE sequence, but not to the mutated sequence (Figure 23B), the HIF-2 $\alpha$ /HIF-3 $\alpha$  complex did not bind to either sequence (Figure 23B), suggesting two potential ways for HIF-3 $\alpha$  of modulating HIF-2 activity.

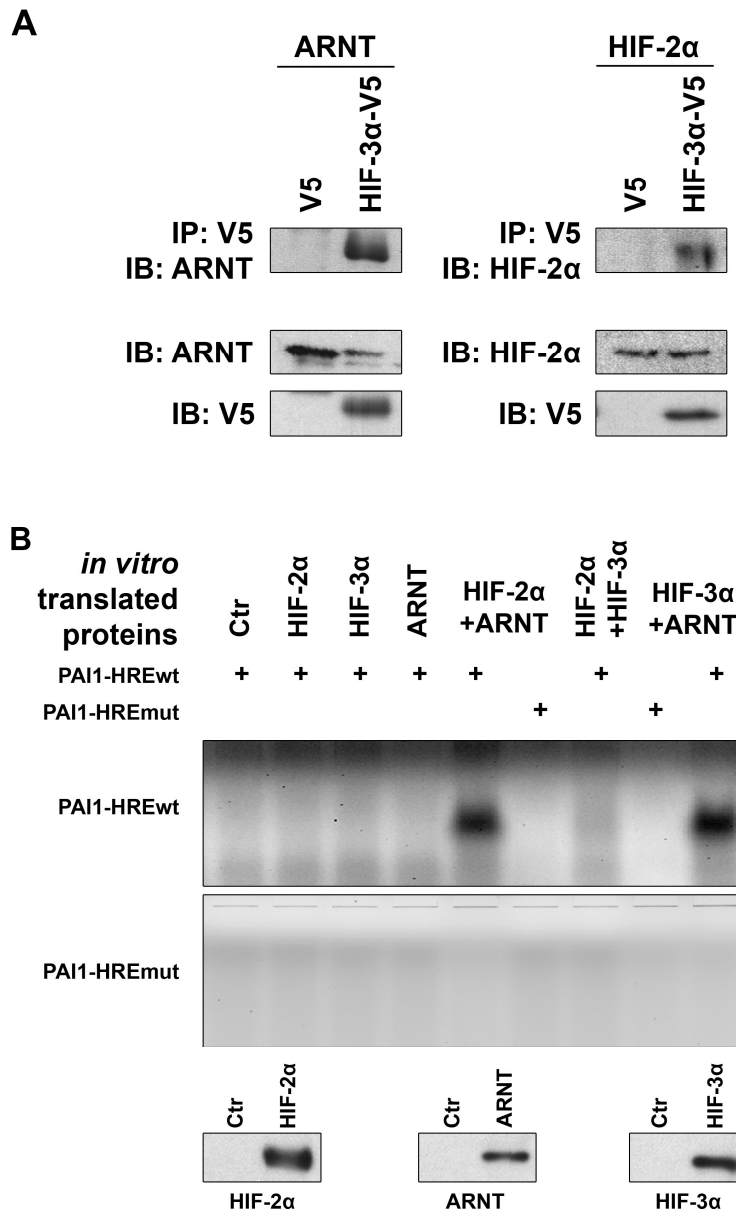


**Figure 23: HIF-3 $\alpha$  binds to DNA in complex with ARNT but not with HIF-2 $\alpha$ .**

HEK293T cells were cotransfected with V5-tagged HIF-3 $\alpha$ 1 and either HIF-2 $\alpha$  or ARNT. After lysis, proteins were immunoprecipitated with V5 antibody and detected by Western blot analysis using antibodies specific for HIF-2 $\alpha$  or ARNT (A). Western blot panels are representative for 3 independent experiments. *In vitro* translated HIF-subunits (HIF-2 $\alpha$ , ARNT and HIF-3 $\alpha$ ) were mixed in combinations according to labeling with Cy5-labeled DNA probe containing the published HRE sequence located at -197/-188 base pairs of the *PAI1* promoter. The mixture was separated on an agarose gel and formation of DNA-protein complexes was identified by scanning the gel for fluorescence (B). Gel is representative for 3 independent experiments. *In vitro* translated HIF subunits were identified by Western blot analysis with antibodies against: HIF-2 $\alpha$ , HIF-3 $\alpha$  and ARNT (C).

#### 4.2.6 HIF-3 $\alpha$ /ARNT binds to *PAI1* promoter

Based on our results, HIF-3 $\alpha$  modulates HIF-2 activity by preventing HIF-2 $\alpha$  from binding to the HRE of the target gene promoter either by interacting with HIF-2 $\alpha$  itself, forming a  $\alpha/\alpha$ -dimer, or by the interaction with the  $\beta$ -subunit ARNT with a subsequent occupation of the HRE by the HIF-3 $\alpha$ /ARNT complex.

To further examine these two scenarios, HMEC-1 cells were depleted from *HIF2A* or *HIF3A*, exposed to hypoxia for 48 hours, a time point at which HIF-3 $\alpha$  is presumably expressed and active (Figure 17). Cells were subsequently fixed with formaldehyde for chromatin immunoprecipitation (ChIP) assay. After cell lysis, precipitation of HIF-2 $\alpha$  and ARNT was performed. Co-precipitated DNA was analyzed by qPCR using primers specific for the region of the *PAI1* promoter containing the HRE-2 sequence.

Occupation of the analyzed *PAI1* promoter region by HIF-2 $\alpha$  was only marginally increased in control cells by hypoxia, but was significantly increased in HIF-3 $\alpha$  deficient cells under hypoxia (Figure 24A) indicating that HIF-3 $\alpha$  limits HIF-2 $\alpha$  occupation of the *PAI1* promoter under hypoxic conditions. In line, when *HIF2A* and *HIF3A* were simultaneously depleted, HIF-2 $\alpha$  binding to the *PAI1* promoter was abolished. Next, we determined ARNT occupation of the same *PAI1* promoter region. Under hypoxic conditions, ARNT occupation of the *PAI1* promoter was enhanced as expected. Depletion of HIF-3 $\alpha$  did not affect normoxic or hypoxic *PAI1* promoter occupancy by ARNT (Figure 24B). However, binding of ARNT to the *PAI1* promoter was abolished in response to hypoxia when both, *HIF2A* and *HIF3A* were silenced suggesting that at sustained hypoxia HIF-2 $\alpha$  or HIF-3 $\alpha$  would be the preferential interaction partners for ARNT to bind to *PAI1* promoter region (Figure 24B). Our results suggest two possible mechanisms for the observed inhibition of HIF-2 $\alpha$  activity by HIF-3 $\alpha$ : either by competition of HIF-2 $\alpha$  and HIF-3 $\alpha$  for ARNT or, assuming an excess of ARNT, by competition of the complexes HIF-2 $\alpha$ /ARNT and HIF-3 $\alpha$ /ARNT for binding to DNA. To evaluate both possibilities, HMEC-1 cells were exposed to hypoxia for increasing time periods and co-immunoprecipitation of HIF-2 $\alpha$  with ARNT was performed. While ARNT interacted with HIF-2 $\alpha$  when cells were exposed to hypoxia for 8 hours, this interaction diminished at longer time points (Figure 24C) suggesting that at prolonged

hypoxia HIF-3 $\alpha$  outcompeted HIF-2 $\alpha$  in binding for ARNT thereby controlling *PAI1* expression.

A

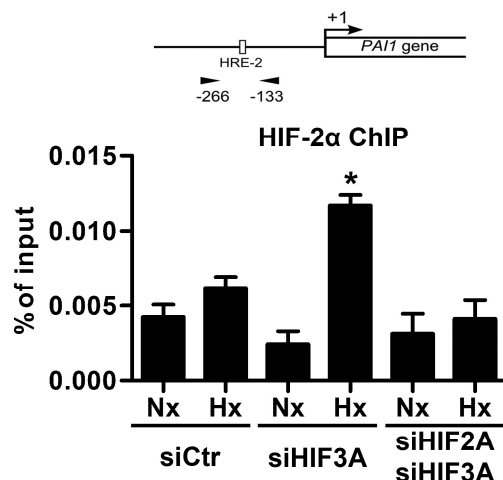
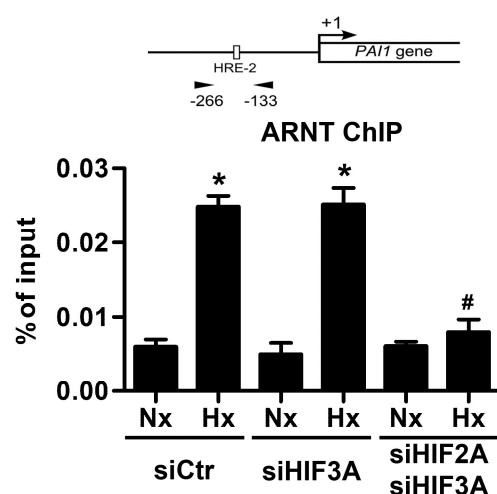


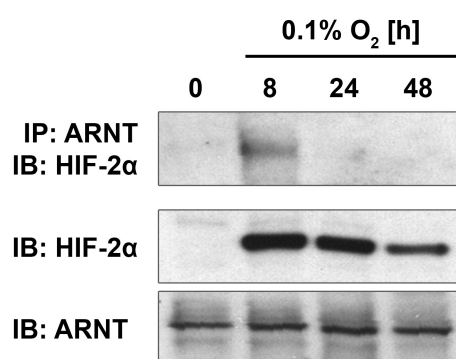
**Figure 24: HIF-3 $\alpha$  inhibits HIF-2 by outcompeting HIF-2 $\alpha$  for the interaction with ARNT subsequently binding to DNA.**

HMEC-1 were transfected with siRNA against either *HIF1A* or *HIF2A* or *HIF3A* or with scrambled RNA (siCtr) and exposed to hypoxia (0.1% O<sub>2</sub>) for 48 hours or not and subsequently fixed with formaldehyde for chromatin immunoprecipitation (ChIP) assay. After cell lysis, precipitation of HIF-2 $\alpha$  (A) and ARNT (B) was performed. Co-precipitated DNA was analyzed by qPCR using primers specific for the region of the *PAI1* promoter containing the HRE sequence and is presented as percent of the input (n = 3, \*p < 0.05 vs. normoxic siCtr, #p < 0.05 vs. hypoxic siHIF3A). (C) HMEC-1 were exposed to hypoxia (0.1% O<sub>2</sub>) for increasing time periods. After lysis, proteins were immunoprecipitated with ARNT antibody and detected by Western blot analysis using antibodies specific for HIF-2 $\alpha$  or ARNT. Western blot panels are representative for 3 independent experiments.

B

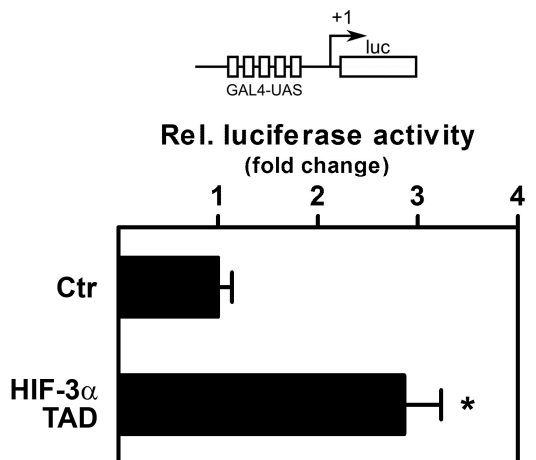
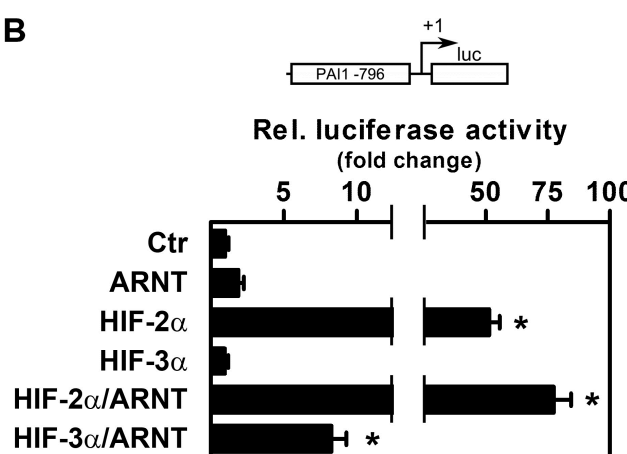
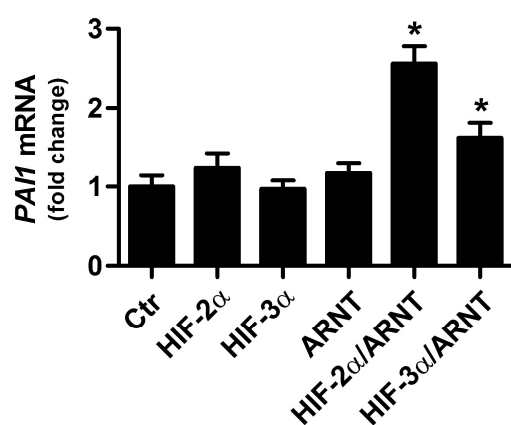


C



#### 4.2.7 Exogenous HIF-3 $\alpha$ /ARNT induces *PAI1* expression

Besides the postulation of an inhibitory role of HIF-3 $\alpha$  in the response to hypoxia, it was also shown before, that co-expression of the HIF-3 $\alpha$ /ARNT complex exerts a mild transactivation effect on selected HIF target genes (Heikkilä et al. 2011). We could show that endogenous HIF-3 $\alpha$ /ARNT complex does bind to genomic *PAI1* promoter, which resulted in intermediate *PAI1* expression levels under sustained hypoxia rather than completely blocking it. Hence, we tested the transactivatory properties of HIF-3 $\alpha$  including the effect of exogenous HIF-3 $\alpha$ /ARNT on *PAI1* expression in our system. First, we provided evidence, that the C-terminally located TAD domain of HIF-3 $\alpha$  exerts moderate transactivation characteristics. This result was achieved by a luciferase assay with a GAL4-DNA binding domain/HIF-3 $\alpha$ -NTAD fusion protein which activated a GAL4-upstream activation sequence 2.89 fold (SD  $\pm$ 0.33) compared to control (Figure 25A). In addition, we analysed exogenous coexpression of HIF-3 $\alpha$  and ARNT on a *PAI1* promoter containing luciferase reporter construct by transfecting HEK293T cells with the respective plasmids. While expression of HIF-3 $\alpha$  or ARNT alone did not show significant activation (Figure 25B), coexpressing HIF-3 $\alpha$  and ARNT clearly increased *PAI1* promoter activity ( $8.41 \pm 1.07$ ). HIF-2 $\alpha$  alone or coexpressed with ARNT led to a more than 50 fold increase compared to control vector (50.3 fold and 76.1 fold, respectively). For assessing the effect of coexpressed HIF-3 $\alpha$ /ARNT on endogenous *PAI1* gene expression, HMEC-1 cells were either transfected with solely HIF-2 $\alpha$ , HIF-3 $\alpha$  or ARNT, or cotransfected with HIF-2 $\alpha$ /ARNT or HIF-3 $\alpha$ /ARNT. Cells were kept under ambient conditions for 48 hours before *PAI1* mRNA levels were analysed by RT-qPCR. Whereas coexpression of HIF-2 $\alpha$ /ARNT clearly increased mRNA levels of *PAI1* ( $2.58 \pm 0.33$ ) (Figure 25C), expression of the single HIF-subunits did not significantly change *PAI1* expression, probably by limited availability of ARNT. Interestingly, we found a mild increase of *PAI1* mRNA levels in cells overexpressing HIF-3 $\alpha$ /ARNT ( $1.71 \pm 0.15$ ) (Figure 25C), indicating that in the presence of ARNT HIF-3 $\alpha$  can, although to a lower extent than HIF-2 $\alpha$ , induce transactivation of *PAI1*.

**A****B****C**

**Figure 25: HIF-3 $\alpha$  exerts transactivatory properties on PAI1 when coexpressed with ARNT.**

HEK293T cells were cotransfected with (A) a plasmid coding for a GAL4 DNA binding domain/ HIF-3 $\alpha$  TAD fusion protein and a GAL4 upstream activation sequence (UAS) containing luciferase reporter plasmid or (B) with solely HIF-2 $\alpha$ , HIF-3 $\alpha$  or ARNT, or contranfected with HIF-2 $\alpha$ /ARNT or HIF-3 $\alpha$ /ARNT together with a *PAI1* promoter containing luciferase reporter plasmid. Subsequently luciferase assay was performed. Values  $\pm$  SD represent the fold induction of luciferase activity (n = 4; \*p < 0.05 vs. control). (C) HMEC-1 cells were either transfected with solely HIF-2 $\alpha$ , HIF-3 $\alpha$  or ARNT, or contranfected with HIF-2 $\alpha$ /ARNT or HIF-3 $\alpha$ /ARNT. Cells were kept under ambient conditions for 48 hours before endogenous *PAI1* mRNA levels were analysed by RT-qPCR. RT-qPCR values were normalized to  $\beta$ -actin. Cells transfected with control construct mRNA levels were set to 1. mRNA data are shown as relative increase to control (n = 3; \*p < 0.05).

## 5 Discussion

In the present study, we investigated the molecular mechanism determining the basal transcription of *HIF3A* in cell lines HMEC-1, HeLa and MCF7. We showed that *HIF3A* abundance differs between cell types, which is dependent on epigenetic mechanisms, such as genomic DNA methylation and histone modifications at the distal promoter region of *HIF3A*. Moreover, we found that HIF-3 $\alpha$  protein negatively regulates HIF-2-driven PAI-1 expression in HMEC-1 cells, resulting in a moderate PAI-1-mediated angiogenesis in endothelial cells under prolonged hypoxia. Moreover, we show that HIF-3 $\alpha$  exerts its modulatory properties by outcompeting HIF-2 $\alpha$  for the interaction with ARNT resulting in binding of the HIF-3 $\alpha$ /ARNT complex to DNA, exerting moderate transactivatory properties. Taken together, our data suggest an important role of HIF-3 $\alpha$  in fine-tuning of the HIF system in sustained hypoxia. Given its absence in some tumor cell lines and its modulating properties regarding angiogenic processes, *HIF3A* might be involved in tumor suppression or at least serve as a tumor marker.

### 5.1 *HIF3A* expression in different cell lines

The description of human *HIF3A* by Gu et al. brought up a new HIF subunit which was, based on luciferase assays, characterized as potentially regulating the classical HIF system (Gu et al. 1998; Hara et al. 2001). It also led to a controversial discussion about its endogenous expression levels, as others (based on personal communication) and we could not unambiguously identify endogenous HIF-3 $\alpha$  protein. Thus, we determined transcript levels of *HIF3A* in different cell lines as a potential surrogate of its function. In the present study we showed differential basal expression of transcript variants in different cell lines as shown by gene expression analysis. We chose different tumor cell lines (HeLa, MCF7, LNCaP, DU145, and HEK293T), which are widely used in cancer research, thereby representing degenerated and unphysiological cellular properties. Representing primary cell lines with physiologic morphology and functionality, PASMC and SGBS preadipocytes were chosen. In addition, immortalized HMEC-1 cell line was selected due to its similarity with normal human micro-

vascular endothelial cells with retained morphologic, phenotypic, and functional characteristics of normal human microvascular endothelial cells (Ades et al. 1992). The initial investigation of consensus *HIF3A* transcripts revealed an interesting grouping. Whereas sensitivity of qPCR was hardly high enough for detecting *HIF3A* in tumor cell lines, the basal expression of *HIF3A* in primary and primary-like cells was around 1000 times higher. Despite this striking difference, the number of different cell lines used does not allow a conclusive connection between *HIF3A* levels and tumor status. For our downstream analyses including the detailed quantification of different transcript variants, HeLa, MCF7 and HMEC-1 cells were chosen. Primary cell lines were not included due to their limited life span for subsequent experiments.

In order to investigate all ten described and suggested transcript variants (tv) (Maynard et al. 2003; Pasanen et al. 2010), we exemplarily chose the first three RefSeq annotated mRNAs of *HIF3A* in the nucleotide database of NCBI, each representing a transcript with an alternative first exon: *HIF3Atv1* (RefSeq accession number: NM\_152794) originating from exon 1c, *HIF3Atv2* (NM\_022462) originating from exon 1b and *HIF3Atv3* (NM\_152795) originating from exon 1a (compare **Figure 11A**). For our analysis, we also included the detection of transcript variant BC (GenBank accession number: BC\_026308) due to its structural similarity (but not identity) to the murine IPAS, which was described and characterized as an inhibitory isoform of *Hif3a*. Similarly to our findings on *HIF3A* consensus transcripts, we detected for each analysed transcript highly diverging basal expression levels in the tested cell lines, with low (*HIF3Atv1* and *HIF3Atv2*) to undetectable (*HIF3Atv3* and *HIF3AtvBC*) levels in HeLa and MCF7 cells. In HMEC-1 cells, expression of all variants was detected and was 2-3 orders of magnitudes higher compared to detectable variants in HeLa and MCF7 cells. Thereby we confirmed recent findings of Pasanen et al. (2010) showing low to undetectable levels of transcripts originating from exon 1a, 1b and 1c of the *HIF3A* locus in various cancer cell lines. We also extended their findings of higher basal expression levels of *HIF3A* transcripts in cDNA from fetal and adult tissues by showing increased basal expression of *HIF3A* in non-tumor HMEC-1 cell line. Although several reports show that detection of *HIF3A* is highly variable in different tissues (Maynard et al. 2005; Pasanen et al. 2010), a detailed characterization

of *HIF3A* expression clearly indicating its function is still not published. Our results are adding another piece of puzzle by showing differential *HIF3A* expression between different cell lines, representing tumor and non-tumor cells. It remains unclear, whether the presence of a distinct isoform alone or the levels of different transcripts reflects diverging physiological functions, thus meriting further investigation.

## **5.2 DNA accessibility and chromatin remodeling**

As shown previously by Weis and colleagues, besides modification or degradation of mRNA, the accessibility of the respective promoter is closely linked to the expression levels of a distinct gene (Zabel et al. 2000). When we assessed the accessibility of two regions (a distal region close to exons 1a and 1b and a proximal region around exon 1c) in the *HIF3A* promoter by DNaseI digestion and a subsequent quantification of distinct DNA fragments by qPCR, we found in HMEC-1 a high accessibility in both regions, whereas in HeLa and MCF7 cells the accessibility was low. We thereby could correlate the expression levels with accessibility of two regions within the promoter of *HIF3A*. A recent report of Druliner et al. (2013) developed a model linking the general and locus-specific roles of chromatin structure to lung cancer progression. In this context, our results of *HIF3A* promoter being highly accessible in non-tumor HMEC-1 cells and low accessible in tumor cell lines HeLa and MCF7 support this model indicating tumor related regulation of *HIF3A* expression.

It has been described by Cedar and Bergman, that accessibility of genomic DNA is mainly determined by chromatin remodeling (Cedar and Bergman 2009). This dynamic process of chromatin structure modification tightly controls gene expression by providing or denying access for the transcription machinery to DNA. Essentially, two mechanisms contribute to the repositioning of histones within the chromatin, namely a covalent bonding of functional groups (e.g. by histone acetyl transferases and histone methyl transferases) and an ATP-driven nucleosome movement (e.g. by SWI/SNF) (Clapier and Cairns 2009). These epigenetic mechanisms were shown to be involved in cancer-associated silencing of known tumor suppressor genes (Jones and Baylin 2002; Oshiro et al. 2003); thus we investigated whether genomic DNA

methylation is associated with the downregulation/inactivation of *HIF3A* in tumor cell lines.

### **5.3 DNA methylation**

Analysis of DNA methylation by genomic bisulfite sequencing showed a correlation of *HIF3A* expression with the extent of methylation of specific CpG dinucleotides located in CpG island 1 spanning exon 1a. Interestingly, the degree of hypomethylation observed in HMEC-1 cells was less profound than we expected based on the differences in mRNA levels. We found only 12-15% less methylated CpGs in HMEC-1 compared to MCF7 and HeLa, which could be attributed to the immortalized status of HMEC-1 compared to classical primary cell lines.

In contrast, CpG island 2 spanning exons 1c and 2 was extensively hypermethylated in all tested cell lines, suggesting a regulatory role of only CpG island 1 but not CpG island 2 in the transcription of *HIF3A*. We thereby extended recent findings of Maha-patra et al. (2012) who suggested *HIF3A* as a biomarker for prostate cancer. Their suggestion is based on a hypermethylation CpG island 1 in the *HIF3A* promoter in prostate cancer samples with hypomethylation of adjacent non tumor tissue. It is interesting to note that none of the CpG sites within CpG island 2 itself is differentially methylated in tested cell lines. In contrast, such a difference is observed for sites NM\_152794.3:c.1-6627 and NM\_152794.3:c.1-6751 in CpG island 1. Whereas these sites are fully methylated in MCF7 and HeLa cells, in HMEC-1 methylation of the aforementioned CpG sites is aberrant. These positions might represent distinct binding sites for chromatin remodeling proteins such as the methyl CpG binding protein 2 (MeCP2) which serves as a cofactor in the chromatin remodeling by binding to methylated DNA with a subsequent recruitment of histone deacetylases. Minor changes in DNA methylation might also contribute to the regulation of the expression of *HIF3A* transcripts including those originating from downstream located alternative transcription start sites. It should still be noted, that the differences in methylation within tested cell lines does not fully account to the observed huge differences in mRNA levels, as current studies consider unmethylated CpG islands to be linked with active transcription of the respective gene (Weber et al. 2007). However, a recent study by

Buck et al. (2013) on clear cell renal cell carcinoma found a decreased chromatin accessibility while the level of DNA-methylation remained unchanged. Moreover, another study revealed that a cluster of methylated CpG sites instead of CpG islands resulted in silencing of certain genes. (Zou et al. 2006). Thus, an analysis containing a larger number of specimens might elucidate whether hypomethylation of particular sites contribute to the observed increased *HIF3A* transcription or whether it is rather a DNA-methylation independent mechanism.

Interestingly, a recent publication by Dick and colleagues revealed that increased body-mass index (BMI) is associated with increased CpG methylation at the *HIF3A* locus in blood cells and adipose tissue (2014). The three probes, which showed a statistically highly significant association, are located in intron 1. Thus, they are outside of the two described CpG islands in the 5' region of the *HIF3A* locus, which were analyzed in the present study. Meta-analyses performed in the above mentioned BMI study suggest that increased CpG methylation of the *HIF3A* locus is not causing higher BMI but rather is the result of it (Dick et al. 2014). However, they observed an inverse association between CpG methylation and expression of *HIF3A*, which we also found in our studies. Although neither they nor we did reveal the underlying mechanism for the correlation of methylation and expression of *HIF3A*, it does show the importance of HIF signaling and its regulation by DNA methylation. Further work needs to be done to decipher the association of *HIF3A* methylation and its pathophysiological meaning not only in obesity, but also in cancer.

## **5.4 Histone modification**

Although DNA methylation represents a major mechanism of epigenetic regulation, it has also been described that gene expression is controlled by both, DNA methylation and histone modifications (Cedar and Bergman 2009). While DNA hypermethylation is invariably associated with gene silencing (Jaenisch and Bird 2003), H3 acetylation is a typical feature of active genes (Koch et al. 2007). Conversely, H3K9me3 is a histone modification consistently associated with gene repression (Wang et al. 2008). In the present study, we sought to investigate these associations on the *HIF3A* promoter. This choice was based on the consideration that the observed difference in DNA

methylation status of the distal *HIF3A* promoter is limited to two CpGs. Our results show that association of the activating histone marks H3Ac to the distal *HIF3A* promoter is increased in HMEC-1 cells compared to HeLa and MCF7 cells. It is therefore likely that reduced H3Ac association to the distal *HIF3A* promoter, along with an increased frequency of DNA hypermethylation at specific CpG dinucleotides, contributes to the lower expression of *HIF3A* transcripts seen in HeLa and MCF7 cells. Of note, the enrichment of *HIF3A* promoter fragments differed substantially amongst the three tested cell lines (compare Figure 14). This observation was steady throughout several experiments and might be linked to the cell physiology ending up in different absolute amounts of precipitated DNA.

Although we found a potential reason for the presence and absence of *HIF3A* transcripts in different cell lines, there are certain limitations, which should be addressed in further investigations.

One interesting aspect is the dynamics of the epigenetical status under hypoxic conditions. Recently, Baugh and colleagues could show a hypoxia induced hypermethylation of the *THY1* promoter but rather on long (days) than short (hours) term hypoxia (Robinson et al. 2012). Also Shahrzad and colleagues observed a change in methylation pattern upon hypoxic stimulation, however they observed a general hypomethylation. Nevertheless, the reported effect was again linked with pronounced chronic hypoxia (Shahrzad et al. 2007). Although our results underline a pronounced silencing of *HIF3A* in selected cell lines, we cannot exclude the transcription of *HIF3A* under sustained hypoxic stress conditions.

Another aspect is for sure the mechanism how distinct genes, in particular genes that are associated with tumor suppression (maybe including *HIF3A*) are being shut off by chromatin remodelling. Currently, only the factors involved in that process are known; but how the selection of the respective gene is established and how the cells sense the negative feedback loop is only at the beginning of its elucidation.

In summary, our results demonstrate that basal expression of *HIF3A* is controlled on an epigenetic level in HMEC-1, HeLa and MCF7. DNA methylation of a region around exon 1a was shown to be involved in the control of *HIF3A* expression, since local hypermethylation leads to *HIF3A* silencing in HeLa and MCF7 cells, while the

absence of methylation of particular CpG sites is associated with abundant *HIF3A* expression observed in HMEC-1. More importantly, the fraction of acetylated histone 3 is markedly increased over H3K9me3 in HMEC-1 cells. Our data raise the possibility that previously described differences in the abundance of *HIF3A* transcripts in different cells and tissues (Pasanen et al. 2010) may be generally related to differential patterns of DNA methylation and histone modifications thereby regulating the function of HIF-3 $\alpha$  protein. Nevertheless, the observed epigenetic differences in the regulatory regions of *HIF3A* do not fully account for its differential basal expression.

When we observed an inverse correlation of *HIF3A* expression and epigenetic markers for inactive chromatin in various cell lines, we were assuming a correlation with retained physiologic properties. To get an idea about the relationship of substantial expression of *HIF3A* and cellular degeneration, cDNA from 8 tissues with different tumor stages were analyzed. The samples were taken either from adjacent tissue with normal appearance or from tumor tissue stages I to IV (in total 12 samples per tissue). We observed *HIF3A* levels spreading up to 50 fold within single tissues and almost 300 fold overall. The detected 1.86 fold elevated *HIF3A* levels in normal tissue compared to cancer tissue did not turn out to be statistically significant. Although we observed an inverse correlation of tumor stage and *HIF3A* transcript levels in lung tissue, the sample size was far to low to perform high quality statistics and to get a profound result. However, this experiment was thought to get an initial idea about an inverse association of *HIF3A* expression and tumor status thus it can be considered as a starting point for an analysis of *HIF3A* transcript levels in larger cohorts.

However, when looking for published data pointing towards a role for an association of *HIF3A* with tumor status, only few are available. Amongst it the results from “The Human Protein Atlas” showing profound immunostaining of cancer and normal tissue (Uhlen et al. 2010). Importantly, they state that protein reliability is uncertain as results are based on one antibody, which is in line with our own experience. In addition, data available from the database GENT (Gene Expression across Normal and Tumor tissue) indicates a difference in HIF3A mRNA levels in normal and tumor tissue (Shin et al. 2011). However, although the mean expression in normal tissue tends to be

slightly increased over mean expression in cancer tissue, this data from Affymetrix U133A or U133plus2 platforms also differs amongst different types of tissues and seems not to be significant. In addition, the results for *HIF3A* expression in normal tissues pancreas and liver are contradictory with database results from “Expression Atlas”, where *HIF3A* is described to be low to absent in pancreas and liver (Petryszak et al. 2014).

## 5.5 *Induction of HIF3A*

Concomitantly with the description of HIF-3 $\alpha$ , the speculation about its distinct role began. In fact, already Gu et al. started to enlight the properties of HIF-3 $\alpha$  especially in the context of hypoxia (1998). IPAS, an isoform of the murine HIF-3 $\alpha$ , was characterized as a negative regulator of HIF-1 $\alpha$  (Makino et al. 2001). In addition, as functional counterparts of IPAS, human HIF-3 $\alpha$ 1 and HIF-3 $\alpha$ BC were described (Hara et al. 2001; Maynard et al. 2005; Maynard et al. 2007; Heikkilä et al. 2011). Two features of HIF-3 $\alpha$  qualify it to act dominant negatively on the HIF system under sustained hypoxia: not containing a C-terminal transactivation domain, and being upregulated in the later phase of hypoxia (Hara et al. 2001; Pasanen et al. 2010; Augstein et al. 2011). Maynard et al. suggested on the basis of the differences in the domain structure a modulatory role of HIF-3 $\alpha$  towards the classical HIF-subunits HIF-1 $\alpha$  and HIF-2 $\alpha$  in response to hypoxia (2005). Although it was shown that human HIF-3 $\alpha$  decreased both hypoxia- and HIF-induced transactivation, these results were essentially all achieved by using exogenous HIF-3 $\alpha$  on reporter gene assays (Gu et al. 1998; Hara et al. 2001; Pasanen et al. 2010). Although these outcomes pointed to an inhibitory role of HIF-3 $\alpha$ , they nevertheless lack a physiological connection. As spatiotemporal properties of HIF-3 $\alpha$  under hypoxic conditions are virtually unknown, an exogenous overexpression of any of the HIF-3 $\alpha$  isoforms might does not reflect its endogenous function.

In this study we demonstrated that in human microvascular endothelial cells (HMEC-1), *HIF3A* mRNA levels were induced up to 72 hours of sustained hypoxia (Figure 17), extending the previous finding of Pasanen et al. (2010), who showed *HIF3A* mRNA levels induced in hepatoma cells (Hep3B) and neuroblastoma cells

(Kelly) after 24 hours of hypoxia. We found the strongest induction of *HIF3A* mRNA levels at 0.1% oxygen, suggesting a role in the adaptation to severe hypoxic conditions. These findings are in support with Forristal et al. whose study proposes that *HIF3A* is upregulated under sustained hypoxic conditions, may taking over the initial, transient role of HIF-1 $\alpha$  (Forristal et al. 2010). Of note, they were using a 5 % environmental oxygen tension in human embryonic stem cell line Hues-7, thus a direct comparison with the 0.1% O<sub>2</sub> in standard cell lines is not reliable.

Our data also shows that induction of HIF-1 $\alpha$  and HIF-2 $\alpha$  protein under prolonged hypoxia is independent of their gene transcription. Particularly the significant decay of *HIF1A* mRNA over the time seemingly contradicts the concomitantly induced protein levels. Recently, Kračun et al. suggested that this effect is mediated by  $\beta$ -3 integrin inhibiting NF $\kappa$ B triggered *HIF1A* induction (Kračun et al. 2014).

Furthermore, we chose exemplarily two HIF-1 and HIF-2 target genes in each case to analyse the effects of HIF-3 $\alpha$  silencing. For both HIF-1 target genes (*PGK1* and *EGLN3*) we found a profound induction under hypoxic condition, which is in line with previous reports (Pescador et al. 2005; Dayan et al. 2006). From the very few published HIF-2 target genes, we analysed *PAI1* and *CD82*. Whereas the latter did not change upon hypoxic stimulation, *PAI1* was found to be upregulated in hypoxia. We speculate that the discrepancy of published *CD82* expression via HIF-2 in HUVECs and our results is based both on cell line and oxygen tension differences.

## **5.6 Limitations of the reporter gene assay**

Here we show that exogenous HIF-3 $\alpha$  inhibits hypoxia-driven luciferase activity, thereby extending findings, that overexpression of HIF-3 $\alpha$  diminished HIF-1 induced luciferase levels (Hara et al. 2001; Maynard et al. 2005; Maynard et al. 2007). Although several studies reported the inhibitory effect of exogenous HIF-3 $\alpha$  in a luciferase assay (Hara et al. 2001; Maynard et al. 2005; Maynard et al. 2007), the effects of HIF-3 $\alpha$  on endogenous HIF target genes are still controversial, ranging from moderate activation to clear inhibition (Hara et al. 2001; Maynard et al. 2005; Augstein et al. 2011; Heikkilä et al. 2011).

Reporter gene assays are a powerful instrument for getting a first idea about a specific transcriptional mechanism, especially if a proper normalization and standardization is carried out. However, the results of others and ours regarding functional role of *HIF3A* can be easily misinterpreted due to two major limitations. The first shortcoming is the status of the reporter gene containing plasmid, which is episomal and moreover histone free. Thus, the conditions for the endogenous regulatory element and its counterpart within the vector are different regarding cellular localization and accessibility. The second disadvantage is the unknown spatiotemporal behavior of the studied transcription factor. Especially in the case of HIF-3 $\alpha$ , when neither the presence itself nor the appearance nor the concentration is well known, an often carried out exogenous overexpression of a HIF-3 $\alpha$  variant might lead to artificial effects. Considering the affiliation of HIF-3 $\alpha$  with the PAS protein superfamily, a massive flooding of the cell with highly unphysiological levels of HIF-3 $\alpha$  protein may end up in artificial interactions with other PAS proteins and thus in hard to interpret results. Taking into account that we and others found *HIF3A* expression upregulated in the later phase of hypoxia (Hara et al. 2001; Pasanen et al. 2010; Augstein et al. 2011) concomitantly with an early HIF-1 $\alpha$  appearance, the proclaimed inhibition of HIF-1 $\alpha$  by HIF-3 $\alpha$  is theoretically possible but might not biologically relevant due to their asynchronous appearance. Due to the above-mentioned drawbacks of a reporter gene assay, we aimed for the characterization of endogenous HIF-3 $\alpha$ . Nevertheless, the results obtained with HIF-3 $\alpha$  in reporter gene assay can be interpreted as a hint towards the involvement in the hypoxic response. In particular, reports about HIF-3 $\alpha$  being an activating transcription factor with ARNT in excess (Gu et al. 1998; Hara et al. 2001) point out a complex function of HIF-3 $\alpha$ .

## **5.7 Heterogeneous effect of HIF subunit knockdown**

We started the analysis of endogenous HIF-3 $\alpha$  by verifying our siRNAs directed against the different HIF-alpha subunits. Besides the confirmation of an efficient knockdown of its respective target, we observed a compensatory increase of HIF-1 $\alpha$  protein after *HIF2A* depletion, which appeared not on mRNA level. The underlying mechanism of this effect has recently been described by Schulz et al. (2012) when

they found a RNA binding protein that mediated enhanced translation of HIF-1 $\alpha$  concomitantly with the depletion of *HIF2A*. In addition, we were able to confirm a recent finding that *HIF3A* is a HIF-1 target gene (Pasanen et al. 2010); whether this finding exerts a regulatory negative feedback loop on HIF-1 $\alpha$  activity or the activation of a secondary HIF-member not involved in the HIF-1 $\alpha$  regulation remains elusive.

Tested HIF target genes showed different responses after depletion of *HIF1A* or *HIF2A*. As expected, HIF-1 $\alpha$  target gene *PGK1* exerted decreased or no hypoxic induction upon *HIF1A* depletion, respectively. With depletion of *HIF2A*, a hypoxic induction of *PGK1* was not be observed, suggesting that only a subset of HIF-1 target genes is susceptible for compensation by HIF-2. In contrast, *HIF2A* silencing completely abolished the hypoxic induction of *PAI1*.

When silencing *HIF3A* no alteration of *PGK1* levels could be observed. Although these findings may point to a dispensable role of *HIF3A* in the inhibition of HIF-1 $\alpha$ , we cannot exclude an effect of HIF-3 $\alpha$  also on HIF-1 activity under different conditions. Eventually, we found that plasminogen activator inhibitor 1 (*PAI1*) is a HIF-2 target gene in vascular endothelial cells, which is in line with previous reports (Sato et al. 2004; Diebold et al. 2010; Stiehl et al. 2011). Notably, the effects of HIF- $\alpha$  subunit depletion observed on mRNA level could also be monitored on protein level, particularly the depletion of *HIF3A* increased PAI-1 protein levels.

## **5.8 Functional effects of *HIF3A* depletion**

After we demonstrated that at sustained hypoxia HIF-2-driven *PAI1* expression is inhibited by HIF-3 $\alpha$ , we confirmed our observation on functional level by the inhibitory effect of HIF-3 $\alpha$  on PAI-1-mediated tube formation. By using supernatants of HIF subunit depleted and hypoxia-stimulated cells for the stimulation of cells in ambient conditions, we were mimicking the paracrine cell cell communication observed in vasculature. In addition, we minimized side effects of hypoxia on the cells. Whereas supernatant of hypoxic control cells increased tube formation, supernatant from *HIF2A* depleted hypoxic cells showed no change in tube formation clearly pointing to an indispensable role of HIF-2 $\alpha$  in the angiogenic process. In line with our previous results, supernatant of cells depleted of *HIF3A* and to a lesser extent *HIF1A* in-

creased tube formation compared to supernatant of hypoxic control cells, suggesting a pivotal role of PAI-1 in tube formation. This idea was strongly supported by the use of an inhibitory antibody against human PAI-1, which was mixed with the supernatant of *HIF3A* depleted hypoxic cells resulting in abandoned tube formation.

When discussing about angiogenesis, it is also necessary to mention the role of VEGF-A. In our setup however, paracrine signaling by VEGF-A seems to be less important, as the depletion of *HIF1A* and thus also of HIF-1 $\alpha$  target gene *VEGFA* has minor effects compared to the increased PAI-1 signaling in these cells. Our results support the idea that under physiological conditions endothelial cells are highly sensitive to VEGF-A secreted by many cell types, but usually not by endothelial cells themselves. In contrast to previous reports, our study provides a description about a functional effect of endogenous human HIF-3 $\alpha$ .

## **5.9 Revealing the modulatory mechanism of HIF-3 $\alpha$ by interaction studies**

We next focused on the investigation of the underlying mechanism of modulatory properties of human HIF-3 $\alpha$ . While the murine HIF-3 $\alpha$  isoform *lpas* was found to interact with HIF-1 $\alpha$  but not with ARNT (Makino et al. 2001), protein-protein interactions of all human HIF-3 $\alpha$  splice variants with HIF-1 $\alpha$ , HIF-2 $\alpha$  and ARNT were described in an *in vitro* system (Pasanen et al. 2010), of which we confirmed the interaction of HIF-3 $\alpha$  with HIF-2 $\alpha$  and of HIF-3 $\alpha$  with ARNT in the present study.

It is well known that heterodimerization of different HIF subunits occur *via* their N-terminally located bHLH-PAS domains. Considering the presence of 19 mammalian bHLH-PAS genes and the similarity of PAS domains amongst their transcripts (Bersten et al. 2013), it is not surprising to observe an interaction between members of the respective protein family when overexpressed. However, the tool of co-immunoprecipitation of exogenous proteins provides a first insight to potential endogenous interactions.

Subsequently to the protein-protein interactions, we showed that HIF-3 $\alpha$  is binding in a complex with ARNT to the HRE-2 sequence in the *PAI1* promoter in human endo-

thelial cells by using a cell free electromobility shift assay. In addition, both HIF-2 $\alpha$ /ARNT and HIF-3 $\alpha$ /ARNT did not bind to a mutated HRE probe, indicating that both dimers do bind to the core HRE sequence. Among human HIF-3 $\alpha$  isoforms, so far only HIF-3 $\alpha$ BC, the structural analogue to IPAS, was reported to bind *in vitro* to a HIF response element in a complex with HIF-1 $\alpha$  and HIF-2 $\alpha$ , but not with ARNT (Maynard et al. 2005; Maynard et al. 2007). However, due to the limited length of the probe and the histone free status, the observed binding properties of HIF-3 $\alpha$  can only be regarded as another hint about a possible physiological mechanism. The potential of HIF dimers for HRE binding *in vitro* might be dependent on the isoform and the chosen HRE and may not reflect endogenous situation. Nevertheless, our findings indicate two potential mechanisms, how HIF-3 $\alpha$  interferes in the HIF-2 $\alpha$ /ARNT driven transactivation of *PAI1*: either HIF-3 $\alpha$  interacts with HIF-2 $\alpha$ , thus preventing the formation of an active HIF-2 $\alpha$ /ARNT complex or HIF-3 $\alpha$  interacts with ARNT subsequently binding to the HRE in the promoter thereby sterically blocking the binding site for a HIF-2 $\alpha$ /ARNT complex. Thus we aimed for analysing the properties of endogenous HIF-3 $\alpha$ .

## **5.10 HIF-3 $\alpha$ is modulating HIF-2 $\alpha$ activity by competing for ARNT**

The detection and identification of human endogenous HIF-3 $\alpha$  is still ambiguous, so we designed experiments, which indirectly demonstrate the impact and role of endogenous HIF-3 $\alpha$  protein. In a chromatin immunoprecipitation assay we found only little HIF-2 $\alpha$  bound to the *PAI1* promoter region under prolonged hypoxia, which is in accordance with our previous results showing an intermediate transactivation of *PAI1*. We hypothesize, that with prolonged hypoxia HIF-3 $\alpha$  already started to exert its modulatory properties. Thus, with a knockdown of *HIF3A*, *PAI1* promoter occupation by HIF-2 $\alpha$  increased significantly clearly suggesting a direct impact of HIF-3 $\alpha$  presence on HIF-2 $\alpha$  activity. Concomitantly, occupation of the same promoter region by ARNT under hypoxia was already profound under control conditions and did not change with the knockdown of *HIF3A*. We therefore concluded, that in hypoxic con-

tral cells HIF-3 $\alpha$  is complexed with ARNT and bound to the *PAI1* promoter region containing the HRE-2 site. With depletion of *HIF3A*, HIF-2 $\alpha$ /ARNT complex is unhamperedly binding to the *PAI1* promoter, which can be seen in HIF-2 $\alpha$  occupation but not in ARNT occupation. Only with depletion of both, *HIF2A* and *HIF3A*, the fraction of promoter-bound ARNT under hypoxic conditions clearly decreased, excluding other interaction partners for ARNT in this setup. Thereby we demonstrated, that under sustained hypoxia also endogenous HIF-3 $\alpha$  binds in complex with ARNT to the HRE in the *PAI1* promoter (Figure 24A/B), thus elucidating the mechanism of modulating HIF-2 $\alpha$  activity and additionally confirming the physiological relevance of HIF-3 $\alpha$ /ARNT dimerization. However, it is not yet clear, whether the dimerization of HIF-3 $\alpha$  and ARNT occurs in parallel to a HIF-2 $\alpha$ /ARNT dimerization or as a competitive dimerization of HIF-3 $\alpha$  and HIF-2 $\alpha$  for ARNT.

To address this issue we performed a co-immunoprecipitation in which the hypoxia induced interaction of HIF-2 $\alpha$  and ARNT is abolished at 24 hours concomitant to still elevated HIF-2 $\alpha$  protein levels. Based on our observations of *HIF3A* mRNA levels, we assumed an induction of HIF-3 $\alpha$  protein upon prolonged hypoxic stimulation. Thus, we suggest that HIF-3 $\alpha$  outcompeted HIF-2 $\alpha$  in binding for ARNT. Although ARNT is known as a ubiquitous protein involved in different cellular processes, our results suggest that under sustained hypoxia ARNT is a limiting factor for dimerization with HIF- $\alpha$  subunits. Considering that HIF-3 $\alpha$  cannot only interact with HIF-1 $\alpha$  but also with HIF-2 $\alpha$  or ARNT *in vitro* (Pasanen et al. 2010), we assume that the observed dimerization of HIF-1 $\alpha$ /HIF-3 $\alpha$  and HIF-2 $\alpha$ /HIF-3 $\alpha$  could be endogenously attributed to the restricted pool of ARNT, thereby enabling also the dimerization of alpha subunits in between themselves and thus negatively regulating HIF-mediated gene expression. To address the question whether dimerization of HIF-3 $\alpha$  with other HIF- $\alpha$  subunits occurs endogenously under hypoxic conditions, a reliable and highly sensitive antibody against HIF-3 $\alpha$  would be necessary, which is to our knowledge currently not in sight.

## 5.11 Transactivatory properties of HIF-3 $\alpha$

In addition to the occupation of the HRE by HIF-3 $\alpha$ /ARNT, we were wondering about the transactivatory function of this complex. Thus, we performed luciferase assays with either the isolated HIF-3 $\alpha$  TAD domain fused to a GAL4 DNA binding domain or with the full-length HIF subunits. We observed not only a transactivation of an upstream activation sequence by the GAL4-HIF-3 $\alpha$ -TAD construct but also an induction of *PAI1* promoter activity by HIF-3 $\alpha$ /ARNT complex, while both proteins showed not substantial changes when overexpressed alone. Besides a strong transcriptional upregulation of endogenous *PAI1* mRNA level by HIF-2 $\alpha$ /ARNT, we observed mildly increased *PAI1* levels after coexpressing HIF-3 $\alpha$  and ARNT. Thereby, we confirmed a recent finding of Heikkilä et al. showing that coexpression of HIF-3 $\alpha$  and ARNT resulted in mild transcriptional upregulation of certain HIF target genes (2011). Whereas in our setup HIF-3 $\alpha$  alone did not significantly alter *PAI1* mRNA levels, in their report overexpression of HIF-3 $\alpha$  without the coexpression of ARNT did not show upregulation of transcription but rather downregulation of respective target genes (Heikkilä et al. 2011). The observed differences might be attributed to the differences in exogenous HIF-3 $\alpha$  and ARNT protein levels, as their overexpression is rather uncontrolled.

## 5.12 Perspectives

Based on our results we propose a model in which HIF-3 $\alpha$  is upregulated with progression of hypoxia, and interacts with HIF-2 $\alpha$ , thereby preventing further high-level transcription from its respective target genes. The impact of HIF-3 $\alpha$  on the HIF system might be dependent on the amount of HIF-3 $\alpha$  protein present in the cell. At the onset of hypoxia, HIF-3 $\alpha$  levels are low and HIF-1 and HIF-2 target genes are transactivated by HIF-1 $\alpha$ /ARNT or HIF-2 $\alpha$ /ARNT. However, with progression of hypoxia, HIF-1 induced HIF-3 $\alpha$  levels increase and modulate HIF-2-mediated gene expression. An additional modulating effect might be the interaction with HIF- $\alpha$  subunits thereby preventing dimerization with ARNT and the subsequent activation of HIF target genes. However, due to technical limitations, this point remains elusive. Accord-

ing to our findings, the predominant modulatory effect is based on the interaction of HIF-3 $\alpha$  with ARNT, thus subsequently maintaining basal transcription necessary for coping with chronic hypoxic conditions.

To summarize, we suggest that the so far described and published effects of HIF-3 $\alpha$ , inhibitory or activating, are both correct, depending on the time point of withdrawal or introduction of HIF-3 $\alpha$  in the respective cellular context.

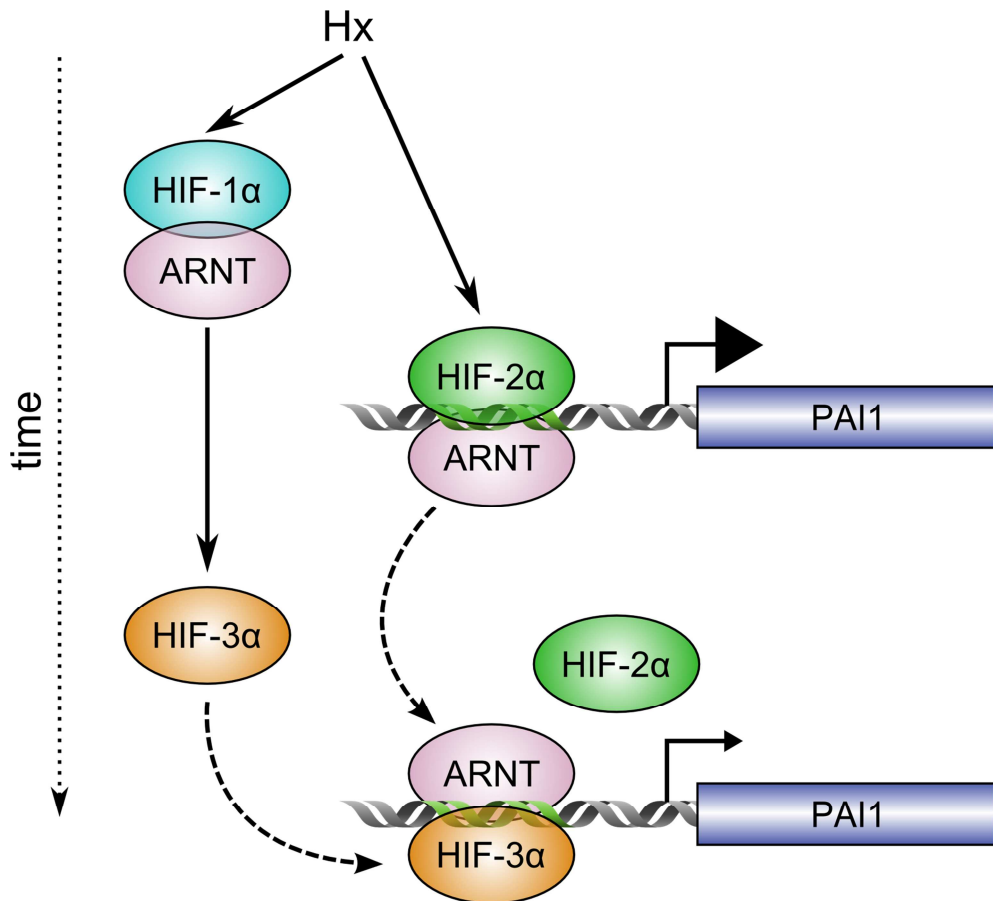


**Figure 26: Suggested mechanism of modulatory action of HIF-3 $\alpha$  on HIF-2 $\alpha$  under hypoxia.**

Upon hypoxic conditions HIF-1 $\alpha$  and ARNT dimerize and activate the respective target genes, amongst others *HIF3A*. Consecutively, HIF-2 $\alpha$ /ARNT dimers are active with prolonged hypoxia and trigger besides others genes participating in the regulation of angiogenic processes. With sustained hypoxia, the HIF-1 mediated HIF-3 $\alpha$  expression is competing with HIF-2 $\alpha$  for the binding with ARNT thereby blocking HIF-2 from binding, preventing immoderate transactivation and maintaining intermediate expression levels of target genes.

Although few studies reported an inhibitory role of HIF-3 $\alpha$  in angiogenic processes by modulating *VEGFA* (Makino et al. 2001; Augstein et al. 2011), both, identification of the inhibited factor as well as the mechanistic background were discussed ever

since. The distinct structures of human and murine HIF-3 $\alpha$  variants adds another level of complexity to the sustainable understanding of their individual physiological or pathophysiological role. The initial description of the HIF3A gene in both organisms suggested profound overlap in structure and function (Gu et al. 1998; Hara et al. 2001). However, with the report about the inhibitory murine IPAS and its unique exon 4a by Makino and colleagues, the search for a structural equivalent in human started (Makino et al. 2001; Makino et al. 2002). Due to only partial overlap of human splicing variants of human *HIF3A* with murine *Ipas* mRNA, only functional but not structural counterparts of murine IPAS were suggested. While Maynard and colleagues suggested HIF-3 $\alpha$ 4 as a dominant negative variant towards the HIF system, the group around Augstein proposed HIF-3 $\alpha$ 2 and HIF-3 $\alpha$ 3 to exert inhibitory properties on HIF (Maynard et al. 2005; Augstein et al. 2011). Considering the limited comparability of murine and human orthologs and the varying description about human *HIF3A* variants, comprehensive studies are necessary to elucidate the function of HIF-3 $\alpha$  in the respective organism.

In addition, more “HIF-3 $\alpha$  target genes” remain to be revealed in further studies. Based on our findings of *HIF3A* being induced at prolonged hypoxia, we expect a significant overlap with HIF-2 target genes rather than HIF-1 target genes.

Our data give a good insight in the relevance of HIF-3 $\alpha$  for proliferative responses of vascular endothelial cells. Bearing in mind, that HIF-3 $\alpha$  exerts modulatory properties in endothelial cells, its pathophysiological significance is subject to speculations. Proper endothelial function is inevitable in vascular biology, assuring barrier purposes, homeostasis of blood pressure and vascular tone as well as angiogenesis (Vita 2011). However, disordered endothelial cell proliferation along with concurrent exuberant neoangiogenesis results in the formation of glomeruloid structures known as the plexiform lesions, which are common pathological features of the pulmonary vessels of patients with pulmonary arterial hypertension (PAH) (Budhiraja et al. 2004). In addition, HIF-2 $\alpha$  seems to be contributing to pulmonary hypertension as shown by a gain of function mutation HIF-2 $\alpha$  in mice (Tan et al. 2013). Thus, it is tempting to speculate, that a missing modulation of HIF-2 $\alpha$  by HIF-3 $\alpha$  is contributing to the development of pulmonary hypertension and thus might exert a therapeutical value.

In addition, angiogenesis is also an important step in the transition of tumors from a confined to malignant state (Carmeliet 2000). Anti-angiogenic therapy targets vascular growth within tumors, with the aim of suppressing tumor growth and metastasis (Kubota 2012). It is known that anti-angiogenic treatment e.g. by VEGF blockade damages not only tumor vessels but also healthy vessels and results in severe problems such as hemorrhagic and thrombotic event (Verheul and Pinedo 2007; Kubota 2012). To overcome the mentioned drawbacks, HIF-3 $\alpha$  might be considered a candidate for preventing excessive angiogenesis towards a moderate and controlled neovascularization.

However, more direct insight in the role of HIF-3 $\alpha$  in regulation of proliferative pathologies developing under sustained hypoxia requires good and translatable models. Thus, confirming and extending our results by a multidimensional approach, including clinical and molecular parameters might have therapeutical implications.

## 6 Summary

The evolutionary conserved hypoxia-inducible factor (HIF) system plays a key role in an appropriate adaptation to decreased oxygen tension, ranging from systemic effects like triggering EPO secretion and angiogenic processes to cellular effects like switching pathways of energy production. In its active form, HIF is a heterodimer consisting of a constitutively expressed  $\beta$ -subunit (ARNT) and a regulated  $\alpha$ -subunit. While the function of human HIF-1 $\alpha$  and HIF-2 $\alpha$  has been well characterized, the functional role of human HIF-3 $\alpha$  is less understood.

The thesis aimed at the characterization of the transcriptional regulation of human *HIF3A* gene and the modulatory function of human HIF-3 $\alpha$  protein. A special focus was put on its effect under hypoxia on HIF-2 driven gene expression.

When analyzing the transcription of *HIF3A*, we found that its basal expression is profound in human endothelial microvascular cells (HMEC-1), a cell line with retained physiological features. In contrast, in degenerated cervical and breast cancer cell lines (HeLa and MCF-7, respectively) *HIF3A* transcripts are low to undetectable. A comparative DNasel assay revealed high accessibility of the *HIF3A* promoter in HMEC-1, in HeLa and MCF-7 cells however the accessibility was intermediate and low, respectively, indicating differential regulation of basal *HIF3A* transcription. Subsequently, we performed bisulfite sequencing of the *HIF3A* promoter region to assess its epigenetical status. We found a strong hypermethylation of tested CpG sites in HeLa and MCF-7 cells. In contrast methylation of the same region in HMEC-1 cells was less severe. Last, we analysed the chromatin status of the *HIF3A* promoter region by chromatin immune precipitation of modified histones. Whereas we found enriched levels of acetylated histone 3 (H3Ac), a marker for active chromatin, in HMEC-1 cells, a marker for inactive chromatin, trimethylated lysine 9 of histone 3 (H3K9me3), was decreased. Compared to HMEC-1 cells, the ratio of H3Ac and H3K9me3 was clearly lower in HeLa and MCF-7 cells. The analysis of regulation of human *HIF3A* in different cell lines revealed an epigenetic dependency of its basal transcription and give rise to speculations about its role in tumor cells.

When we analysed the functional role of HIF-3 $\alpha$ , we found that exposure of HMEC-1 to severe hypoxia (0.1% oxygen) increased *HIF3A* mRNA levels around 8 to 16

hours, and this response was diminished by depletion of HIF-1 $\alpha$ . In a luciferase assay, over-expressed HIF-3 $\alpha$  decreased hypoxia-stimulated promoter activity of the HIF-target gene plasminogen activator-inhibitor-1 (*PAI1*), compared to control. Oppositely, depletion of *HIF3A* by RNAi further enhanced the hypoxia-driven *PAI1* promoter activity supporting the hypothesis of HIF-3 $\alpha$  acting inhibitory on the HIF system. Consequently, depletion of *HIF3A* by RNAi increased expression of *PAI1* at later time points of hypoxia (>24h). In line, we could demonstrate that knockdown of *HIF2A* but not *HIF1A* abolished *PAI1* expression in HMEC-1 under hypoxia.

Co-immunoprecipitation assays revealed that HIF-3 $\alpha$  is able to interact with HIF-1 $\alpha$  and HIF-2 $\alpha$  as well as with ARNT. By gel shift assays, we could demonstrate that HIF-3 $\alpha$ /ARNT but not  $\alpha/\alpha$  dimers can bind to HIF-response elements on DNA. Chro-matin immunoprecipitation analysis showed that HIF-2 $\alpha$  binding to the *PAI1* promoter was maximal at 24h of hypoxia, but declined after 48h. Knockdown of *HIF3A* did not affect HIF-2 $\alpha$  binding to the *PAI1* promoter at 24h but increased HIF-2 $\alpha$  occupation of the *PAI1* promoter at 48h. In contrast, ARNT occupation of the *PAI1* promoter was stable at 24h and 48h. However, depletion of both, HIF-2 $\alpha$  and HIF-3 $\alpha$ , abolished ARNT binding to the *PAI1* promoter. These findings indicate that a HIF-3 $\alpha$ /ARNT complex competes with DNA binding of HIF-2 $\alpha$  after prolonged hypoxia. Additional studies showed weak transactivatory properties of overexpressed HIF-3 $\alpha$ /ARNT complexes in luciferase assay as well as on endogenous *PAI1* expression level. Considering these results, HIF-3 $\alpha$  seems to play a rather modulatory than inhibitory role under hypoxia. This effect was also found in a functional angiogenesis assay. With depleted HIF-3 $\alpha$ , tube formation was increased compared to control conditions, whereas knockdown of HIF-2 $\alpha$  resulted in decreased formation of tube like structures. Taken together, this study shows a diverging epigenetic regulation of basal *HIF3A* expression in different cell lines. In addition, we showed that HIF-3 $\alpha$  modulates HIF-2 activity by interacting with ARNT and a subsequent binding to the *PAI1* promoter under prolonged hypoxia. Considering suggested proangiogenic role of HIF-2 $\alpha$  in hypoxic regions of many solid tumors, our findings of an epigenetic regulation of *HIF3A* expression and the modulatory role of HIF-3 $\alpha$  under hypoxic conditions could be of potential therapeutical value.

## 7 Zusammenfassung

Die Verfügbarkeit von Sauerstoff spielt eine zentrale Rolle bei oxidativer Phosphorylierung und damit der Energieversorgung in eukaryotischen Zellen. Bei zellulärer Sauerstoffunversorgung (Hypoxie) koordinieren die evolutionär konservierten Hypoxie-induzierbaren Faktoren (HIFs) die Anpassung durch systemische sowie zelluläre Prozesse. In seiner aktiven Form besteht der Transkriptionsfaktor HIF aus einem Heterodimer aus konstitutiv exprimierter  $\beta$ -Untereinheit ARNT und einer regulierten  $\alpha$ -Untereinheit. Während HIF-1 $\alpha$  und HIF-2 $\alpha$  gut untersucht und charakterisiert sind, werden Regulation und Funktion des humanen HIF-3 $\alpha$  bisher kontrovers diskutiert.

In dieser Arbeit wurde sowohl die transkriptionelle Regulation des *HIF3A* Gens als auch die modulierende Funktion des HIF-3 $\alpha$  Proteins näher untersucht. Im Besonderen wurde der Effekt von HIF-3 $\alpha$  auf die durch HIF-2 induzierte Genexpression analysiert.

Die Expression des *HIF3A* Gens unter basalen Bedingungen war in den untersuchten Zelllinien sehr heterogen. Während in der primär-ähnlichen Zelllinie HMEC-1 hohe Spiegel von *HIF3A* Transkripten nachgewiesen wurden, konnte in verschiedenen Tumorzelllinien, darunter HeLa und MCF7, nur sehr geringe *HIF3A* Expression festgestellt werden. Dies korrelierte mit der Zugänglichkeit des *HIF3A* Promoters, welche in HMEC-1 als hoch, in HeLa und MCF7 dagegen nur als niedrig bis intermediär eingestuft wurde. Die Methylierungsanalyse des *HIF3A* Promoters in den verschiedenen Zelllinien durch Bisulfitsequenzierung ergab eine nahezu vollständige Hypermethylierung der CpG-Stellen bei HeLa und MCF7, während in HMEC-1 Zellen der gleiche Bereich weniger ausgeprägt methyliert war. Bei der Analyse der Histonmodifikationen in der Promotorregion mittels Chromatinimmunpräzipitation zeigte sich eine Anreicherung von azetyliertem Histon 3 in HMEC-1 Zellen. In HeLa und MCF7 Zellen wurde dieser Marker für aktives Chromatin in deutlich geringerem Maße nachgewiesen. Dagegen war die Anreicherung des Markers für inaktives Chromatin, trimethyliertes Lysin 9 in Histon 3, in HeLa und MCF7 Zellen deutlich stärker als in HMEC-1 Zellen. Unsere Ergebnisse deuten auf eine epigenetische Regulation des *HIF3A*-Gens hin, die in verschiedenen Zelllinien zu einer unterschiedlichen basalen Regula-

tion führen und damit zu Spekulationen hinsichtlich der Rolle von HIF-3 $\alpha$  bei Tumorzellen führen.

Zusätzlich zur Untersuchung der Transkription von *HIF3A* analysierten wir die Funktion von HIF-3 $\alpha$  in der zellulären Reaktion auf Hypoxie. Dazu wurden HMEC-1 Zellen bei 0,1% Sauerstoff kultiviert und in Ermangelung zuverlässiger Antikörper die Spiegel von *HIF3A* mRNA gemessen. Wir konnten zeigen, dass der deutliche Anstieg der *HIF3A* Transkriptionsrate zwischen 8 und 16 Stunden Hypoxie HIF-1 abhängig ist. Anschließend konnte mittels Luciferase-Assay die inhibitorische Eigenschaften von HIF-3 $\alpha$  auf die Hypoxie-induzierte Aktivität des Promotors des HIF-Zielgens *PAI1* (Plasminogen-Aktivator-Inhibitor 1) gezeigt werden. Eine Abreicherung von HIF-3 $\alpha$  durch siRNA führte dagegen zu einer verstärkten Aktivität des *PAI1*-Promotors und parallel dazu auch zu einer erhöhten Expression von endogenem *PAI1* in HMEC-1 Zellen unter hypoxischen Bedingungen. Dabei konnte gezeigt werden, dass die hypoxische Expression von *PAI1* in HMEC-1 Zellen HIF-2 und nicht HIF-1-abhängig ist. Die Charakterisierung von HIF-3 $\alpha$  mittels Coimmunopräzipitation ergab mögliche Proteininteraktionen sowohl mit HIF-1 $\alpha$  als auch HIF-2 $\alpha$  und ARNT. Beim folgenden Gel shift assay zeigte sich, dass nur HIF-3 $\alpha$ /ARNT, nicht jedoch  $\alpha/\alpha$ -Dimere an HIF reaktive Elemente der DNA binden können. Mit Hilfe von Chromatinimmunopräzipitation konnte nachgewiesen werden, dass die Bindung von HIF-2 $\alpha$  am endogenen *PAI1* Promotor nach 24 Stunden Hypoxie am höchsten war, nach 48 Stunden jedoch wieder geringer wurde. Die Abreicherung von *HIF3A* durch siRNA führte zu einer erhöhten Bindung des *PAI1* Promotors durch HIF-2 $\alpha$  nach 48 Stunden Hypoxie, während bei 24 Stunden keine Änderung beobachtet wurde. Der Anteil durch ARNT gebundene *PAI1* Promotor DNA blieb bei 24 und 48 Stunden Hypoxie sowohl unter Kontrollbedingungen als auch nach Abreicherung von *HIF3A* stabil. Die gleichzeitige Abreicherung von *HIF2A* und *HIF3A* jedoch führte zu einer vollständigen Aufhebung der ARNT-Bindung an den Promotor. Unsere Ergebnisse zeigen, dass unter anhaltender Hypoxie der HIF-3 $\alpha$ /ARNT Komplex mit HIF-2 $\alpha$  um die Bindung an die DNA konkurriert und damit die Expression des Zielgens reguliert. Zusätzlich konnte gezeigt werden, dass überexprimierte HIF-3 $\alpha$ /ARNT Komplexe sowohl im Luciferase assay als auch bei der Expression des endogenen *PAI1* moderate transaktivatorische Effekte ausüben.

sche Eigenschaften aufweisen. Vor diesem Hintergrund scheint HIF-3 $\alpha$  eher eine modulierende als inhibierende Wirkung auf das HIF-System zu besitzen. Der modulierende Effekt von HIF-3 $\alpha$  konnte in einem sogenannten *tube formation assay* bestätigt werden, in dem unter hypoxischen Bedingungen die Abreicherung von *HIF3A* zu einer verstärkten Aussprossung von endothelialen Strukturen führt. Demgegenüber führte eine Abreicherung von *HIF2A* zu einer abgeschwächten Bildung dieser Strukturen.

Zusammengefasst zeigt diese Studie eine unterschiedliche epigenetische Regulation der basalen Transkription von *HIF3A* in verschiedenen Zelllinien. Zusätzlich konnten wir bei anhaltender Hypoxie in HMEC-1 Zellen eine modulierende Funktion von HIF-3 $\alpha$  auf die Aktivität von HIF-2 $\alpha$  am *PAI1* Promotor zeigen. Dies basiert auf einer kompetitiven Interaktion von HIF-3 $\alpha$  und HIF-2 $\alpha$  mit ARNT und einer anschließenden Bindung eines HIF-3 $\alpha$ /ARNT-Komplexes an die entsprechende Bindungsstelle. Dieser Komplex zeigt schwache transaktivatorische Eigenschaften, so dass HIF-3 $\alpha$  als modulierender und nicht inhibierender Faktor bei Hypoxie zu beschreiben ist.

Unter Berücksichtigung der proangiogenen Eigenschaften von HIF-2 $\alpha$  in hypoxischen Arealen solider Tumoren sind nach weiterer Charakterisierung von HIF-3 $\alpha$  vielfältige therapeutische Möglichkeiten denkbar.

## 8 References

Ades EW, Candal FJ, Swerlick RA, et al (1992) HMEC-1: establishment of an immortalized human microvascular endothelial cell line. *J Invest Dermatol* 99:683–690.

Aggarwal S, Gross CM, Sharma S, et al (2013) Reactive oxygen species in pulmonary vascular remodeling. *Compr Physiol* 3:1011–1034. doi: 10.1002/cphy.c120024

Alberts B, Johnson A, Lewis J, et al (2002) Molecular Biology of the Cell, 4th edn. Garland Science

Altschul SF, Gish W, Miller W, et al (1990) Basic local alignment search tool. *J Mol Biol* 215:403–410. doi: 10.1016/S0022-2836(05)80360-2

Anand P, Kunnumakara AB, Sundaram C, et al (2008) Cancer is a Preventable Disease that Requires Major Lifestyle Changes. *Pharm Res* 25:2097–2116. doi: 10.1007/s11095-008-9661-9

Aragonés J, Schneider M, Van Geyte K, et al (2008) Deficiency or inhibition of oxygen sensor Phd1 induces hypoxia tolerance by reprogramming basal metabolism. *Nat Genet* 40:170–180. doi: 10.1038/ng.2007.62

Augstein A, Poitz DM, Braun-Dullaeus RC, et al (2011) Cell-specific and hypoxia-dependent regulation of human HIF-3 $\alpha$ : inhibition of the expression of HIF target genes in vascular cells. *Cell Mol Life Sci* 68:2627–2642. doi: 10.1007/s00018-010-0575-4

Bajou K, Noël A, Gerard RD, et al (1998) Absence of host plasminogen activator inhibitor 1 prevents cancer invasion and vascularization. *Nat Med* 4:923–928.

Baylin SB, Ohm JE (2006) Epigenetic gene silencing in cancer - a mechanism for early oncogenic pathway addiction? *Nat Rev Cancer* 6:107–116. doi: 10.1038/nrc1799

Bersten DC, Sullivan AE, Peet DJ, Whitelaw ML (2013) bHLH-PAS proteins in cancer. *Nat Rev Cancer* 13:827–841. doi: 10.1038/nrc3621

Bock C, Reither S, Mikeska T, et al (2005) BiQ Analyzer: visualization and quality control for DNA methylation data from bisulfite sequencing. *Bioinformatics* 21:4067–4068. doi: 10.1093/bioinformatics/bti652

Bonello S, Zähringer C, Belaiba RS, et al (2007) Reactive oxygen species activate the HIF-1 $\alpha$  promoter via a functional NF $\kappa$ B site. *Arterioscler Thromb Vasc Biol* 27:755–61. doi: 01.ATV.0000258979.92828.bc

Boron WF, Boulpaep EL (2008) Medical Physiology. Elsevier Health Sciences

Boutilier RG (2001) Mechanisms of cell survival in hypoxia and hypothermia. *J Exp Biol* 204:3171–3181.

Buck MJ, Raaijmakers LM, Ramakrishnan S, et al (2013) Alterations in chromatin accessibility and DNA methylation in clear cell renal cell carcinoma. *Oncogene*. doi: 10.1038/onc.2013.455

Budhiraja R, Tuder RM, Hassoun PM (2004) Endothelial Dysfunction in Pulmonary Hypertension. *Circulation* 109:159–165. doi: 10.1161/01.CIR.0000102381.57477.50

Carmeliet P (2000) Mechanisms of angiogenesis and arteriogenesis. *Nat Med* 6:389–395. doi: 10.1038/74651

Carmeliet P, Dor Y, Herbert JM, et al (1998) Role of HIF-1alpha in hypoxia-mediated apoptosis, cell proliferation and tumour angiogenesis. *Nature* 394:485–490. doi: 10.1038/28867

Cedar H, Bergman Y (2009) Linking DNA methylation and histone modification: patterns and paradigms. *Nat Rev Genet* 10:295–304. doi: 10.1038/nrg2540

Chi P, Allis CD, Wang GG (2010) Covalent histone modifications: miswritten, misinterpreted, and miserased in human cancers. *Nat Rev Cancer* 10:457–469. doi: 10.1038/nrc2876

Clapier CR, Cairns BR (2009) The biology of chromatin remodeling complexes. *Annu Rev Biochem* 78:273–304. doi: 10.1146/annurev.biochem.77.062706.153223

Cooper GM (2000) The Mechanism of Oxidative Phosphorylation. <http://www.ncbi.nlm.nih.gov/books/NBK9885/>. Accessed 29 Jul 2014

Covello KL, Kehler J, Yu H, et al (2006) HIF-2alpha regulates Oct-4: effects of hypoxia on stem cell function, embryonic development, and tumor growth. *Genes Dev* 20:557–570. doi: 10.1101/gad.1399906

Covello KL, Simon MC, Keith B (2005) Targeted replacement of hypoxia-inducible factor-1alpha by a hypoxia-inducible factor-2alpha knock-in allele promotes tumor growth. *Cancer Res* 65:2277–2286. doi: 10.1158/0008-5472.CAN-04-3246

Crews SE (2003) PAS Proteins: Regulators and Sensors of Development and Physiology: Regulators and Sensors of Development and Physiology. Springer

Dayan F, Roux D, Brahimi-Horn MC, et al (2006) The Oxygen Sensor Factor-Inhibiting Hypoxia-Inducible Factor-1 Controls Expression of Distinct Genes through the Bifunctional Transcriptional Character of Hypoxia-Inducible Factor-1α. *Cancer Res* 66:3688–3698. doi: 10.1158/0008-5472.CAN-05-4564

De Leval MR, Deanfield JE (2010) Four decades of Fontan palliation. *Nat Rev Cardiol* 7:520–527. doi: 10.1038/nrccardio.2010.99

Denko NC (2008) Hypoxia, HIF1 and glucose metabolism in the solid tumour. *Nat Rev Cancer* 8:705–713. doi: 10.1038/nrc2468

Dick KJ, Nelson CP, Tsaprouni L, et al (2014) DNA methylation and body-mass index: a genome-wide analysis. *Lancet* 383:1990–1998. doi: 10.1016/S0140-6736(13)62674-4

Dickson KM, Gustafson CB, Young JI, et al (2013) Ascorbate-induced generation of 5-hydroxymethylcytosine is unaffected by varying levels of iron and 2-oxoglutarate. *Biochem Biophys Res Commun* 439:522–527. doi: 10.1016/j.bbrc.2013.09.010

Diebold I, Flügel D, Becht S, et al (2010) The hypoxia-inducible factor-2alpha is stabilized by oxidative stress involving NOX4. *Antioxid Redox Signal* 13:425–436. doi: 10.1089/ars.2009.3014

Diebold I, Kraicun D, Bonello S, Görlach A (2008) The “PAI-1 paradox” in vascular remodeling. *Thromb Haemost* 100:984–91.

Dorsam RT, Gutkind JS (2007) G-protein-coupled receptors and cancer. *Nat Rev Cancer* 7:79–94. doi: 10.1038/nrc2069

Druliner BR, Fincher JA, Sexton BS, et al (2013) Chromatin patterns associated with lung adenocarcinoma progression. *Cell Cycle* 12:1536–1543. doi: 10.4161/cc.24664

Dunwoodie SL (2009) The role of hypoxia in development of the Mammalian embryo. *Dev Cell* 17:755–773. doi: 10.1016/j.devcel.2009.11.008

Elliott S, Sinclair A, Collins H, et al (2014) Progress in detecting cell-surface protein receptors: the erythropoietin receptor example. *Ann Hematol* 93:181–192. doi: 10.1007/s00277-013-1947-2

Elvert G, Kappel A, Heidenreich R, et al (2003) Cooperative interaction of hypoxia-inducible factor-2alpha (HIF-2alpha) and Ets-1 in the transcriptional activation of vascular endothelial growth factor receptor-2 (Flk-1). *J Biol Chem* 278:7520–7530. doi: 10.1074/jbc.M211298200

Ema M, Taya S, Yokotani N, et al (1997) A novel bHLH-PAS factor with close sequence similarity to hypoxia-inducible factor 1alpha regulates the VEGF expression and is potentially involved in lung and vascular development. *Proc Natl Acad Sci USA* 94:4273–4278.

Evans AM, Hardie DG, Peers C, Mahmoud A (2011) Hypoxic pulmonary vasoconstriction: mechanisms of oxygen-sensing. *Curr Opin Anaesthesiol* 24:13–20. doi: 10.1097/ACO.0b013e3283421201

Fakhrejahani E, Toi M (2012) Tumor angiogenesis: pericytes and maturation are not to be ignored. *J Oncol* 2012:261750. doi: 10.1155/2012/261750

Fearon ER, Vogelstein B (1990) A genetic model for colorectal tumorigenesis. *Cell* 61:759–767.

Fink T, Kazlauskas A, Poellinger L, et al (2002) Identification of a tightly regulated hypoxia-response element in the promoter of human plasminogen activator inhibitor-1. *Blood* 99:2077–2083.

Flamme I, Fröhlich T, von Reutern M, et al (1997) HRF, a putative basic helix-loop-helix-PAS-domain transcription factor is closely related to hypoxia-inducible factor-1 alpha and developmentally expressed in blood vessels. *Mech Dev* 63:51–60.

Forristal CE, Wright KL, Hanley NA, et al (2010) Hypoxia inducible factors regulate pluripotency and proliferation in human embryonic stem cells cultured at reduced oxygen tensions. *Reproduction* 139:85–97. doi: 10.1530/REP-09-0300

Gey GO, Bang FB (1951) Viruses and cells: a study in tissue culture applications. I. Cells involved; availability and susceptibility. *Trans N Y Acad Sci* 14:15–24.

Gnaiger E, Steinlechner-Maran R, Méndez G, et al (1995) Control of mitochondrial and cellular respiration by oxygen. *J Bioenerg Biomembr* 27:583–596.

Goda N, Kanai M (2012) Hypoxia-inducible factors and their roles in energy metabolism. *Int J Hematol* 95:457–463. doi: 10.1007/s12185-012-1069-y

Görlach A, Diebold I, Schini-Kerth VB, et al (2001) Thrombin activates the hypoxia-inducible factor-1 signaling pathway in vascular smooth muscle cells: Role of the p22(phox)-containing NADPH oxidase. *Circ Res* 89:47–54.

Grabmaier K, A de Weijert MC, Verhaegh GW, et al (2004) Strict regulation of CAIX(G250/MN) by HIF-1alpha in clear cell renal cell carcinoma. *Oncogene* 23:5624–5631. doi: 10.1038/sj.onc.1207764

Graham FL, Smiley J, Russell WC, Nairn R (1977) Characteristics of a human cell line transformed by DNA from human adenovirus type 5. *J Gen Virol* 36:59–74.

Gu YZ, Moran SM, Hogenesch JB, et al (1998) Molecular characterization and chromosomal localization of a third alpha-class hypoxia inducible factor subunit, HIF3alpha. *Gene Expr* 7:205–13. doi: 9840812

Hanahan D, Weinberg RA (2000) The hallmarks of cancer. *Cell* 100:57–70.

Hara S, Hamada J, Kobayashi C, et al (2001) Expression and characterization of hypoxia-inducible factor (HIF)-3alpha in human kidney: suppression of HIF-mediated gene expression by HIF-3alpha. *Biochem Biophys Res Commun* 287:808–13. doi: 11573933

Heikkilä M, Pasanen A, Kivirikko KI, Myllyharju J (2011) Roles of the human hypoxia-inducible factor (HIF)-3 $\alpha$  variants in the hypoxia response. *Cell Mol Life Sci* 68:3885–3901. doi: 10.1007/s00018-011-0679-5

Hirose K, Morita M, Ema M, et al (1996) cDNA cloning and tissue-specific expression of a novel basic helix-loop-helix/PAS factor (Arnt2) with close sequence simi-

larity to the aryl hydrocarbon receptor nuclear translocator (Arnt). *Mol Cell Biol* 16:1706–1713.

Hirota N, Martin JG (2013) Mechanisms of airway remodeling. *Chest* 144:1026–1032. doi: 10.1378/chest.12-3073

Hochachka PW, Lutz PL, Sick TJ, Rosenthal M (1993) *Surviving Hypoxia: Mechanisms of Control and Adaptation*. CRC Press

Hoeben A, Landuyt B, Highley MS, et al (2004) Vascular Endothelial Growth Factor and Angiogenesis. *Pharmacol Rev* 56:549–580. doi: 10.1124/pr.56.4.3

Hogenesch JB, Chan WK, Jackiw VH, et al (1997) Characterization of a subset of the basic-helix-loop-helix-PAS superfamily that interacts with components of the dioxin signaling pathway. *J Biol Chem* 272:8581–8593.

Holmquist L, Jögi A, Pählman S (2005) Phenotypic persistence after reoxygenation of hypoxic neuroblastoma cells. *Int J Cancer* 116:218–225. doi: 10.1002/ijc.21024

Holmquist-Mengelbier L, Fredlund E, Löfstedt T, et al (2006) Recruitment of HIF-1 $\alpha$  and HIF-2 $\alpha$  to common target genes is differentially regulated in neuroblastoma: HIF-2 $\alpha$  promotes an aggressive phenotype. *Cancer Cell* 10:413–423. doi: 10.1016/j.ccr.2006.08.026

Horoszewicz JS, Leong SS, Chu TM, et al (1980) The LNCaP cell line--a new model for studies on human prostatic carcinoma. *Prog Clin Biol Res* 37:115–132.

Huang LE, Arany Z, Livingston DM, Bunn HF (1996) Activation of hypoxia-inducible transcription factor depends primarily upon redox-sensitive stabilization of its  $\alpha$  subunit. *J Biol Chem* 271:32253–32259.

Huang LE, Gu J, Schau M, Bunn HF (1998) Regulation of hypoxia-inducible factor 1 $\alpha$  is mediated by an O<sub>2</sub>-dependent degradation domain via the ubiquitin-proteasome pathway. *Proc Natl Acad Sci USA* 95:7987–7992.

Hu C-J, Iyer S, Sataur A, et al (2006) Differential Regulation of the Transcriptional Activities of Hypoxia-Inducible Factor 1 Alpha (HIF-1 $\alpha$ ) and HIF-2 $\alpha$  in Stem Cells. *Mol Cell Biol* 26:3514–3526. doi: 10.1128/MCB.26.9.3514-3526.2006

Hu C-J, Sataur A, Wang L, et al (2007) The N-terminal transactivation domain confers target gene specificity of hypoxia-inducible factors HIF-1 $\alpha$  and HIF-2 $\alpha$ . *Mol Biol Cell* 18:4528–4542. doi: 10.1091/mbc.E06-05-0419

Hu C-J, Wang L-Y, Chodosh LA, et al (2003) Differential roles of hypoxia-inducible factor 1 $\alpha$  (HIF-1 $\alpha$ ) and HIF-2 $\alpha$  in hypoxic gene regulation. *Mol Cell Biol* 23:9361–9374.

Iyer NV, Kotch LE, Agani F, et al (1998) Cellular and developmental control of O<sub>2</sub> homeostasis by hypoxia-inducible factor 1 alpha. *Genes Dev* 12:149–162.

Jaakkola P, Mole DR, Tian YM, et al (2001) Targeting of HIF-alpha to the von Hippel-Lindau ubiquitylation complex by O2-regulated prolyl hydroxylation. *Science* 292:468–472. doi: 10.1126/science.1059796

Jaenisch R, Bird A (2003) Epigenetic regulation of gene expression: how the genome integrates intrinsic and environmental signals. *Nat Genet* 33 Suppl:245–254. doi: 10.1038/ng1089

Jang MS, Park JE, Lee JA, et al (2005) Binding and regulation of hypoxia-inducible factor-1 by the inhibitory PAS proteins. *Biochem Biophys Res Commun* 337:209–15. doi: S0006-291X(05)02034-6

Jewell UR, Kvietikova I, Scheid A, et al (2001) Induction of HIF-1 $\alpha$  in response to hypoxia is instantaneous. *FASEB J.* doi: 10.1096/fj.00-0732fje

Jiang BH, Rue E, Wang GL, et al (1996) Dimerization, DNA binding, and transactivation properties of hypoxia-inducible factor 1. *J Biol Chem* 271:17771–17778.

Jones PA, Baylin SB (2002) The fundamental role of epigenetic events in cancer. *Nat Rev Genet* 3:415–428. doi: 10.1038/nrg816

Kaelin WG Jr, Ratcliffe PJ (2008) Oxygen sensing by metazoans: the central role of the HIF hydroxylase pathway. *Mol Cell* 30:393–402. doi: 10.1016/j.molcel.2008.04.009

Keith B, Johnson RS, Simon MC (2012) HIF1 $\alpha$  and HIF2 $\alpha$ : sibling rivalry in hypoxic tumour growth and progression. *Nat Rev Cancer* 12:9–22. doi: 10.1038/nrc3183

Kent WJ (2002) BLAT--the BLAST-like alignment tool. *Genome Res* 12:656–664. doi: 10.1101/gr.229202. Article published online before March 2002

Ke Q, Costa M (2006) Hypoxia-Inducible Factor-1 (HIF-1). *Mol Pharmacol* 70:1469–1480. doi: 10.1124/mol.106.027029

Kietzmann T, Cornesse Y, Brechtel K, et al (2001) Perivenous expression of the mRNA of the three hypoxia-inducible factor alpha-subunits, HIF1alpha, HIF2alpha and HIF3alpha, in rat liver. *Biochem J* 354:531–537.

Kietzmann T, Jungermann K, Görlich A (2003) Regulation of the hypoxia-dependent plasminogen activator inhibitor 1 expression by MAP kinases. *Thromb Haemost* 89:666–73. doi: 12669121

Kim J, Tchernyshyov I, Semenza GL, Dang CV (2006) HIF-1-mediated expression of pyruvate dehydrogenase kinase: a metabolic switch required for cellular adaptation to hypoxia. *Cell Metab* 3:177–185. doi: 10.1016/j.cmet.2006.02.002

Klein A, Flügel D, Kietzmann T (2008) Transcriptional regulation of serine/threonine kinase-15 (STK15) expression by hypoxia and HIF-1. *Mol Biol Cell* 19:3667–3675. doi: 10.1091/mbc.E08-01-0042

Koch CM, Andrews RM, Flicek P, et al (2007) The landscape of histone modifications across 1% of the human genome in five human cell lines. *Genome Res* 17:691–707. doi: 10.1101/gr.5704207

Koh MY, Powis G (2012) Passing the baton: the HIF switch. *Trends Biochem Sci* 37:364–372. doi: 10.1016/j.tibs.2012.06.004

Kotch LE, Iyer NV, Laughner E, Semenza GL (1999) Defective vascularization of HIF-1alpha-null embryos is not associated with VEGF deficiency but with mesenchymal cell death. *Dev Biol* 209:254–267. doi: 10.1006/dbio.1999.9253

Kračun D, Rieß F, Kanchev I, et al (2014) The  $\beta$ 3-Integrin Binding Protein  $\beta$ 3-Endonexin Is a Novel Negative Regulator of Hypoxia-Inducible Factor-1. *Antioxid Redox Signal* 20:1964–1976. doi: 10.1089/ars.2013.5286

Krock BL, Skuli N, Simon MC (2011) Hypoxia-Induced Angiogenesis. *Genes Cancer* 2:1117–1133. doi: 10.1177/1947601911423654

Kubota Y (2012) Tumor angiogenesis and anti-angiogenic therapy. *Keio J Med* 61:47–56.

Kuhn RM, Karolchik D, Zweig AS, et al (2009) The UCSC Genome Browser Database: update 2009. *Nucleic Acids Res* 37:D755–761. doi: 10.1093/nar/gkn875

LadyofHats File:Circulatory System no tags.svg - Wikimedia Commons. [http://commons.wikimedia.org/wiki/File:Circulatory\\_System\\_no\\_tags.svg](http://commons.wikimedia.org/wiki/File:Circulatory_System_no_tags.svg). Accessed 17 Aug 2014

Le Bras A, Lionneton F, Mattot V, et al (2007) HIF-2alpha specifically activates the VE-cadherin promoter independently of hypoxia and in synergy with Ets-1 through two essential ETS-binding sites. *Oncogene* 26:7480–7489. doi: 10.1038/sj.onc.1210566

Legrand M, Mik EG, Johannes T, et al (2008) Renal Hypoxia and Dysoxia After Reperfusion of the Ischemic Kidney. *Mol Med* 14:502–516. doi: 10.2119/2008-00006.Legrand

Leonhardt H, Cardoso MC (2000) DNA methylation, nuclear structure, gene expression and cancer. *J Cell Biochem Suppl* 35:78–83.

Lisy K, Peet DJ (2008) Turn me on: regulating HIF transcriptional activity. *Cell Death Differ* 15:642–649. doi: 10.1038/sj.cdd.4402315

Loboda A, Jozkowicz A, Dulak J (2010) HIF-1 and HIF-2 transcription factors--similar but not identical. *Mol Cells* 29:435–442. doi: 10.1007/s10059-010-0067-2

Lodish H, Berk A, Zipursky SL, et al (2000) Oxidation of Glucose and Fatty Acids to CO<sub>2</sub>. <http://www.ncbi.nlm.nih.gov/books/NBK21624/>. Accessed 9 Aug 2014

Mahapatra S, Klee EW, Young CYF, et al (2012) Global methylation profiling for risk prediction of prostate cancer. *Clin Cancer Res* 18:2882–2895. doi: 10.1158/1078-0432.CCR-11-2090

Makino Y, Cao R, Svensson K, et al (2001) Inhibitory PAS domain protein is a negative regulator of hypoxia-inducible gene expression. *Nature* 414:550–4. doi: 11734856

Makino Y, Kanopka A, Wilson WJ, et al (2002) Inhibitory PAS domain protein (IPAS) is a hypoxia-inducible splicing variant of the hypoxia-inducible factor-3alpha locus. *J Biol Chem* 277:32405–8. doi: 12119283

Marcelo KL, Goldie LC, Hirschi KK (2013) Regulation of endothelial cell differentiation and specification. *Circ Res* 112:1272–1287. doi: 10.1161/CIRCRESAHA.113.300506

Marxsen JH, Stengel P, Doege K, et al (2004) Hypoxia-inducible factor-1 (HIF-1) promotes its degradation by induction of HIF-alpha-prolyl-4-hydroxylases. *Biochem J* 381:761–767. doi: 10.1042/BJ20040620

Maxwell PH, Dachs GU, Gleadle JM, et al (1997) Hypoxia-inducible factor-1 modulates gene expression in solid tumors and influences both angiogenesis and tumor growth. *Proc Natl Acad Sci USA* 94:8104–8109.

Maynard MA, Evans AJ, Hosomi T, et al (2005) Human HIF-3alpha4 is a dominant-negative regulator of HIF-1 and is down-regulated in renal cell carcinoma. *FASEB J* 19:1396–406. doi: 19/11/1396

Maynard MA, Evans AJ, Shi W, et al (2007) Dominant-negative HIF-3 alpha 4 suppresses VHL-null renal cell carcinoma progression. *Cell Cycle* 6:2810–6. doi: 4947

Maynard MA, Qi H, Chung J, et al (2003) Multiple splice variants of the human HIF-3 alpha locus are targets of the von Hippel-Lindau E3 ubiquitin ligase complex. *J Biol Chem* 278:11032–40. doi: 12538644

McIlhenny C, George WD, Doughty JC (2002) A comparison of serum and plasma levels of vascular endothelial growth factor during the menstrual cycle in healthy female volunteers. *Br J Cancer* 86:1786–1789. doi: 10.1038/sj.bjc.6600322

Michiels C (2004) Physiological and Pathological Responses to Hypoxia. *Am J Pathol* 164:1875–1882.

Müller U, Bauer C, Siegl M, et al (2014) TET-mediated oxidation of methylcytosine causes TDG or NEIL glycosylase dependent gene reactivation. *Nucleic Acids Res* 42:8592–8604. doi: 10.1093/nar/gku552

Nagao K, Oka K (2011) HIF-2 directly activates CD82 gene expression in endothelial cells. *Biochem Biophys Res Commun* 407:260–265. doi: 10.1016/j.bbrc.2011.03.017

Nguyen CT, Gonzales FA, Jones PA (2001) Altered chromatin structure associated with methylation-induced gene silencing in cancer cells: correlation of acces-

sibility, methylation, MeCP2 binding and acetylation. *Nucleic Acids Res* 29:4598–4606.

Onita T, Ji PG, Xuan JW, et al (2002) Hypoxia-induced, perinecrotic expression of endothelial Per-ARNT-Sim domain protein-1/hypoxia-inducible factor-2alpha correlates with tumor progression, vascularization, and focal macrophage infiltration in bladder cancer. *Clin Cancer Res* 8:471–480.

Oshiro MM, Watts GS, Wozniak RJ, et al (2003) Mutant p53 and aberrant cytosine methylation cooperate to silence gene expression. *Oncogene* 22:3624–3634. doi: 10.1038/sj.onc.1206545

Østergaard L, Gassmann M (2011) Hypoxia Inducible Factor and Hypoxia-mediated Pulmonary Hypertension. *PVRI Review* 3:5. doi: 10.4103/0974-6013.85613

Pasanen A, Heikkilä M, Rautavauma K, et al (2010) Hypoxia-inducible factor (HIF)-3alpha is subject to extensive alternative splicing in human tissues and cancer cells and is regulated by HIF-1 but not HIF-2. *Int J Biochem Cell Biol* 42:1189–1200. doi: 10.1016/j.biocel.2010.04.008

Perez-Perri JI, Acevedo JM, Wappner P (2011) Epigenetics: new questions on the response to hypoxia. *Int J Mol Sci* 12:4705–4721. doi: 10.3390/ijms12074705

Pescador N, Cuevas Y, Naranjo S, et al (2005) Identification of a functional hypoxia-responsive element that regulates the expression of the egl nine homologue 3 (eglN3/phd3) gene. *Biochem J* 390:189–197. doi: 10.1042/BJ20042121

Petryszak R, Burdett T, Fiorelli B, et al (2014) Expression Atlas update—a database of gene and transcript expression from microarray- and sequencing-based functional genomics experiments. *Nucl Acids Res* 42:D926–D932. doi: 10.1093/nar/gkt1270

Pruitt KD, Tatusova T, Maglott DR (2007) NCBI reference sequences (RefSeq): a curated non-redundant sequence database of genomes, transcripts and proteins. *Nucleic Acids Res* 35:D61–65. doi: 10.1093/nar/gkl842

Racker E (1974) History of the Pasteur effect and its pathobiology. *Mol Cell Biochem* 5:17–23.

Raval RR, Lau KW, Tran MGB, et al (2005) Contrasting properties of hypoxia-inducible factor 1 (HIF-1) and HIF-2 in von Hippel-Lindau-associated renal cell carcinoma. *Mol Cell Biol* 25:5675–5686. doi: 10.1128/MCB.25.13.5675-5686.2005

Rea S, Eisenhaber F, O'Carroll D, et al (2000) Regulation of chromatin structure by site-specific histone H3 methyltransferases. *Nature* 406:593–599. doi: 10.1038/35020506

Reyes H, Reisz-Porszasz S, Hankinson O (1992) Identification of the Ah receptor nuclear translocator protein (Arnt) as a component of the DNA binding form of the Ah receptor. *Science* 256:1193–1195.

Ribatti D (2008) Judah Folkman, a pioneer in the study of angiogenesis. *Angiogenesis* 11:3–10. doi: 10.1007/s10456-008-9092-6

Rifkind RA, Marks PA, Bank A, et al (1976) Erythroid differentiation and the cell cycle: some implications from murine foetal and erythroleukemic cells. *Ann Immunol (Paris)* 127:887–893.

Robinson CM, Neary R, Levendale A, et al (2012) Hypoxia-induced DNA hypermethylation in human pulmonary fibroblasts is associated with Thy-1 promoter methylation and the development of a pro-fibrotic phenotype. *Respiratory Research* 13:74. doi: 10.1186/1465-9921-13-74

Rozen S, Skaletsky H (2000) Primer3 on the WWW for general users and for biologist programmers. *Methods Mol Biol* 132:365–386.

Ruan K, Song G, Ouyang G (2009) Role of hypoxia in the hallmarks of human cancer. *J Cell Biochem* 107:1053–1062. doi: 10.1002/jcb.22214

Ruas JL, Poellinger L, Pereira T (2002) Functional analysis of hypoxia-inducible factor-1 alpha-mediated transactivation. Identification of amino acid residues critical for transcriptional activation and/or interaction with CREB-binding protein. *J Biol Chem* 277:38723–38730. doi: 10.1074/jbc.M205051200

Russo J, Soule HD, McGrath C, Rich MA (1976) Reexpression of the original tumor pattern by a human breast carcinoma cell line (MCF-7) in sponge culture. *J Natl Cancer Inst* 56:279–282.

Sarkar S, Horn G, Moulton K, et al (2013) Cancer Development, Progression, and Therapy: An Epigenetic Overview. *Int J Mol Sci* 14:21087–21113. doi: 10.3390/ijms141021087

Sato M, Tanaka T, Maemura K, et al (2004) The PAI-1 gene as a direct target of endothelial PAS domain protein-1 in adenocarcinoma A549 cells. *Am J Respir Cell Mol Biol* 31:209–215. doi: 10.1165/rccb.2003-0296OC

Schneider CA, Rasband WS, Eliceiri KW (2012) NIH Image to ImageJ: 25 years of image analysis. *Nat Meth* 9:671–675. doi: 10.1038/nmeth.2089

Schulz K, Milke L, Rübsamen D, et al (2012) HIF-1 $\alpha$  protein is upregulated in HIF-2 $\alpha$  depleted cells via enhanced translation. *FEBS Lett* 586:1652–1657. doi: 10.1016/j.febslet.2012.04.039

Seagroves TN, Ryan HE, Lu H, et al (2001) Transcription Factor HIF-1 Is a Necessary Mediator of the Pasteur Effect in Mammalian Cells. *Mol Cell Biol* 21:3436–3444. doi: 10.1128/MCB.21.10.3436-3444.2001

Semenza GL (1999) Regulation of mammalian O<sub>2</sub> homeostasis by hypoxia-inducible factor 1. *Annu Rev Cell Dev Biol* 15:551–578. doi: 10.1146/annurev.cellbio.15.1.551

Semenza GL (2010) Oxygen homeostasis. Wiley Interdiscip Rev Syst Biol Med 2:336–361. doi: 10.1002/wsbm.69

Semenza GL (2012) Hypoxia-inducible factors in physiology and medicine. Cell 148:399–408. doi: 10.1016/j.cell.2012.01.021

Semenza GL (2009) Regulation of oxygen homeostasis by hypoxia-inducible factor 1. Physiology (Bethesda) 24:97–106. doi: 10.1152/physiol.00045.2008

Shahrzad S, Bertrand K, Minhas K, Coomber BL (2007) Induction of DNA hypomethylation by tumor hypoxia. Epigenetics 2:119–125.

Shin G, Kang T-W, Yang S, et al (2011) GENT: gene expression database of normal and tumor tissues. Cancer Inform 10:149–157. doi: 10.4137/CIN.S7226

Sogawa K, Nakano R, Kobayashi A, et al (1995) Possible function of Ah receptor nuclear translocator (Arnt) homodimer in transcriptional regulation. Proc Natl Acad Sci USA 92:1936–1940.

Spruijt CG, Gnerlich F, Smits AH, et al (2013) Dynamic readers for 5-(hydroxy)methylcytosine and its oxidized derivatives. Cell 152:1146–1159. doi: 10.1016/j.cell.2013.02.004

Stiehl DP, Bordoli MR, Abreu-Rodríguez I, et al (2011) Non-canonical HIF-2 $\alpha$  function drives autonomous breast cancer cell growth via an AREG–EGFR–ErbB4 autocrine loop. Oncogene 31:2283–2297. doi: 10.1038/onc.2011.417

Stone KR, Mickey DD, Wunderli H, et al (1978) Isolation of a human prostate carcinoma cell line (DU 145). Int J Cancer 21:274–281.

Strahl BD, Allis CD (2000) The language of covalent histone modifications. Nature 403:41–45. doi: 10.1038/47412

Tan Q, Kerestes H, Percy MJ, et al (2013) Erythrocytosis and pulmonary hypertension in a mouse model of human HIF2A gain of function mutation. J Biol Chem 288:17134–17144. doi: 10.1074/jbc.M112.444059

Ten Dijke P, Arthur HM (2007) Extracellular control of TGF $\beta$  signalling in vascular development and disease. Nat Rev Mol Cell Biol 8:857–869. doi: 10.1038/nrm2262

Thompson JD, Gibson TJ, Higgins DG (2002) Multiple sequence alignment using ClustalW and ClustalX. Curr Protoc Bioinformatics Chapter 2:Unit 2.3. doi: 10.1002/0471250953.bi0203s00

Tian H, McKnight SL, Russell DW (1997) Endothelial PAS domain protein 1 (EPAS1), a transcription factor selectively expressed in endothelial cells. Genes & Development 11:72–82. doi: 10.1101/gad.11.1.72

Turner BM (1998) Histone acetylation as an epigenetic determinant of long-term transcriptional competence. Cell Mol Life Sci 54:21–31.

Uhlen M, Oksvold P, Fagerberg L, et al (2010) Towards a knowledge-based Human Protein Atlas. *Nat Biotechnol* 28:1248–1250. doi: 10.1038/nbt1210-1248

Uniacke J, Holterman CE, Lachance G, et al (2012) An oxygen-regulated switch in the protein synthesis machinery. *Nature* 486:126–129. doi: 10.1038/nature11055

Verheul HMW, Pinedo HM (2007) Possible molecular mechanisms involved in the toxicity of angiogenesis inhibition. *Nat Rev Cancer* 7:475–485. doi: 10.1038/nrc2152

Vita JA (2011) Endothelial Function. *Circulation* 124:e906–e912. doi: 10.1161/CIRCULATIONAHA.111.078824

Voelkel NF, Natarajan R, Drake JI, Bogaard HJ (2011) Right ventricle in pulmonary hypertension. *Compr Physiol* 1:525–540. doi: 10.1002/cphy.c090008

Wabitsch M, Brenner RE, Melzner I, et al (2001) Characterization of a human preadipocyte cell strain with high capacity for adipose differentiation. *Int J Obes Relat Metab Disord* 25:8–15.

Wain HM, Bruford EA, Lovering RC, et al (2002) Guidelines for human gene nomenclature. *Genomics* 79:464–470. doi: 10.1006/geno.2002.6748

Wang GL, Jiang BH, Rue EA, Semenza GL (1995) Hypoxia-inducible factor 1 is a basic-helix-loop-helix-PAS heterodimer regulated by cellular O<sub>2</sub> tension. *Proc Natl Acad Sci USA* 92:5510–5514.

Wang GL, Semenza GL (1993) General involvement of hypoxia-inducible factor 1 in transcriptional response to hypoxia. *Proc Natl Acad Sci USA* 90:4304–4308.

Wang Z, Zang C, Rosenfeld JA, et al (2008) Combinatorial patterns of histone acetylations and methylations in the human genome. *Nat Genet* 40:897–903. doi: 10.1038/ng.154

Ward JPT (2008) Oxygen sensors in context. *Biochim Biophys Acta* 1777:1–14. doi: 10.1016/j.bbabi.2007.10.010

Warnecke C, Zaborowska Z, Kurreck J, et al (2004) Differentiating the functional role of hypoxia-inducible factor (HIF)-1alpha and HIF-2alpha (EPAS-1) by the use of RNA interference: erythropoietin is a HIF-2alpha target gene in Hep3B and Kelly cells. *FASEB J* 18:1462–1464. doi: 10.1096/fj.04-1640fje

Watson JA, Watson CJ, McCann A, Baugh J (2010) Epigenetics, the epicenter of the hypoxic response. *Epigenetics* 5:293–296.

Weber M, Hellmann I, Stadler MB, et al (2007) Distribution, silencing potential and evolutionary impact of promoter DNA methylation in the human genome. *Nat Genet* 39:457–466. doi: 10.1038/ng1990

Wheaton WW, Chandel NS (2011) Hypoxia. 2. Hypoxia regulates cellular metabolism. *Am J Physiol Cell Physiol* 300:C385–C393. doi: 10.1152/ajpcell.00485.2010

Wiesener MS, Jürgensen JS, Rosenberger C, et al (2003) Widespread hypoxia-inducible expression of HIF-2alpha in distinct cell populations of different organs. *FASEB J* 17:271–273. doi: 10.1096/fj.02-0445fje

Wiesener MS, Turley H, Allen WE, et al (1998) Induction of endothelial PAS domain protein-1 by hypoxia: characterization and comparison with hypoxia-inducible factor-1alpha. *Blood* 92:2260–2268.

Woo KJ, Lee T-J, Park J-W, Kwon TK (2006) Desferrioxamine, an iron chelator, enhances HIF-1alpha accumulation via cyclooxygenase-2 signaling pathway. *Biochem Biophys Res Commun* 343:8–14. doi: 10.1016/j.bbrc.2006.02.116

Yamashita T, Ohneda O, Nagano M, et al (2008) Abnormal heart development and lung remodeling in mice lacking the hypoxia-inducible factor-related basic helix-loop-helix PAS protein NEPAS. *Mol Cell Biol* 28:1285–1297. doi: 10.1128/MCB.01332-07

Yu AY, Frid MG, Shimoda LA, et al (1998) Temporal, spatial, and oxygen-regulated expression of hypoxia-inducible factor-1 in the lung. *Am J Physiol* 275:L818–826.

Zabel MD, Byrne BL, Weis JJ, Weis JH (2000) Cell-specific expression of the murine CD21 gene depends on accessibility of promoter and intronic elements. *J Immunol* 165:4437–4445.

Zou B, Chim CS, Zeng H, et al (2006) Correlation between the single-site CpG methylation and expression silencing of the XAF1 gene in human gastric and colon cancers. *Gastroenterology* 131:1835–1843. doi: 10.1053/j.gastro.2006.09.050

# Publikationen und Auszeichnungen

## **Publizierte Artikel:**

- Damir Kračun, **Florian Rieß**, Ivan Kanchev, Meinrad Gawaz, Agnes Görlach. „The  $\beta$ 3-integrin binding protein  $\beta$ 3-endonexin is a novel negative regulator of hypoxia-inducible factor-1 (HIF-1)“. *Antioxid Redox Signal*. 2014 May 1;20(13):1964-76
- Rzymski, T, A Petry, D Kračun, **F Rieß**, L Pike, A L Harris, und A Görlach. 2011. „The unfolded protein response controls induction and activation of ADAM17/TACE by severe hypoxia and ER stress“. *Oncogene* (November 21, 2011)

## **Vorträge:**

- **Florian Rieß**, Steve Bonello, Michael Weitnauer, Thomas Kietzmann, John Hess, Agnes Görlach. HIF-3 $\alpha$  inhibits HIF-2 in vascular endothelial cells by dimerization with ARNT. Short talk plenary session at Keystone symposia: Advances in Hypoxic Signaling: From Bench to Bedside; Fairmont Banff Springs, Banff, Alberta, Kanada; 12.-17. Februar 2012
- **Rieß F.**, Bonello S., Weitnauer M., Kietzmann T., Hess J., Görlach A.. HIF-3ALPHA INHIBITS HIF-2 IN VASCULAR ENDOTHELIAL CELLS BY DIMERIZATION WITH ARNT. 91st Annual Meeting of the German Physiological Society, DPG 2012, Dresden, Germany; 22. – 25. März 2012; Abstract in *Acta Physiologica 2012*; Volume 204, Supplement 689 :O12

## **Poster:**

- **Florian Rieß**, Steve Bonello, Michael Weitnauer, Thomas Kietzmann, John Hess, Agnes Görlach. HIF-3 $\alpha$  inhibits HIF-2 in vascular endothelial cells by dimerization with ARNT. Short talk plenary session at Keystone symposia: Advances in Hypoxic Signaling: From Bench to Bedside; Fairmont Banff Springs, Banff, Alberta, Kanada; 12.-17. Februar 2012
- **Rieß F.**, Bonello S., Weitnauer M., Kietzmann T., Hess J., Görlach A.. HIF-3ALPHA INHIBITS HIF-2 IN VASCULAR ENDOTHELIAL CELLS BY DIMERIZATION WITH ARNT. 91st Annual Meeting of the German Physiological Society, DPG 2012, Dresden, Germany; 22. – 25. März 2012; Abstract in *Acta Physiologica 2012*; Volume 204, Supplement 689 :O12
- Kračun D., Kanchev I., **Rieß F.**, Hess J., Görlach A. Low Dose Dexamethasone Treatment Stimulates Vascular Proliferative Responses Involving NADPH Oxidases And The Hif System. 91st Annual Meeting of the German Physiological Society, DPG 2012, Dresden, Germany; 22. – 25. März 2012; Abstract in *Acta Physiologica 2012*; Volume 204, Supplement 689 :P100

- Kračun D., Kanchev I., **Riess F.**, Hess J., Görlach A. Folic Acid Prevents Uncoupling Of NOSynthase And Pulmonary Vascular Remodelling Under Hypoxia. 91st Annual Meeting of the German Physiological Society, DPG 2012, Dresden, Germany; 22. – 25. März 2012; Abstract in *Acta Physiologica 2012*; Volume 204, Supplement 689 :P101

### **Artikel in Vorbereitung:**

- **Florian Rieß**, Damir Kračun, Steve Bonello, Michael Weitnauer, Thomas Kietzmann and Agnes Görlach. „Reconciling the role of HIF-3 $\alpha$ : Inhibition of HIF-2 activity in endothelial cells“.
- **Florian Rieß**, Agnes Görlach. „Differential epigenetic regulation of basal HIF3A expression in human cell lines“.

### **Auszeichnungen:**

- GSK Reise-Stipendium (600,-€) für den Kongress Keystone symposia: Advances in Hypoxic Signaling: From Bench to Bedside in Banff, Kanada,
- Keystone Symposia scholarship (\$1200) für den Kongress Keystone symposia: Advances in Hypoxic Signaling: From Bench to Bedside in Banff, Kanada.